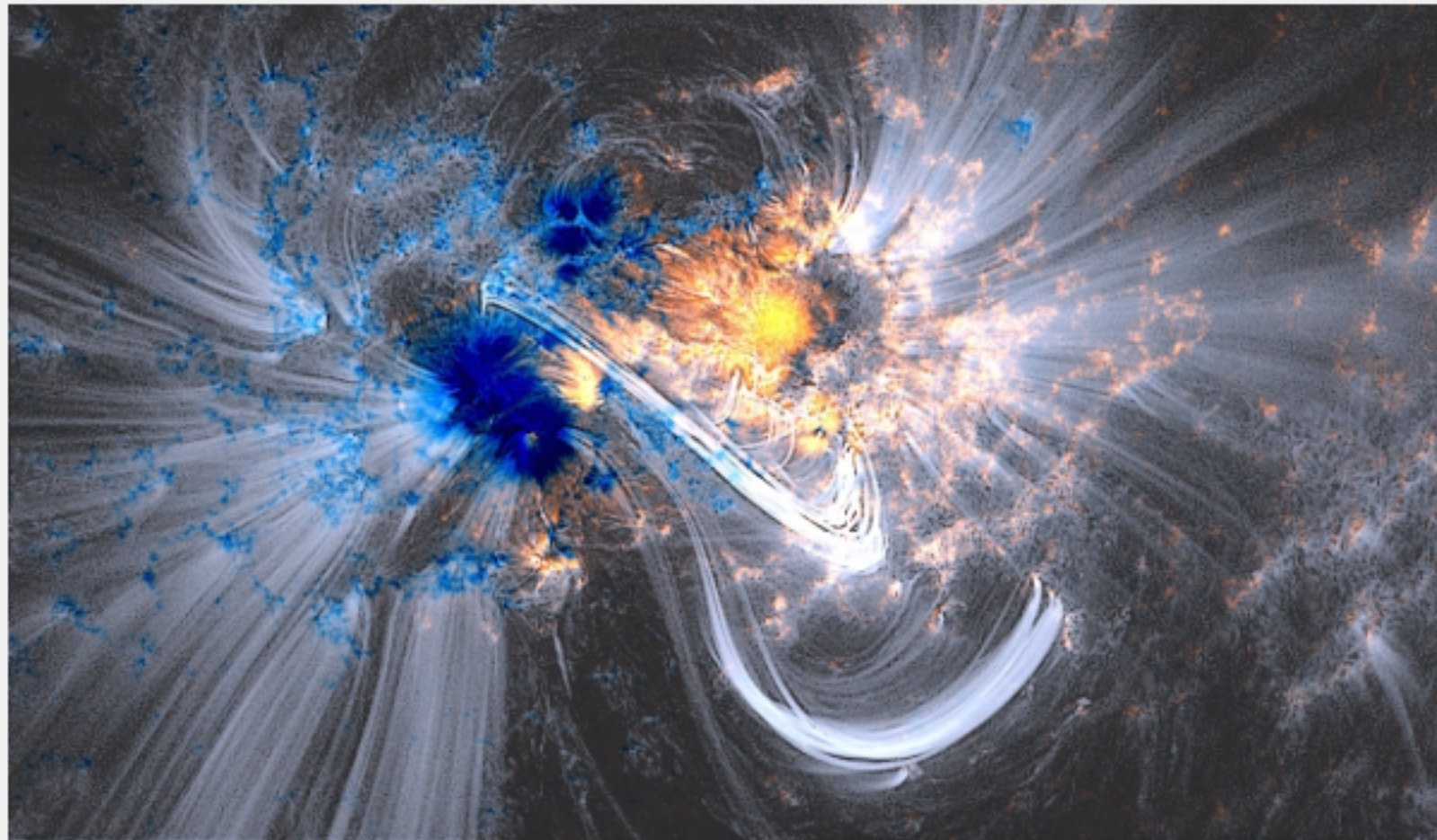


Applications of Bayesian Analysis to Coronal Seismology

Iñigo Arregui



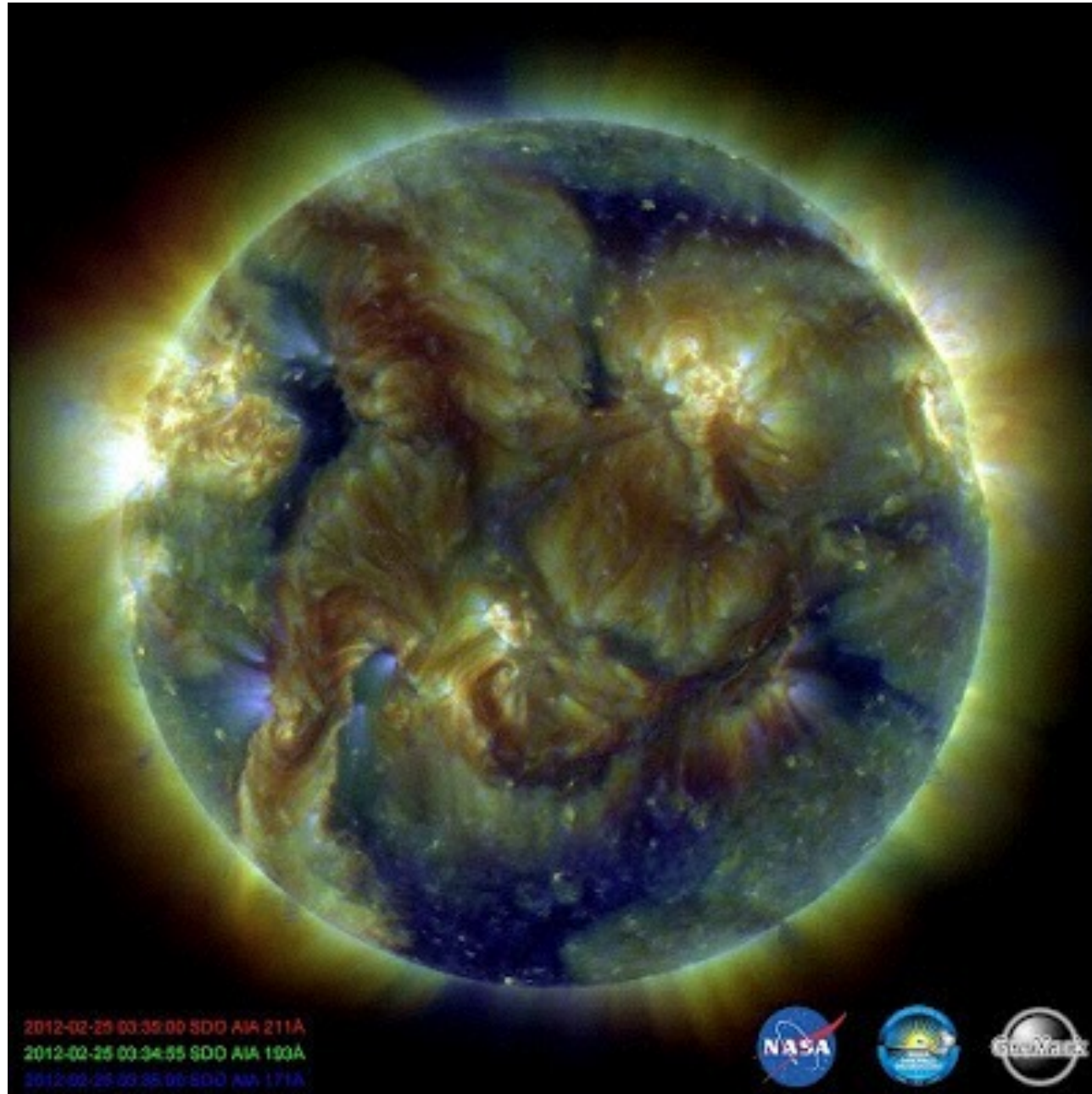
**International Team: Improving the Analysis of Solar and
Stellar Observations**



True, False, and Uncertain

My name is Iñigo Arregui

TRUE



UNCERTAIN

My name is Harry Warren

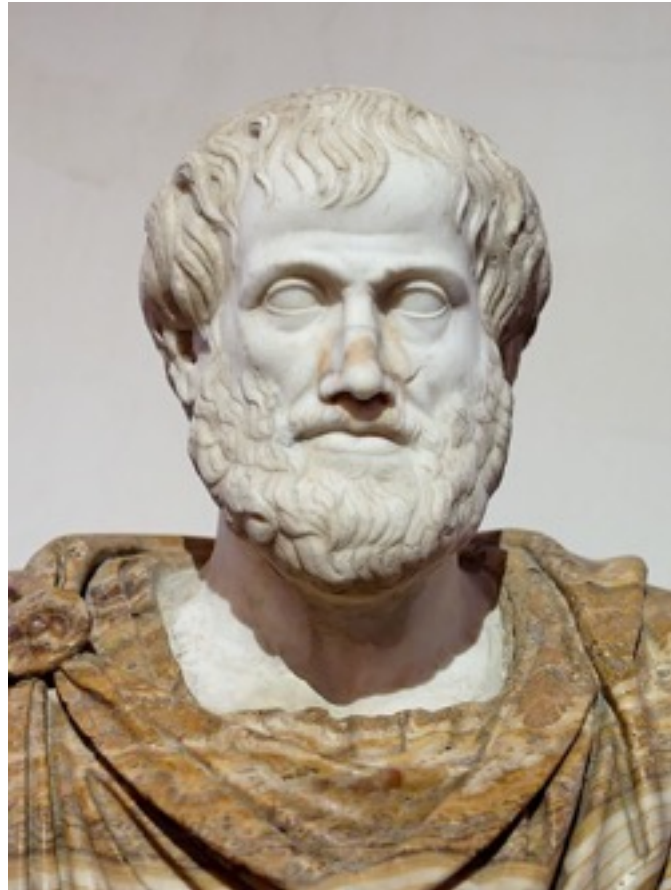
FALSE

But I am happy to be on his Team!

Probability as Extended Logic

Logic

Aristotle



Determines Truth/Falsity

Outcome: True/False

Probability

E. T. Jaynes



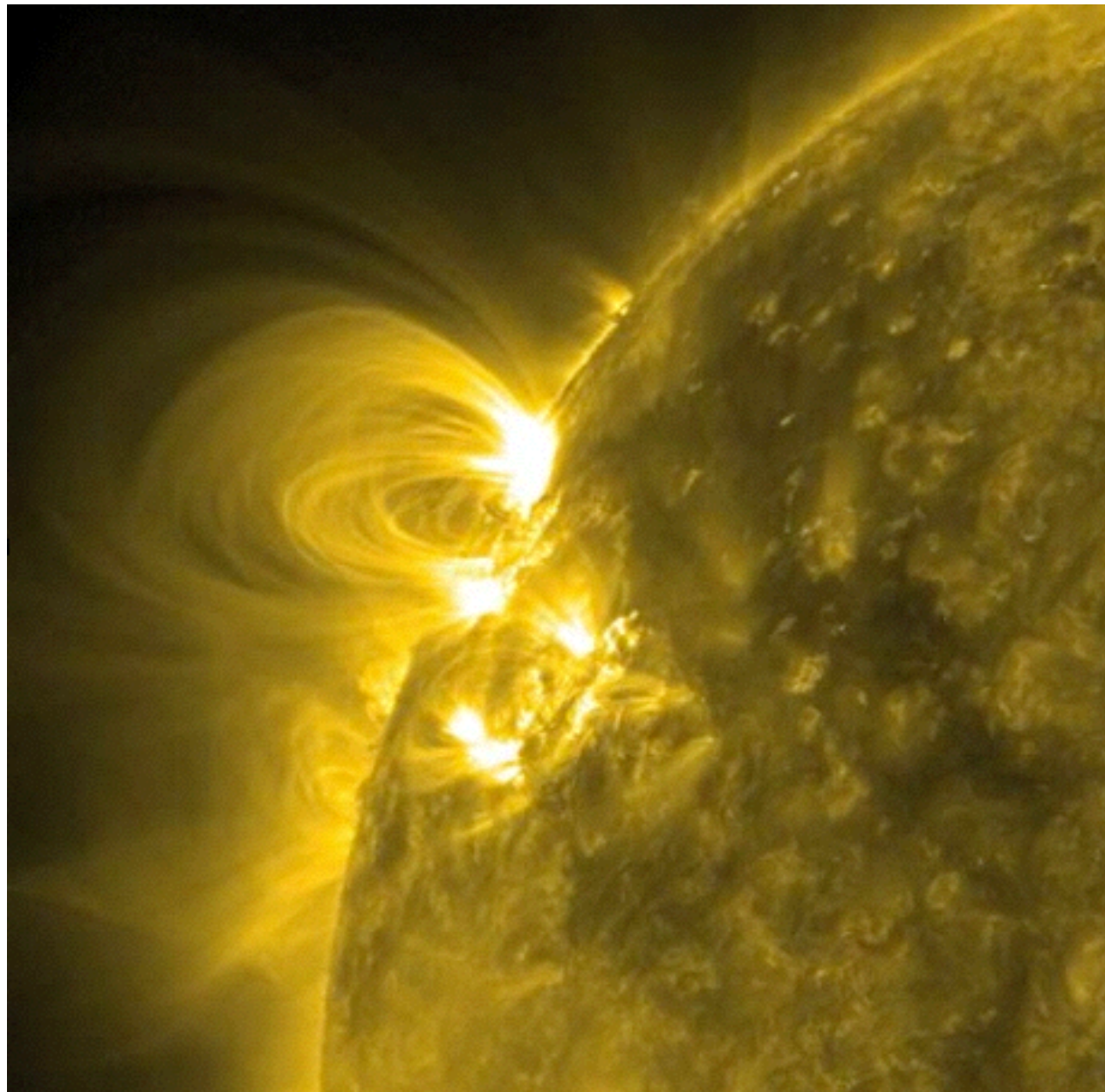
Quantifies Uncertainty

Outcome: Degree of Belief

Seismology of the Solar Atmosphere

Aim: determination of difficult to measure physical parameters in e.g.:

Coronal loops



Prominences



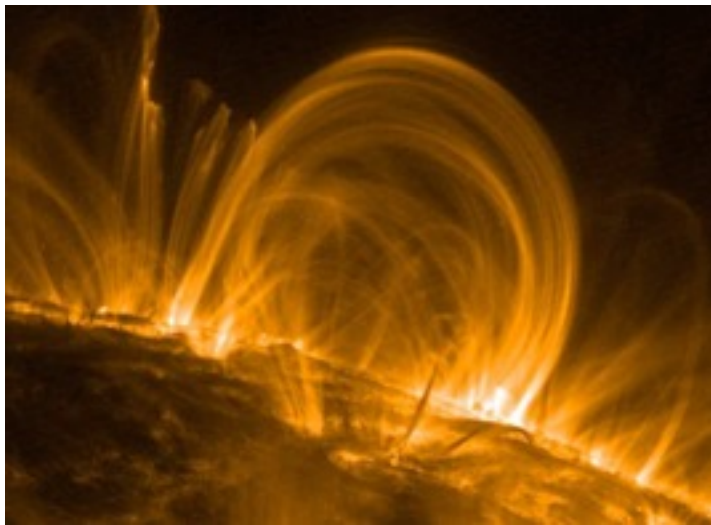
Combination of: { - Observations: Wave activity in the solar atmosphere
- Theory: MHD wave interpretation

Wave Activity - Observations

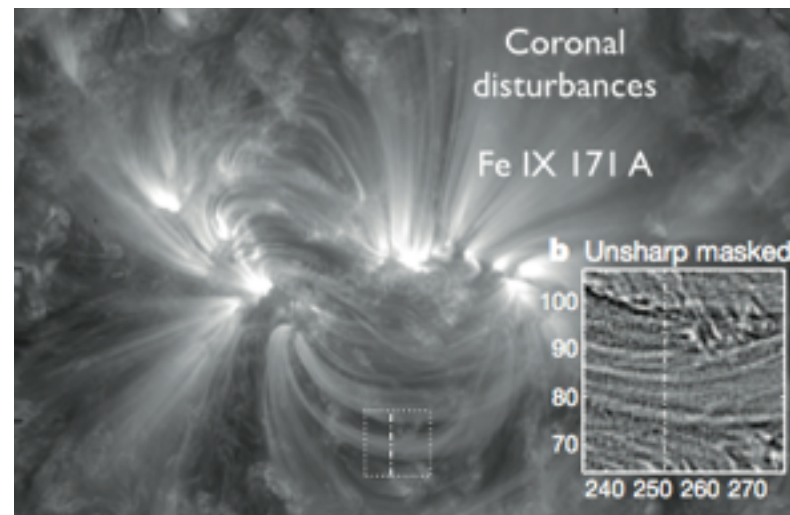
Rosenberg (70); Trotter+(79) ... Aschwanden+(99); Nakariakov+(99); De Pontieu+(07); Okamoto+(07); Cirtain+(07); McIntosh+(11); Kuridze+(13); Morton+(12,13,14); Threlfall+(13); Mathioudakis+(13)...

Existence of wave-like dynamics beyond question

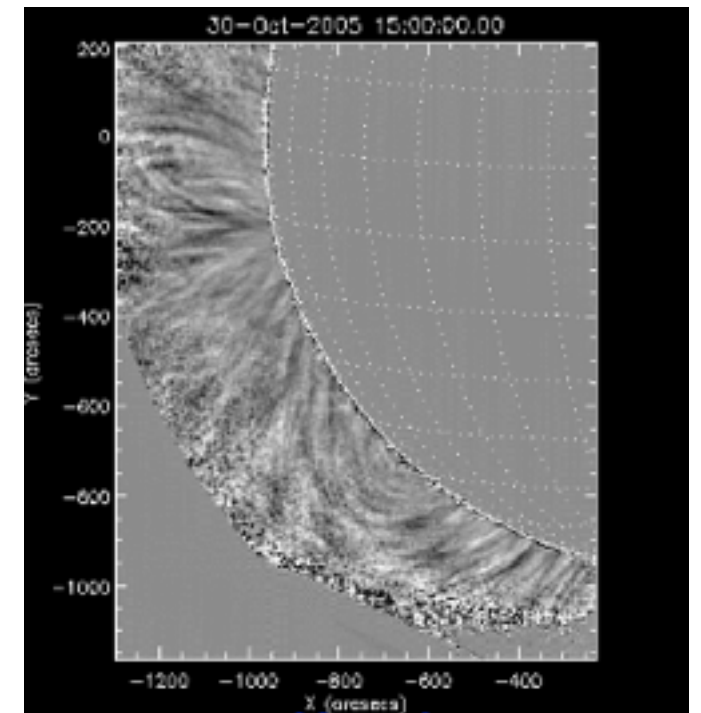
Coronal Loops



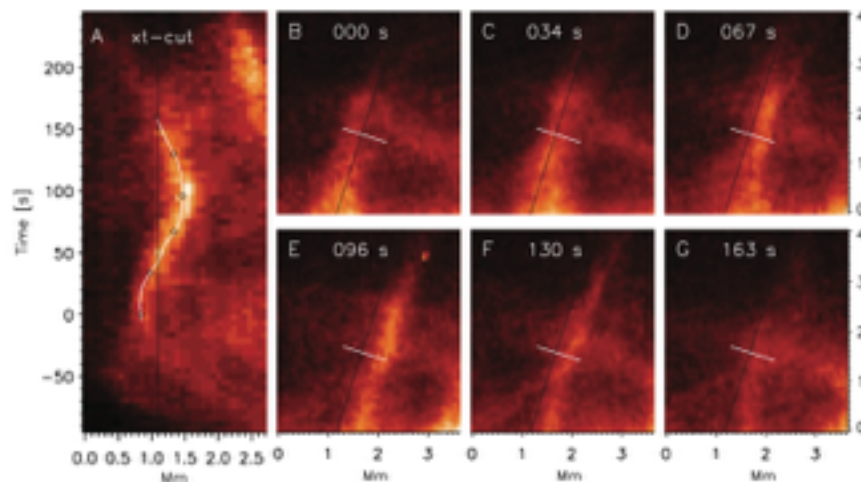
AR Corona



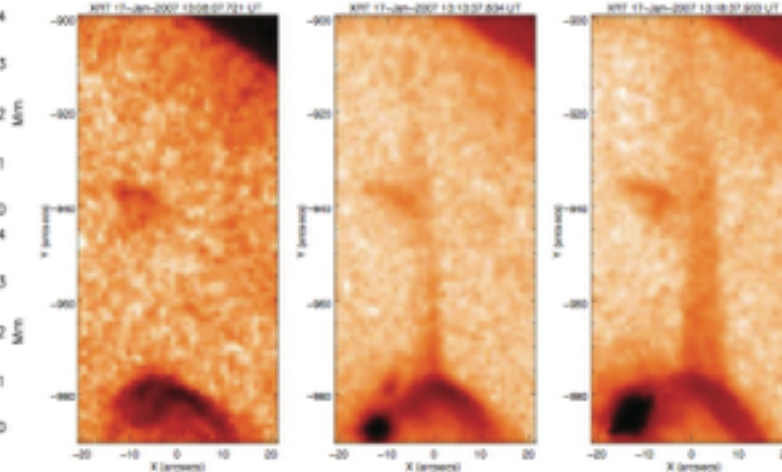
Extended Corona



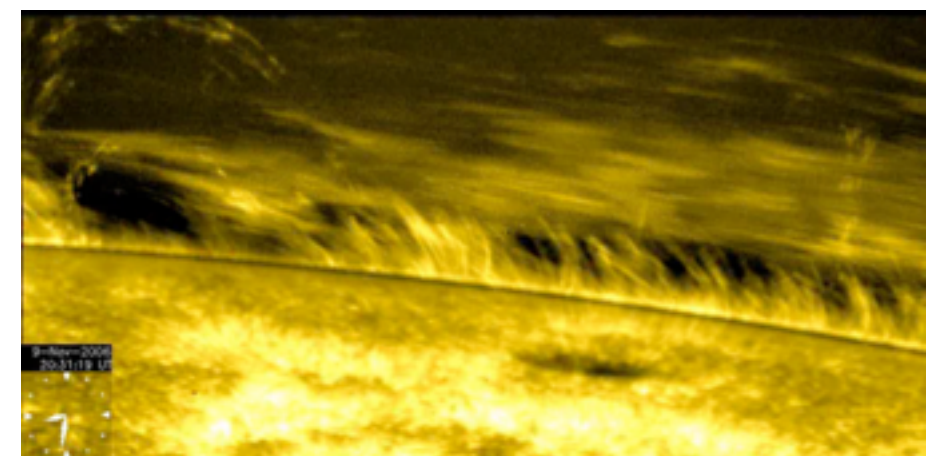
Chromospheric Spicules



X-ray Jets



Prominence plasmas

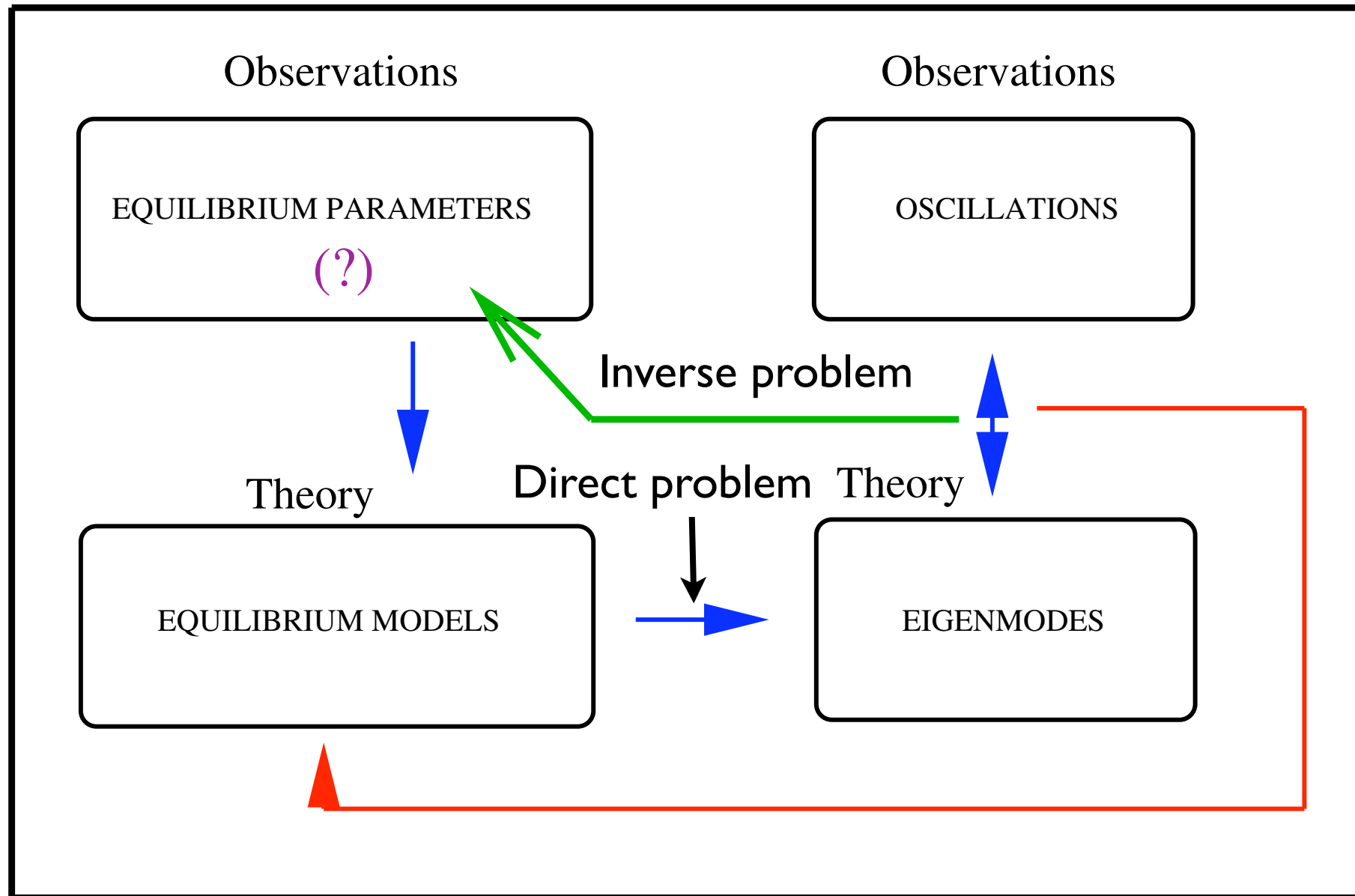


+ chromospheric bright points/mottles + coronal hole structures + filament threads...

Time/spatial variation of **spectral line properties** / **imaged emission**

SST, DST, CoMP, SoHO, TRACE, Hinode, STEREO, SDO, Hi-C, IRIS: **increased detail/coverage**

Method of MHD Seismology



A well established method to obtain information on properties of the solar atmospheric plasma and field

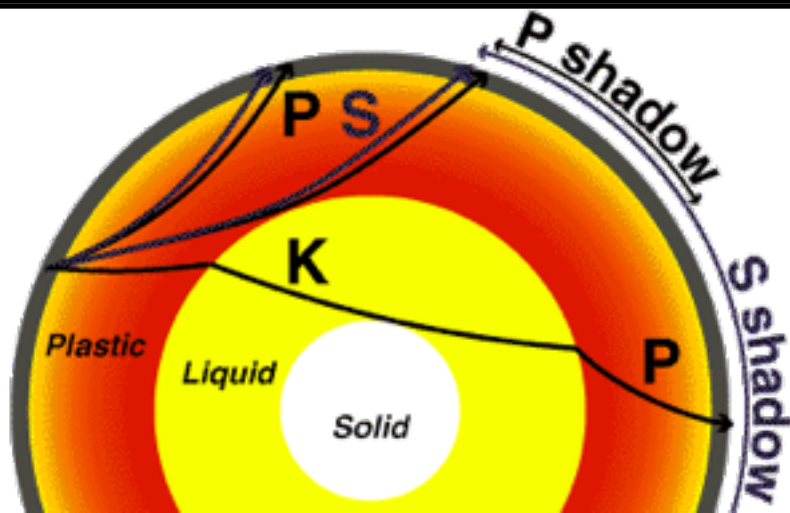
Determination of the magnetic field strength, coronal density scale height, density structuring along and cross coronal loops, etc.

other seismology techniques

↳ asteroseismology

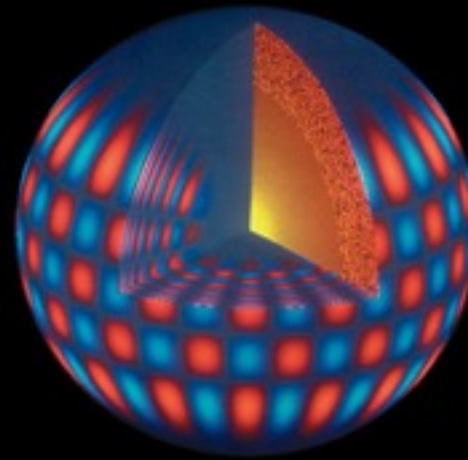
Geoseismology

Earth's interior, earthquakes and related phenomena



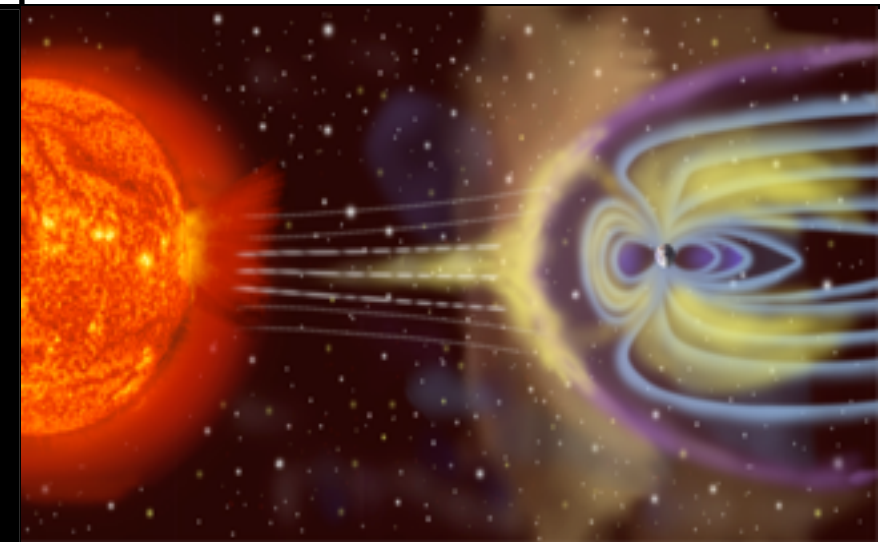
Helioseismology

The interior of the Sun using sound-gravity waves



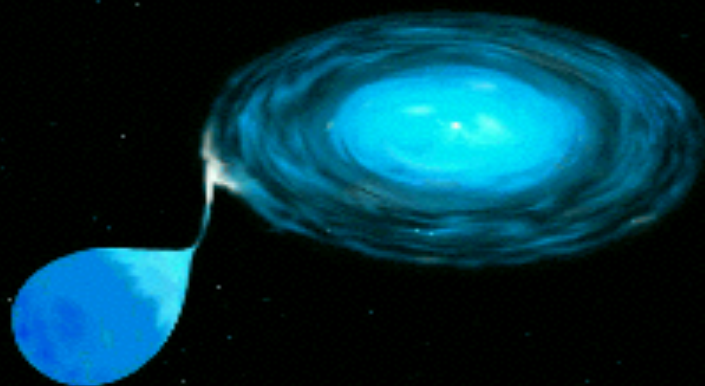
Magnetoseismology

Earth's magnetospheric plasmas

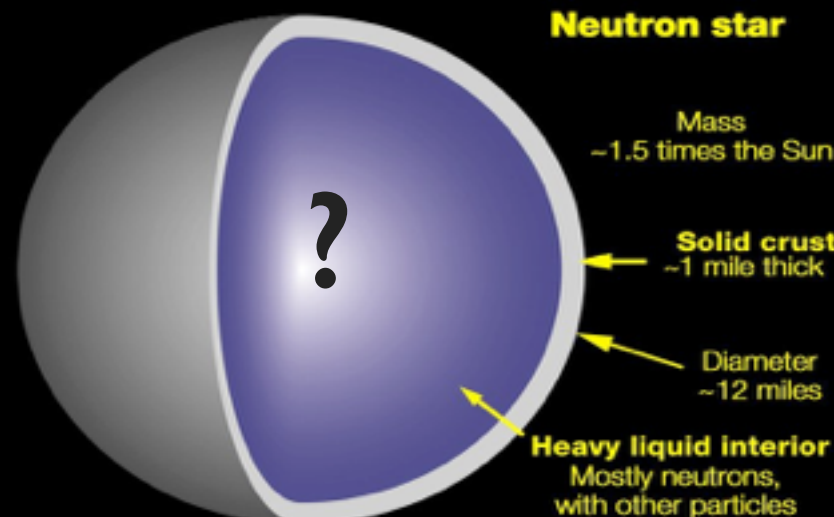


Disk seismology

Accretion disks around compact objects

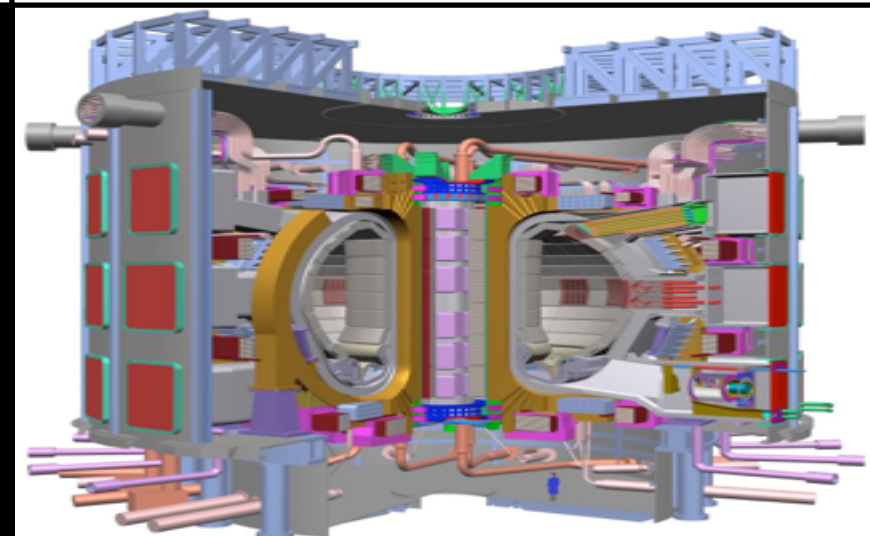


Neutron star seismology



Tokamaks

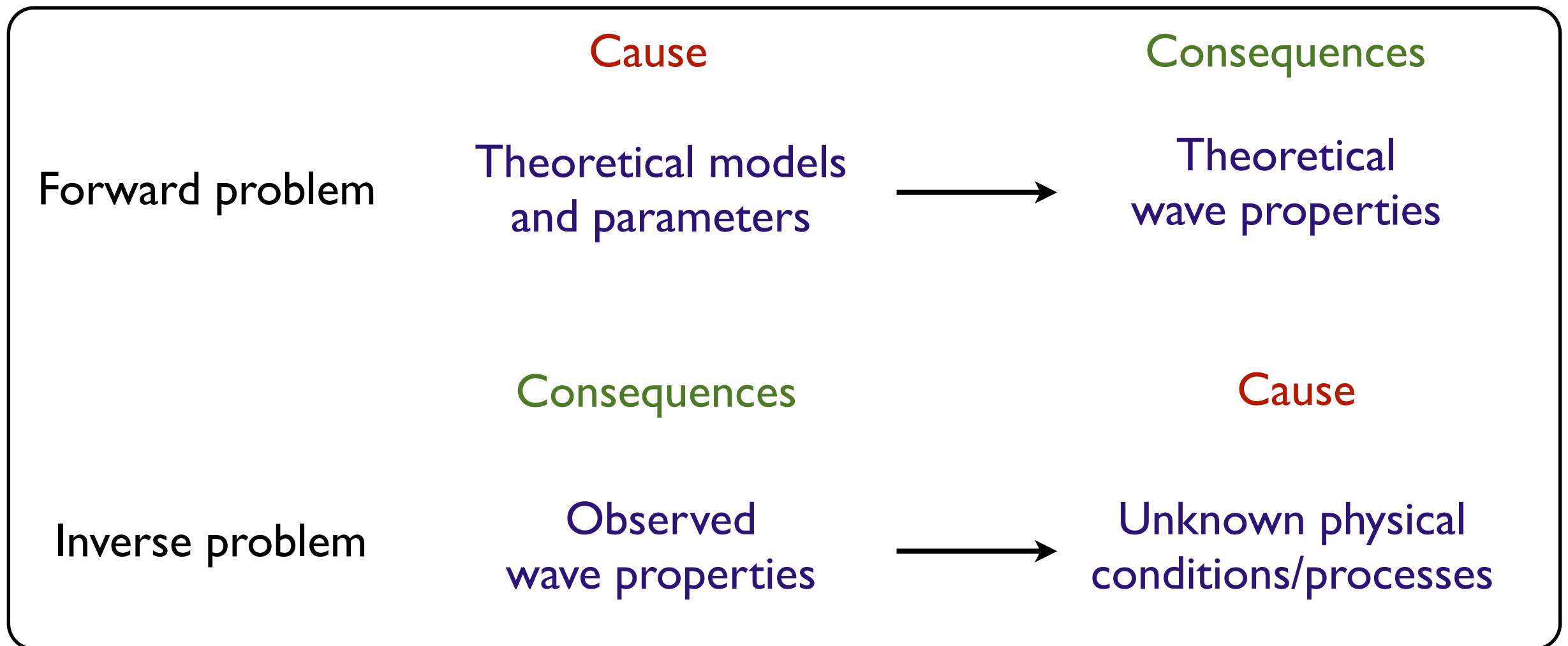
Laboratory/Fusion plasmas



From classic to Bayesian techniques

Confronting observations and theory to infer physical parameters is not an easy task

Seismology involves the solution of **two different problems**



Under conditions in which **information is incomplete and uncertain**

We use the rules of probability to make scientific inference and quantify uncertainty

A one-slide introduction to probability

What is probability: Probability quantifies randomness and uncertainty

What is statistics: Statistics uses probability to make scientific inferences

Use of probability: There are two main schools / lines of thought / religions

	They calculate probabilities of different things!	
	Frequentists Measure frequencies	Bayesians Measure informed belief
Interpretation of probability	Long-run relative frequency in the limit of infinite repetitions	Measure of degree to which a given proposition is supported by data
Focus on	Alternative data: compare probs. of different data realizations	Alternative hypotheses: compare probs. of different hypotheses in view of data
Useful for	Counting Characterizing data	Inference and model comparison

Astrophysics observational science > data are fixed!

The Bayesian framework defines rigorous tools to perform inference and model comparison by looking at how data constrain parameters/models

We cannot state that something is true/false in the solar atmosphere

We just try to quantify what to believe

And accept that as the best we can do



Bayesian Data Analysis

Probabilistic Inference considers the inversion problem as the task of estimating the degree of belief in statements about parameter values/model evidence

Bayes' Rule (Bayes & Price 1763)

$$p(\boldsymbol{\theta} | D, M) = \frac{p(D | \boldsymbol{\theta}, M) p(\boldsymbol{\theta} | M)}{\int d\boldsymbol{\theta} p(D | \boldsymbol{\theta}, M) p(\boldsymbol{\theta} | M)}$$

$p(\boldsymbol{\theta} D, M)$	Posterior
$p(\boldsymbol{\theta} M)$	Prior
$p(D \boldsymbol{\theta}, M)$	Likelihood function
$\int d\boldsymbol{\theta} p(D \boldsymbol{\theta}, M) p(\boldsymbol{\theta} M)$	Evidence

State of knowledge is a combination of what is known a priori independently of data and the likelihood of obtaining a data realisation actually observed as a function of the parameter vector

Parameter Inference

Compute posterior for different combinations of parameters

Marginalise

$$p(\theta_i | d) = \int p(\boldsymbol{\theta} | d) d\theta_1 \dots d\theta_{i-1} d\theta_{i+1} \dots d\theta_N$$

Model Comparison

Compare one model against other

Posterior ratios

$$\frac{p(M_i | d)}{p(M_j | d)} = \frac{p(d | M_i) p(M_i)}{p(d | M_j) p(M_j)}$$

Model Averaging

Posteriors weighted with model evidence

Weighted posterior

$$p(\boldsymbol{\theta} | d) = \sum_{i=1}^N p(\boldsymbol{\theta} | d, M_i) p(M_i | d)$$

List of Applications and Methodologies

APPLICATIONS

Inference of physical parameters in coronal waveguides from observed damped transverse oscillations

Inference of cross-field density structure from damped transverse oscillations

Inference of coronal density scale height and coronal magnetic expansion and comparison between stratified and magnetically non-uniform models

Model comparison for the density structure along and across coronal waveguides

METHODS

Markov Chain Monte Carlo sampling of the posterior

Computation of marginal posteriors from integrals

Computation of marginal likelihood to assess model plausibility

Computation of Bayes factors to assess relative model plausibility

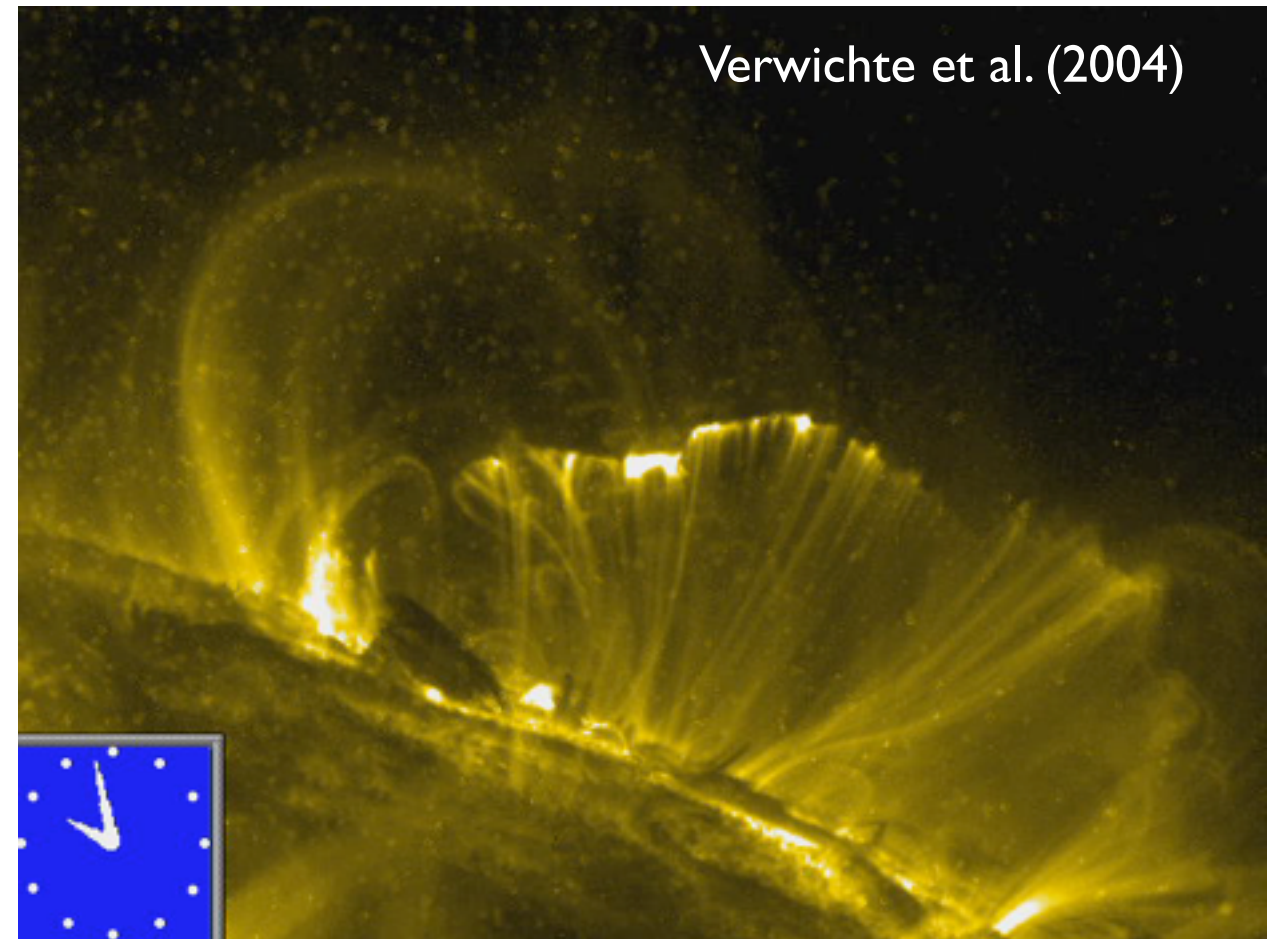
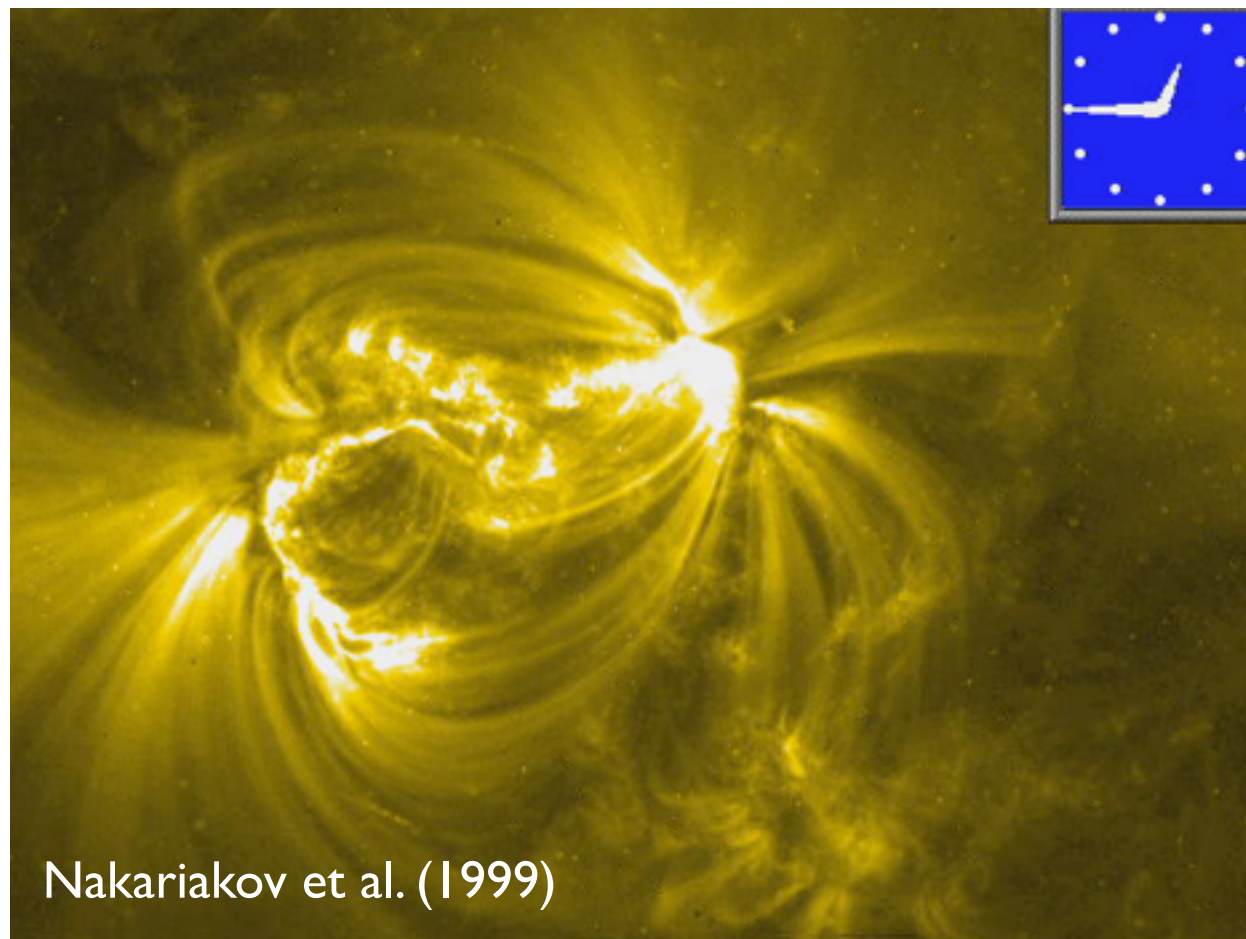
Computation of weighted posterior to perform model averaging

Example #1

Inference of coronal loop parameters from
observations of transverse oscillations

Coronal loop oscillations

Aschwanden et al. (1999); Nakariakov et al. (1999); Aschwanden et al. (2002); Schrijver et al. (2002), Verwichte et al. (2004) ... White & Verwichte (2012)



Periods ~ 2-11 mins

Damping times ~ 3-21 mins

- Transverse standing MHD kink mode of a magnetic flux tube - lateral displacement of the tube (Nakariakov99)- Multiple harmonics (Verwichte04)
- Resonant damping - coupling of global motion to local Alfvén waves (Hollweg & Yang88; Goossens02)

Classic inversion - ID density enhancements

Forward problem

- Thin tube approximation for the period (Edwin & Roberts 1983)

$$P = \tau_{\text{Ai}} \sqrt{2} \left(\frac{\zeta + 1}{\zeta} \right)^{1/2}$$

- Thin boundary approximation for the damping (Goossens et al. 1992; Ruderman & Roberts 2002)

$$\frac{\tau_{\text{d}}}{P} = \frac{2}{\pi} \frac{\zeta + 1}{\zeta - 1} \frac{1}{l/R}$$

Inverse problem

$$P(\zeta, l/R, \tau_{\text{Ai}}) = P_{\text{obs}}$$

$$\frac{\tau_{\text{d}}}{P}(\zeta, l/R) = \left(\frac{\tau_{\text{d}}}{P} \right)_{\text{obs}}$$

3 parameters $(\zeta, l/R, \tau_{\text{Ai}})$

2 observables $(P, \tau_{\text{d}}/P)$

- Observed periods and damping times can be reproduced **by infinite number of models**
- But **they must follow a particular ID solution space** (Arregui et al. 2007)

Inversion in coronal loops

Analytic/numerical inversion schemes

Arregui et al. (2007); Goossens, Arregui, Ballester, Wang (2008)

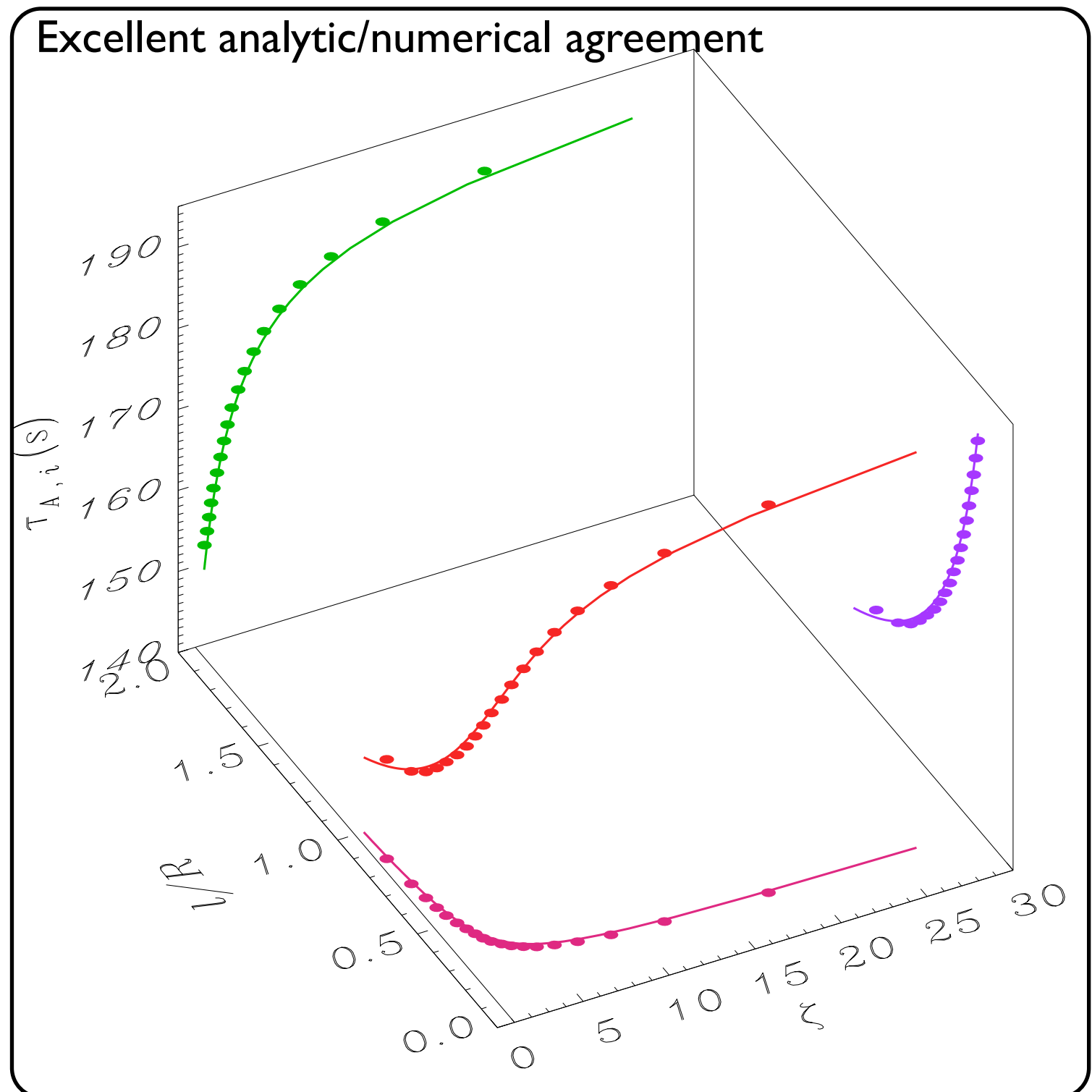
Alfvén speed constrained to a narrow range

Advantages

- No assumption on particular values for parameters
- General solution from which limiting cases can be studied

Limitations

- Infinite number of equally valid solutions
- No clear way to propagate errors from observations to inferred quantities



Bayesian inversion

Arregui & Asensio Ramos (2011, ApJ 740 44)

Prior information

Density contrast:

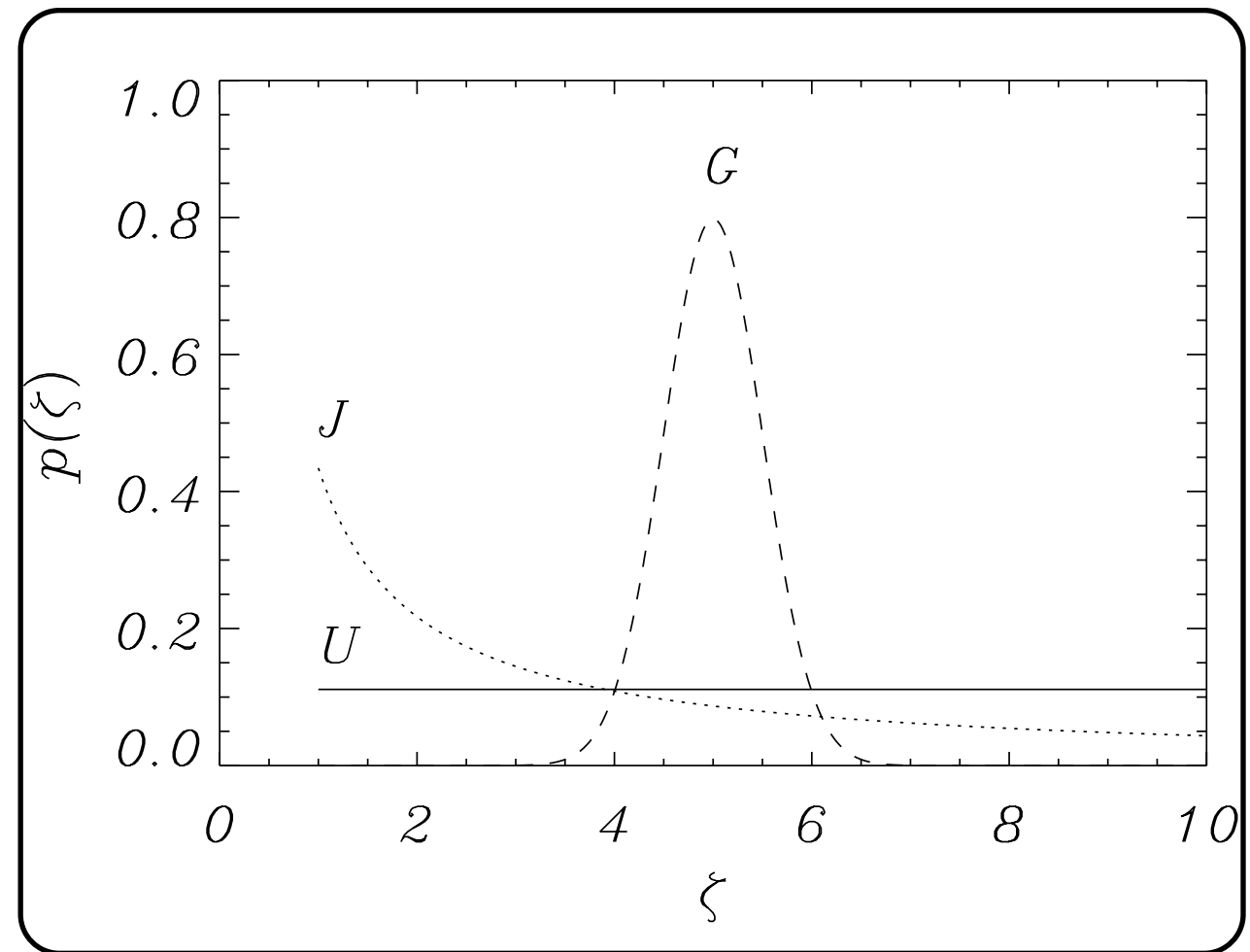
3 different options

Inhomogeneity length-scale:

Uniform in range 0-2

Alfvén travel time:

Uniform in range determined by period



Likelihood function

$$p(d|\boldsymbol{\theta}) = (2\pi\sigma_P\sigma_\tau)^{-1} \exp \left\{ \frac{[P - P^{\text{syn}}(\boldsymbol{\theta})]^2}{2\sigma_P^2} + \frac{[\tau_d - \tau_d^{\text{syn}}(\boldsymbol{\theta})]^2}{2\sigma_\tau^2} \right\}$$

Synthetic data from
forward problem

 σ_P^2
 σ_τ^2

Variances associated to
period and damping time

Optimal results are obtained with density information

Suppose we have some information on densities

Arregui & Asensio Ramos (2011)

$$P = 232 \text{ s}$$

$$\tau_d/P = 3.8$$

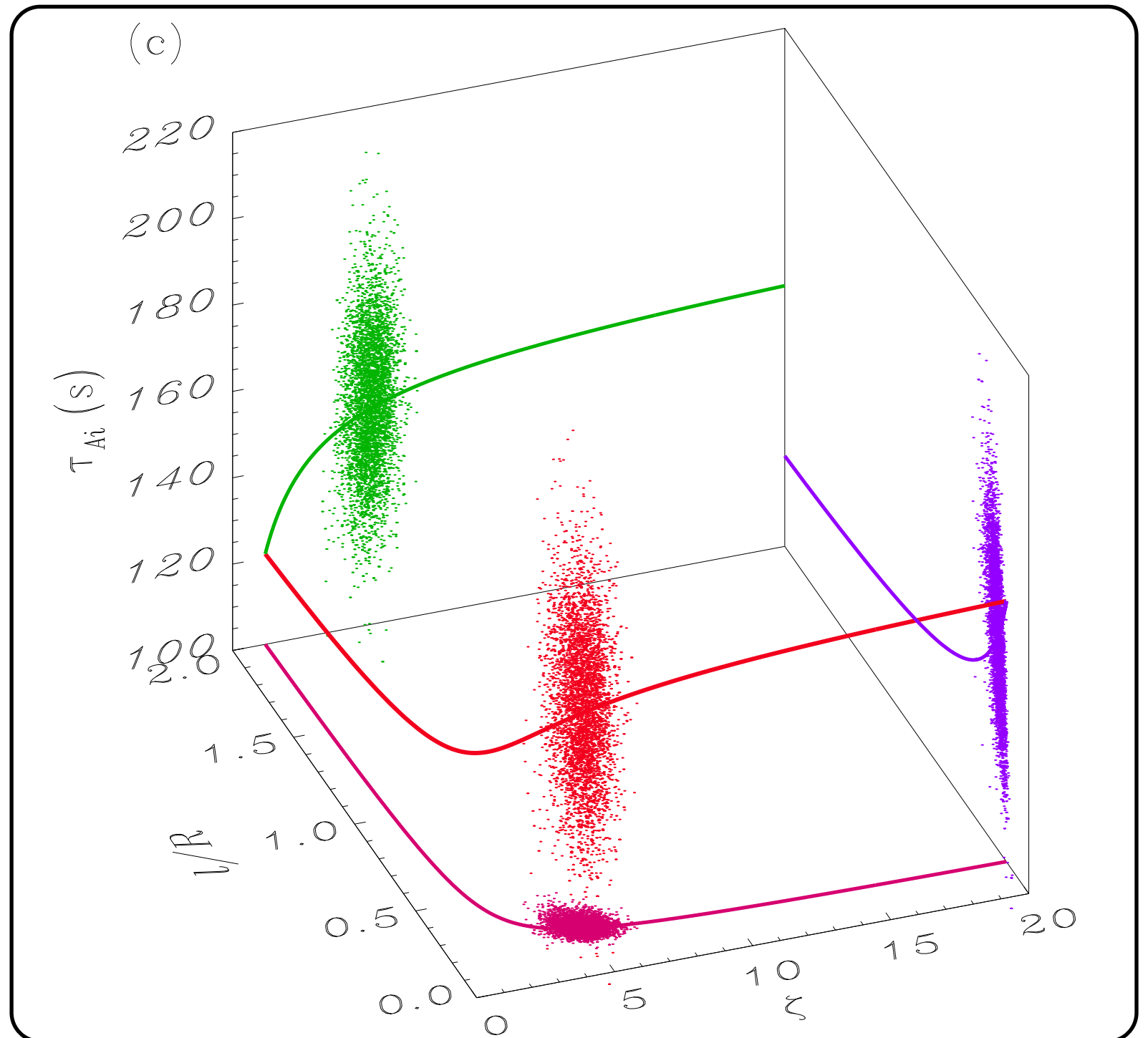
Prior information

Density contrast:
Gaussian centered
in $\zeta = 5$ $\sigma_\zeta = 0.1\zeta$

Inhomogeneity
Uniform in $l/R \in [0 - 2]$

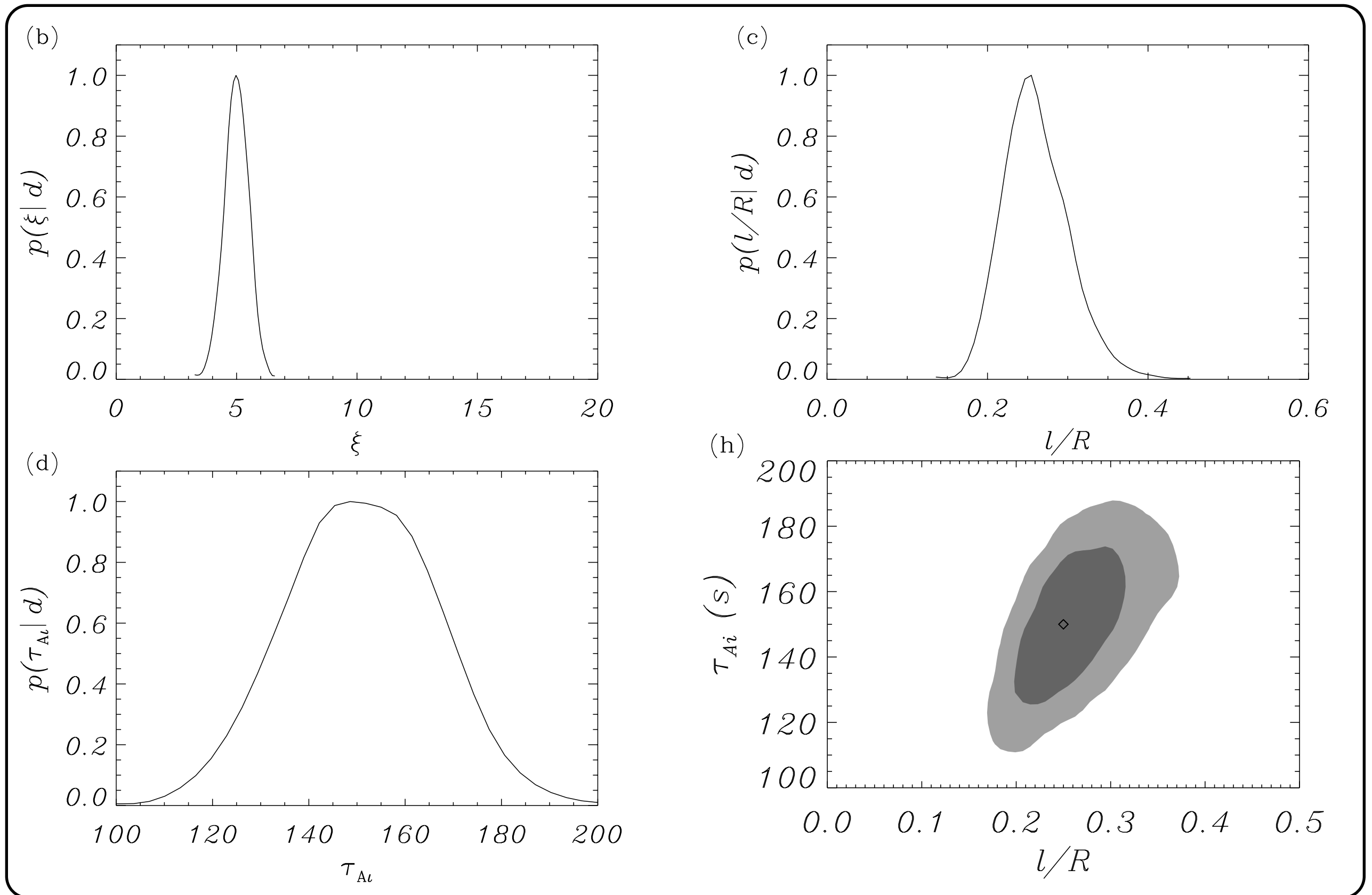
Alfvén travel time
Uniform in $\tau_{Ai} \in [1 - 400]$

**Data is able to
constrain the problem**



Marginal posteriors

All parameters of interest **fully constrained** when info on density inserted



Application to I I loop oscillation events

Table 2. Analytic (A) and Bayesian (B) inversion results for the analyzed loop oscillation events.

Oscillation properties				Inversion results					
				Analytic	Bayesian <small>Jeffreys</small>			Bayesian <small>Gaussian</small> 	
#	P (s)	τ_d (s)	P/τ_d	τ_{Ai} (s)	τ_{Ai} (s)	l/R	τ_{Ai} (s)	l/R	ζ
1	261	870	0.30	145–177	$161.5^{+22.2}_{-19.7}$	$0.36^{+0.27}_{-0.13}$	$169.4^{+17.4}_{-16.9}$	$0.30^{+0.05}_{-0.04}$	$4.99^{+0.50}_{-0.50}$
2	265	300	0.88	163–182	$169.9^{+20.9}_{-21.4}$	$0.92^{+0.47}_{-0.25}$	$167.1^{+17.4}_{-16.9}$	$1.01^{+0.19}_{-0.16}$	$3.76^{+0.64}_{-0.61}$
3	316	500	0.63	189–217	$199.4^{+25.0}_{-24.5}$	$0.76^{+0.61}_{-0.28}$	$196.8^{+17.4}_{-16.9}$	$0.77^{+0.43}_{-0.19}$	$3.53^{+1.88}_{-1.42}$
4	277	400	0.69	168–189	$176.2^{+22.7}_{-22.7}$	$0.73^{+0.53}_{-0.22}$	$167.2^{+17.4}_{-16.9}$	$1.05^{+0.43}_{-0.28}$	$2.56^{+0.98}_{-0.69}$
5	272	849	0.32	151–187	$173.2^{+21.1}_{-22.4}$	$0.34^{+0.26}_{-0.11}$	$159.7^{+17.4}_{-16.9}$	$0.58^{+0.47}_{-0.17}$	$2.18^{+0.75}_{-0.62}$
6	522	1200	0.44	304–359	$329.7^{+43.08}_{-43.8}$	$0.49^{+0.39}_{-0.16}$	$319.9^{+17.4}_{-16.9}$	$0.59^{+0.25}_{-0.13}$	$2.97^{+0.94}_{-0.91}$
7	435	600	0.73	267–299	$281.3^{+33.1}_{-35.4}$	$0.74^{+0.41}_{-0.20}$	$290.9^{+17.4}_{-16.9}$	$0.64^{+0.11}_{-0.09}$	$6.98^{+1.0}_{-1.0}$
8	143	200	0.72	90–98	$90.9^{+12.0}_{-11.4}$	$0.76^{+0.53}_{-0.23}$	$93.8^{+17.4}_{-16.9}$	$0.69^{+0.11}_{-0.10}$	$5.55^{+0.94}_{-0.96}$
9	423	800	0.53	247–291	$265.6^{+35.2}_{-33.0}$	$0.64^{+0.68}_{-0.25}$	$290.5^{+17.4}_{-16.9}$	$0.41^{+0.07}_{-0.06}$	$13.4^{+3.5}_{-3.8}$
10	185	200	0.93	117–126	$119.2^{+14.8}_{-14.8}$	$0.94^{+0.48}_{-0.26}$	$114.4^{+17.4}_{-16.9}$	$1.21^{+0.24}_{-0.20}$	$3.08^{+0.43}_{-0.44}$
11	390	400	0.98	245–270	$250.5^{+29.6}_{-22.7}$	$0.99^{+0.54}_{-0.28}$	$221.5^{+17.4}_{-16.9}$	$1.69^{+0.17}_{-0.25}$	$2.10^{+0.29}_{-0.23}$

 Inversions with Gaussian prior use contrast estimates by Aschwanden et al. (2003)

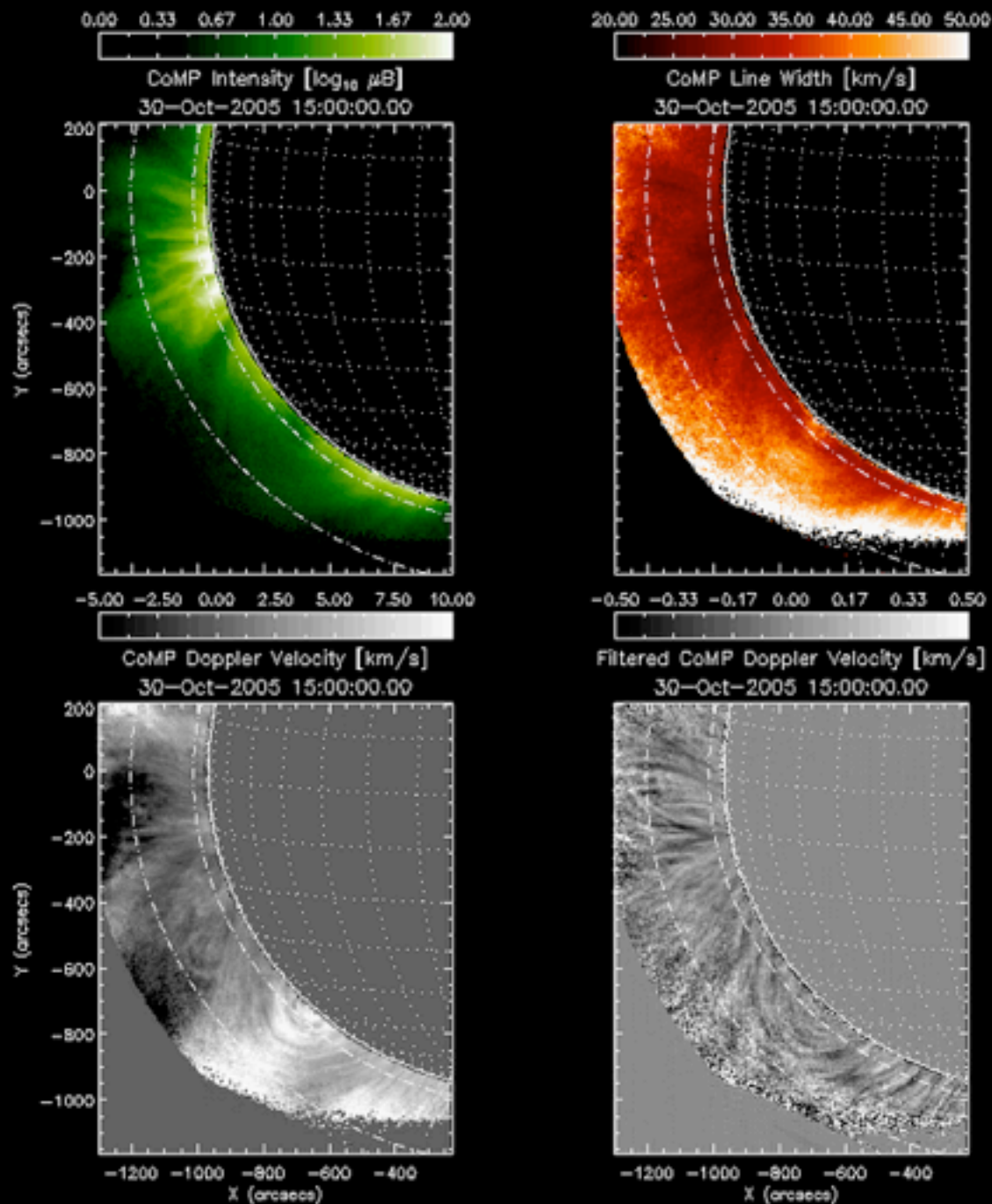
Example #2

Inference of cross-field density structuring
from observations with multiple damping
regimes in propagating coronal waves

Spatially damped transverse coronal waves

Coronal waves

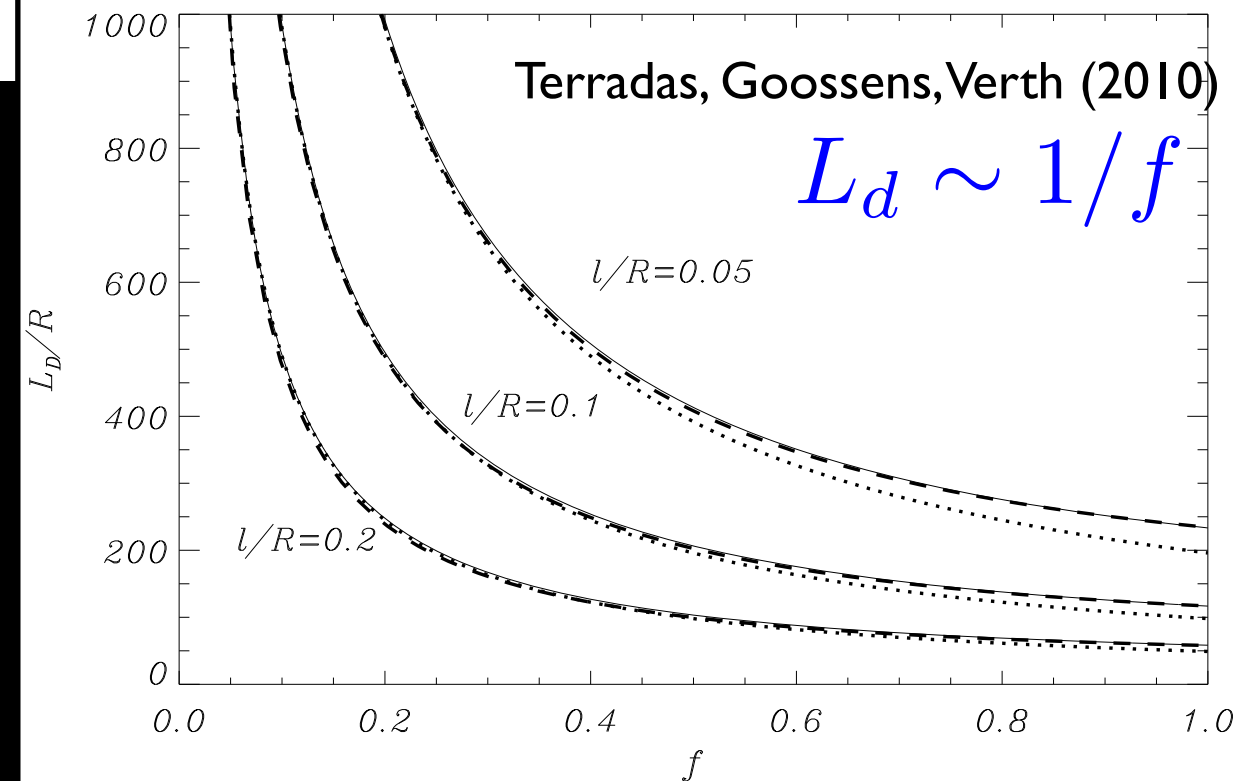
Tomczyk et al. (2007); Tomczyk & McIntosh (2009)



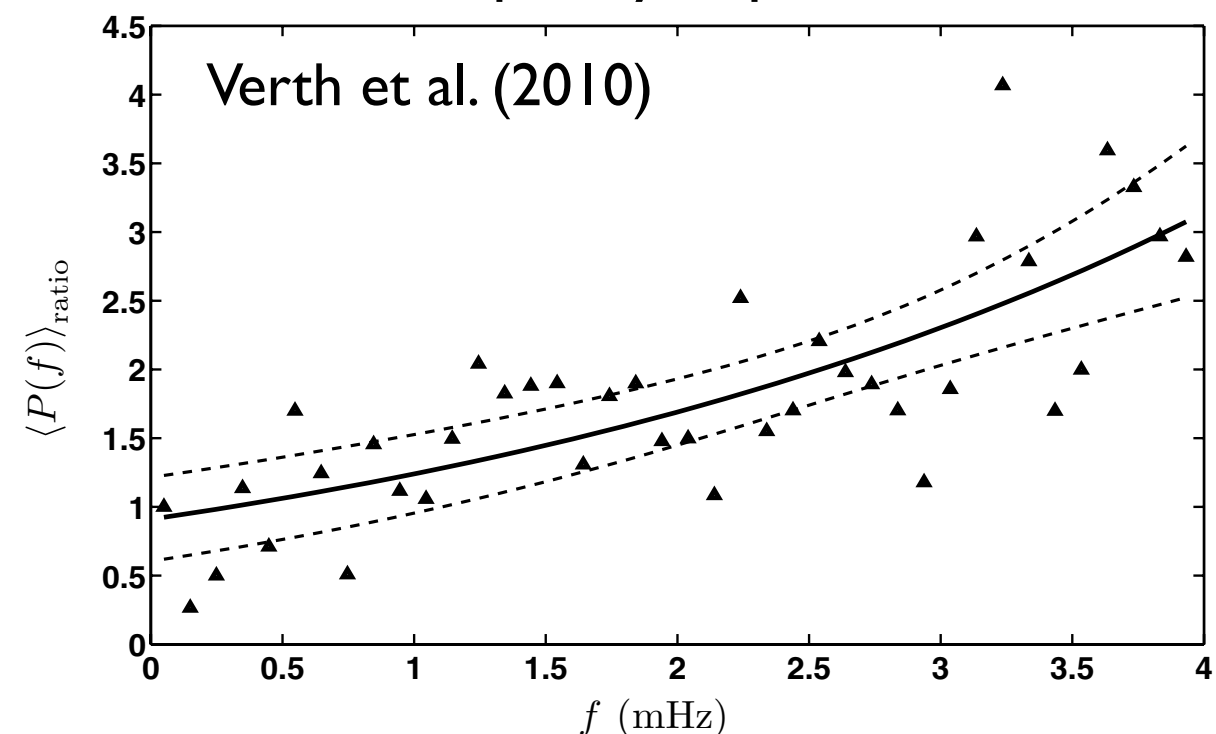
Different inward/outward power

Resonant absorption favours low-f waves

Selective spatial damping



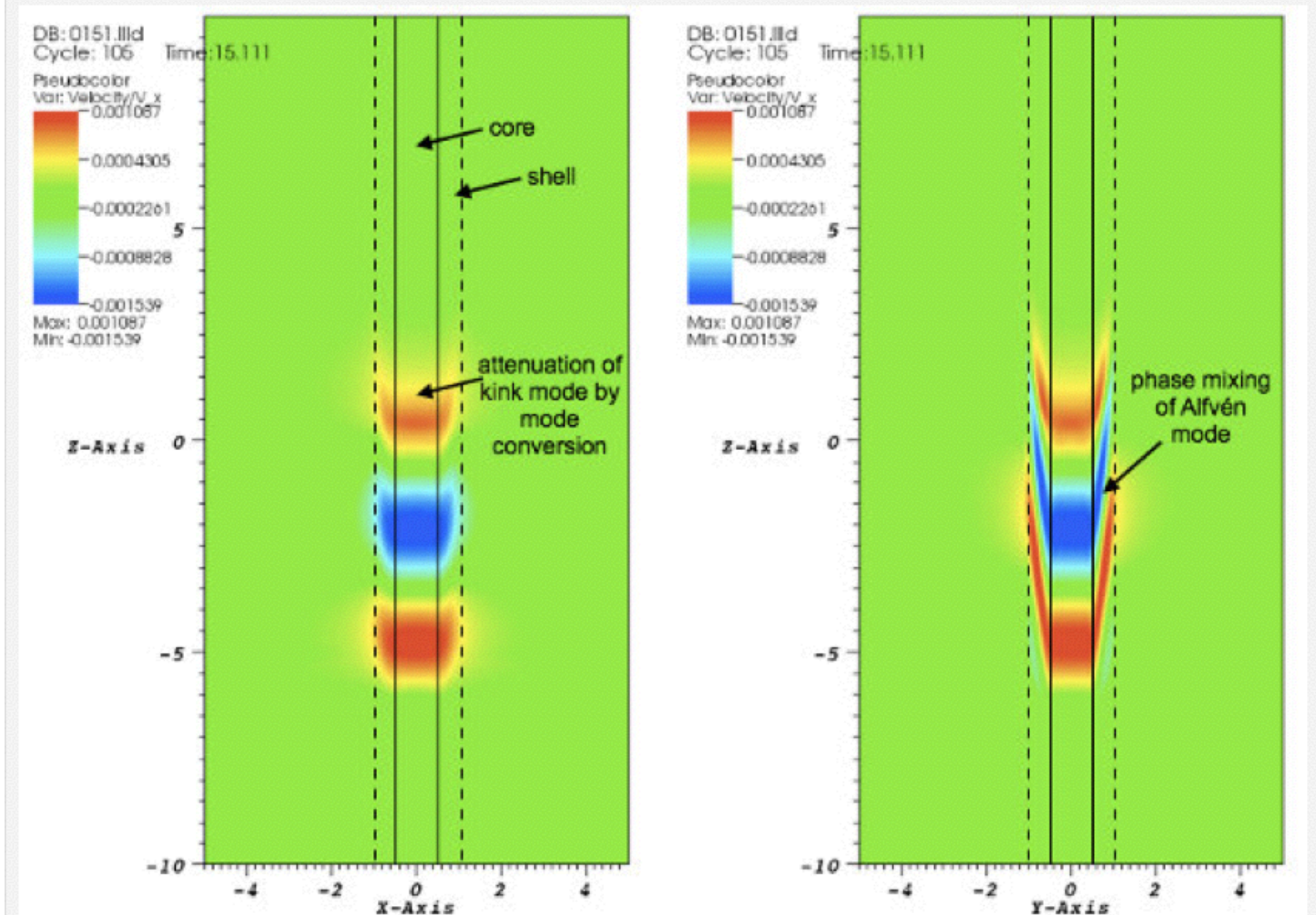
Frequency dependence



Spatial damping of propagating kink waves

Terradas Goossens & Verth (2010) see also Soler et al. (2011a,b) Pascoe, Wright, De Moortel (2010)

For propagating transverse kink waves resonant absorption produces **spatial damping**



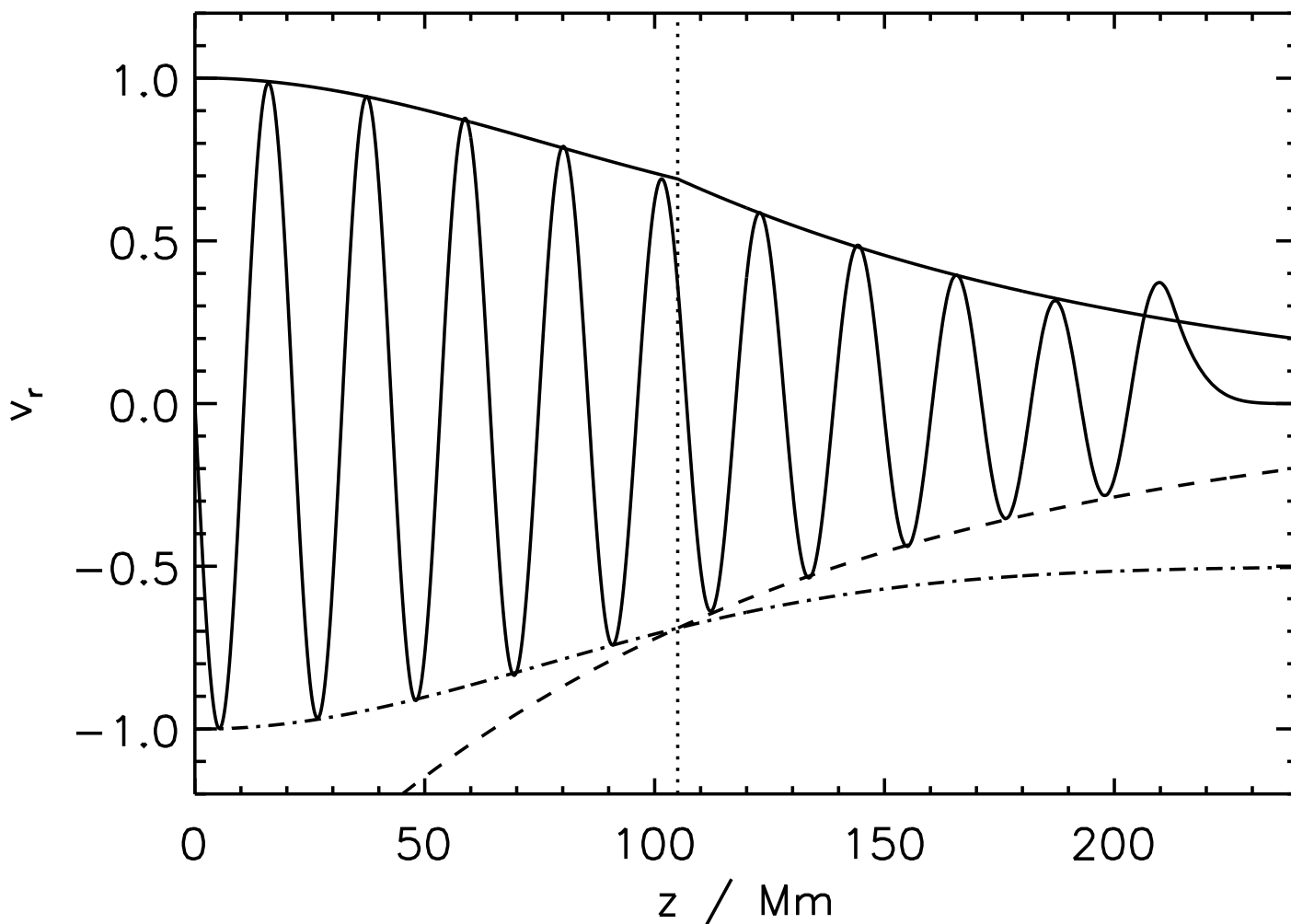
Two damping regimes

Pascoe et al. (2010, 2011, 2012, 2013)

Hood et al. (2013)

Ruderman & Terradas (2013)

The decay of resonantly damped kink oscillations shows 2 distinct regimes:
Initial Gaussian decay + subsequent exponential damping



Gaussian damping

$$\frac{L_g}{\lambda} = \left(\frac{2}{\pi}\right) \left(\frac{R}{l}\right)^{1/2} \left(\frac{\zeta + 1}{\zeta - 1}\right)$$

Exponential damping

$$\frac{L_d}{\lambda} = \left(\frac{2}{\pi}\right)^2 \left(\frac{R}{l}\right) \left(\frac{\zeta + 1}{\zeta - 1}\right)$$

Regime change at location

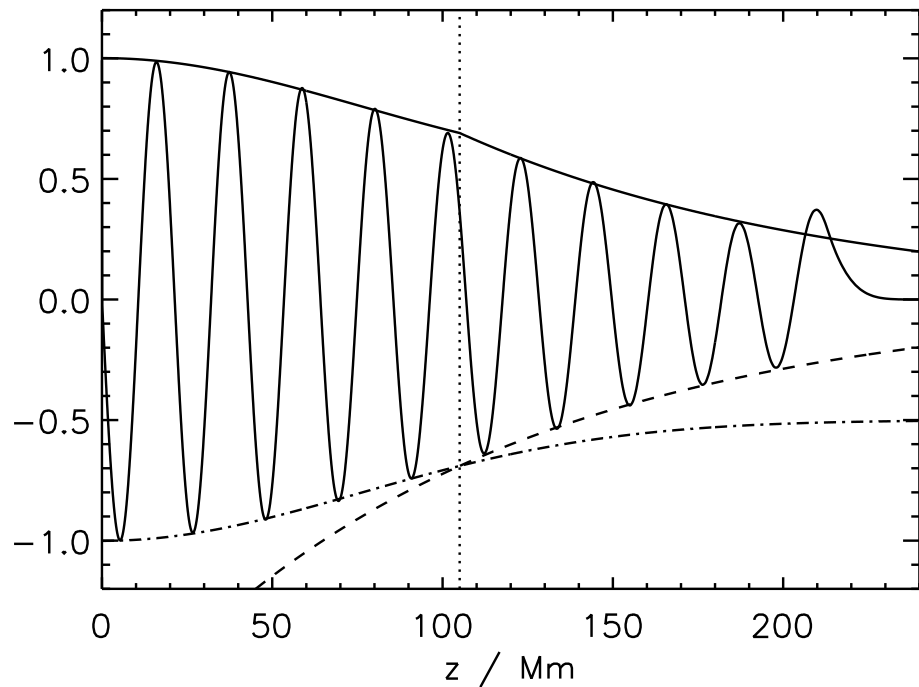
$$h = \frac{L_g^2}{L_d} = \lambda \left(\frac{\zeta + 1}{\zeta - 1}\right)$$

Additional information without the need to include new parameters

Bayesian inference with propagating waves

Arregui, Asensio Ramos, Pascoe (2013, ApJL submitted)

Inversion of density contrast and transverse inhomogeneity length scale using Gaussian damping length and height of change of damping regime as data



Generate synthetic data using analytical forward model

$$\frac{L_g}{\lambda} = \left(\frac{2}{\pi}\right) \left(\frac{R}{l}\right)^{1/2} \left(\frac{\zeta + 1}{\zeta - 1}\right) \quad h = \frac{L_g^2}{L_d} = \lambda \left(\frac{\zeta + 1}{\zeta - 1}\right)$$

Parameter space

$$\zeta = 1.5, 2, 3, 4 \text{ and } l/R = 0.05, 0.15, 0.2, 0.4$$

Likelihood + uniform priors for contrast and length scale

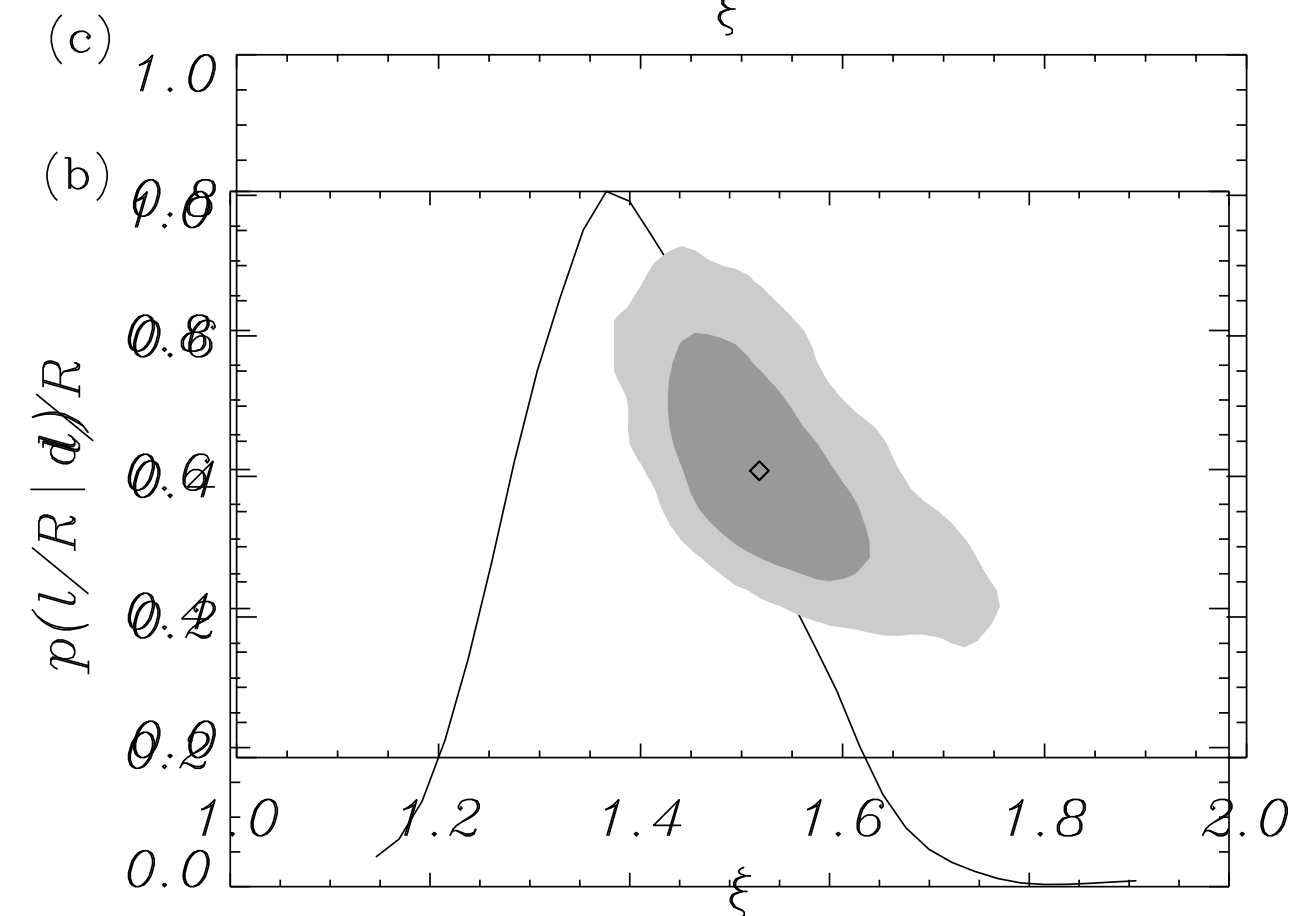
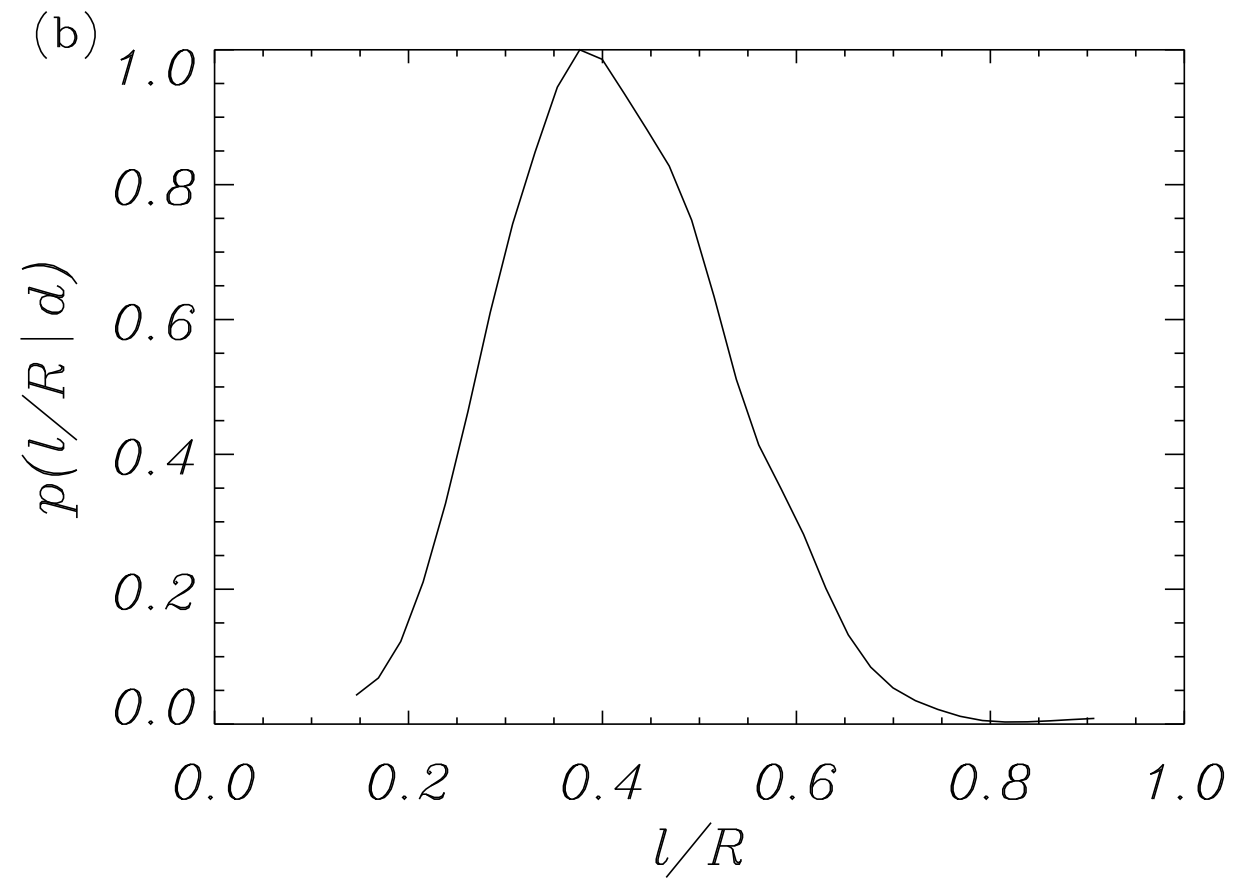
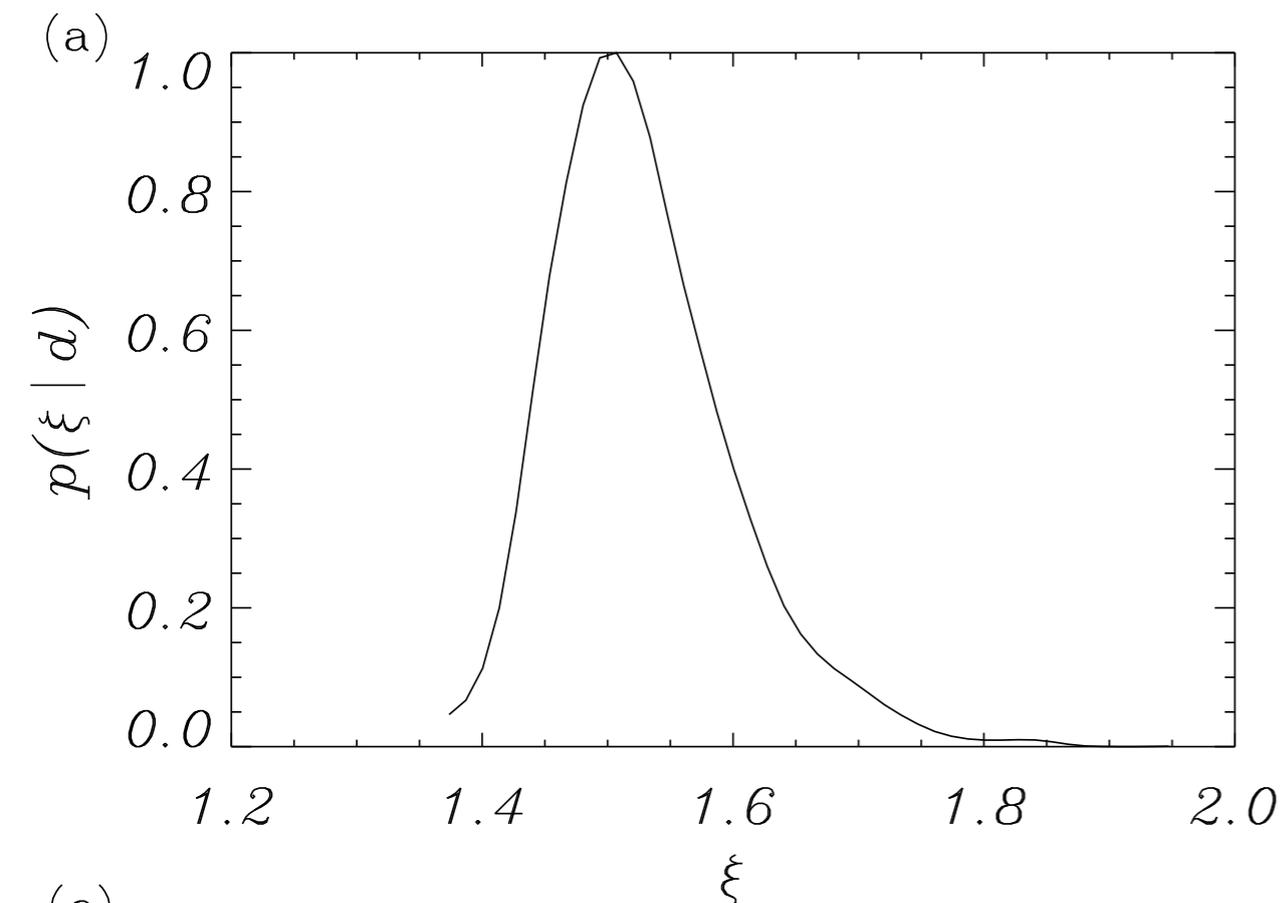
$$p(d|\theta) = (2\pi\sigma_{L_g}\sigma_h)^{-1} \exp \left\{ -\frac{[L_g - L_g^{\text{syn}}(\theta)]^2}{2\sigma_{L_g}^2} - \frac{[h - h^{\text{syn}}(\theta)]^2}{2\sigma_h^2} \right\} \quad p(\theta_i) = \frac{1}{\theta_i^{\text{max}} - \theta_i^{\text{min}}} \text{ for } \theta_i^{\text{min}} \leq \theta \leq \theta_i^{\text{max}}$$

Use Bayes' rule and marginalise

$$p(\theta|D, M) = \frac{p(D|\theta, M)p(\theta|M)}{\int d\theta p(D|\theta, M)p(\theta|M)}$$

$$p(\theta_i|d) = \int p(\theta|d) d\theta_1 \dots d\theta_{i-1} d\theta_{i+1} \dots d\theta_N$$

Inversion result - example



The existence of two damping regimes enables us to constrain the two parameters of interest

They fully determine the cross-field density structuring

Inversion results

Inversion with analytical forward model

Inversion with numerical simulation

Table 1. Inversion of Synthetic Data Using the Analytical Forward Model

Synthetic Parameters		Synthetic Data		Inversion Results	
ζ	l/R	L_g/λ	h/λ	ζ	l/R
1.5	0.05	14.2	5.0	1.51 ^{+0.08} _{-0.06}	0.05 ^{+0.02} _{-0.01}
1.5	0.15	8.2	5.0	1.50 ^{+0.07} _{-0.06}	0.16 ^{+0.05} _{-0.04}
1.5	0.2	7.1	5.0	1.51 ^{+0.07} _{-0.06}	0.21 ^{+0.06} _{-0.05}
1.5	0.4	5.0	5.0	1.50 ^{+0.07} _{-0.05}	0.44 ^{+0.13} _{-0.11}
3	0.05	5.7	2.0	3.11 ^{+0.59} _{-0.38}	0.05 ^{+0.02} _{-0.01}
3	0.15	3.3	2.0	3.09 ^{+0.61} _{-0.40}	0.15 ^{+0.05} _{-0.04}
3	0.2	2.9	2.0	3.13 ^{+0.58} _{-0.41}	0.19 ^{+0.07} _{-0.05}
3	0.4	2.0	2.0	3.10 ^{+0.60} _{-0.41}	0.42 ^{+0.15} _{-0.12}
4	0.05	4.8	1.7	4.31 ^{+1.52} _{-0.79}	0.05 ^{+0.02} _{-0.01}
4	0.15	2.7	1.7	4.39 ^{+1.47} _{-0.85}	0.15 ^{+0.05} _{-0.04}
4	0.2	2.4	1.7	4.38 ^{+1.69} _{-0.85}	0.19 ^{+0.08} _{-0.06}
4	0.4	1.7	1.7	4.38 ^{+1.55} _{-0.86}	0.38 ^{+0.14} _{-0.11}
10	0.5	1.1	1.2	11.54 ^{+4.58} _{-3.88}	0.51 ^{+0.16} _{-0.11}
10	1.0	0.8	1.2	11.55 ^{+4.69} _{-3.81}	1.02 ^{+0.29} _{-0.22}
10	1.5	0.6	1.2	12.29 ^{+4.32} _{-3.89}	1.45 ^{+0.29} _{-0.28}

Table 2. Inversion of Numerical Data From Simulations

Simulation Parameters		Fitted Data		Inversion Results	
ζ	l/R	L_g/λ	h/λ	ζ	l/R
1.5	0.05	11.5	3.8	1.73 ^{+0.12} _{-0.09}	0.05 ^{+0.02} _{-0.01}
1.5	0.15	7.9	4.6	1.56 ^{+0.08} _{-0.07}	0.15 ^{+0.05} _{-0.04}
1.5	0.2	7.0	4.8	1.53 ^{+0.08} _{-0.06}	0.21 ^{+0.07} _{-0.05}
1.5	0.4	5.0	4.9	1.52 ^{+0.07} _{-0.06}	0.39 ^{+0.09} _{-0.08}
3	0.05	5.5	2.1	2.88 ^{+0.46} _{-0.33}	0.06 ^{+0.02} _{-0.02}
3	0.15	3.5	2.2	2.74 ^{+0.44} _{-0.32}	0.16 ^{+0.06} _{-0.04}
3	0.2	3.1	2.2	2.74 ^{+0.41} _{-0.30}	0.21 ^{+0.07} _{-0.05}
3	0.4	2.1	2.0	3.09 ^{+0.57} _{-0.40}	0.38 ^{+0.13} _{-0.11}
4	0.05	4.9	1.7	4.17 ^{+1.32} _{-0.74}	0.05 ^{+0.02} _{-0.01}
4	0.15	3.1	1.9	3.19 ^{+0.64} _{-0.42}	0.16 ^{+0.06} _{-0.05}
4	0.2	2.7	1.9	3.33 ^{+0.74} _{-0.43}	0.21 ^{+0.07} _{-0.06}
4	0.4	2.3	2.2	2.73 ^{+0.43} _{-0.29}	0.38 ^{+0.12} _{-0.10}

Inversion technique correctly recovers input parameters

Analytical forward model accurate enough when compared to simulation inversions

Large density contrasts represent a challenge from observational point of view

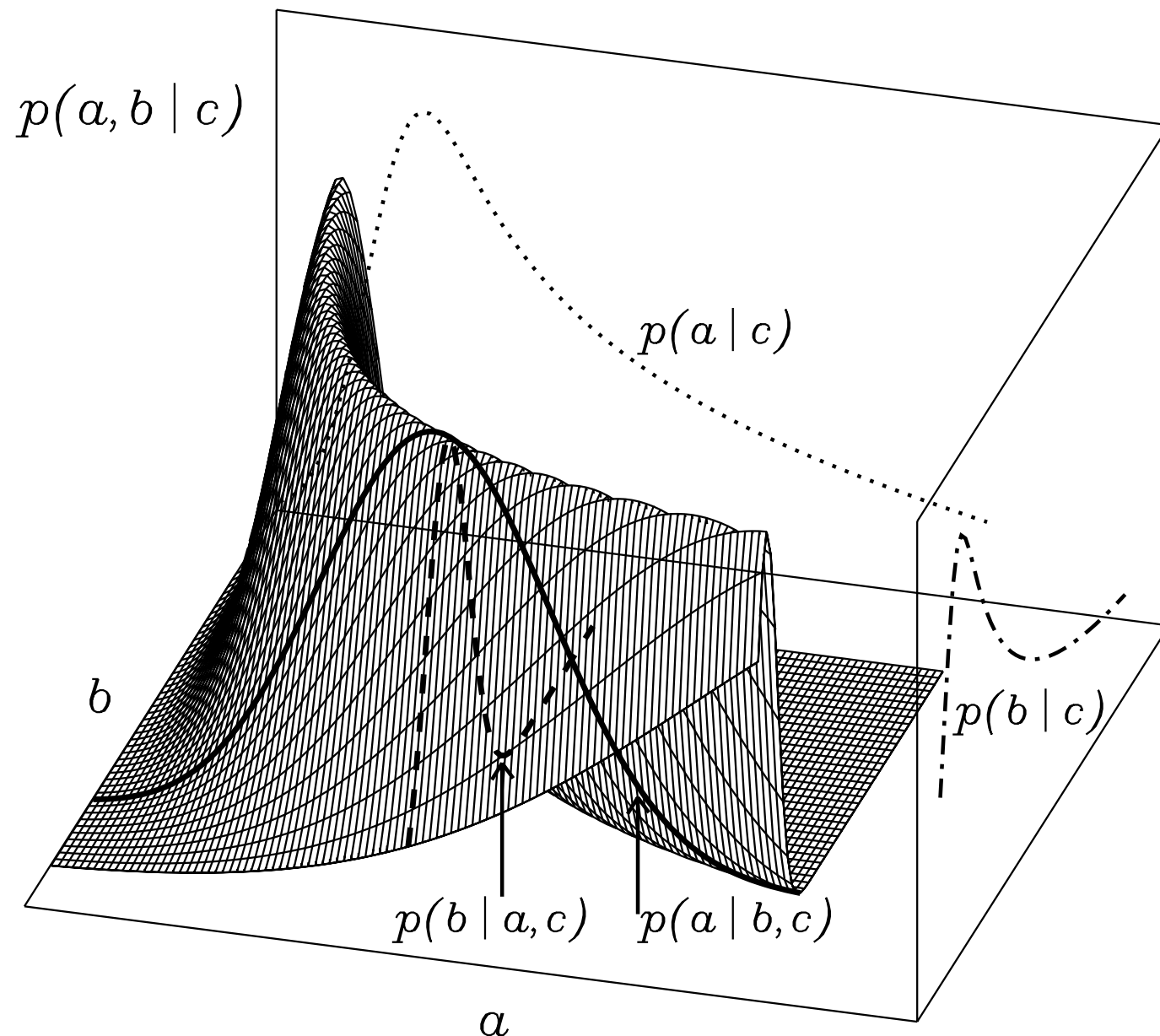
Example #3

Inference of cross-field density structure from damping of transverse waves, joint probability and marginal posteriors

Conditional probability and marginal posteriors

$$c = a \cdot b$$

Joint probability of a and b , given c $p(a,b|c)$



$p(b|a,c)$: probability of b , given a and c

$p(a|b,c)$: probability of a , given b and c

$p(a|c)$: probability of a , given c

$p(b|c)$: probability of b , given c

*All animals are equal,
but some animals are more equal than others*
George Orwell, Animal Farm (1945)

In spite of the fact the c can be obtained by an infinite number of combinations of a and b ,
some parameter values are more plausible than others

The probability of a damping ratio

Application of the previous procedure to obtain:

- density contrast
- transverse inhomogeneity length scale

from the damping ratio of transverse oscillations

Forward model

$$r = \frac{\tau_d}{P} = \frac{2}{\pi} \left(\frac{R}{L} \right) \left(\frac{\zeta + 1}{\zeta - 1} \right)$$

Priors

$$p(\zeta) = \frac{1}{\zeta^{\max} - \zeta^{\min}} \quad \text{for} \quad \zeta^{\min} \leq \zeta \leq \zeta^{\max}$$

$$p(l/R) = \frac{1}{(l/R)^{\max} - (l/R)^{\min}} \quad \text{for} \quad (l/R)^{\min} \leq l/R \leq (l/R)^{\max}$$

Likelihood function

$$p(r|\zeta, l/R) = \frac{1}{\sigma_r \sqrt{2\pi}} \exp \left\{ -\frac{[r_{obs} - r_{model}(\zeta, l/R)]^2}{2\sigma_r} \right\}$$

Marginalise



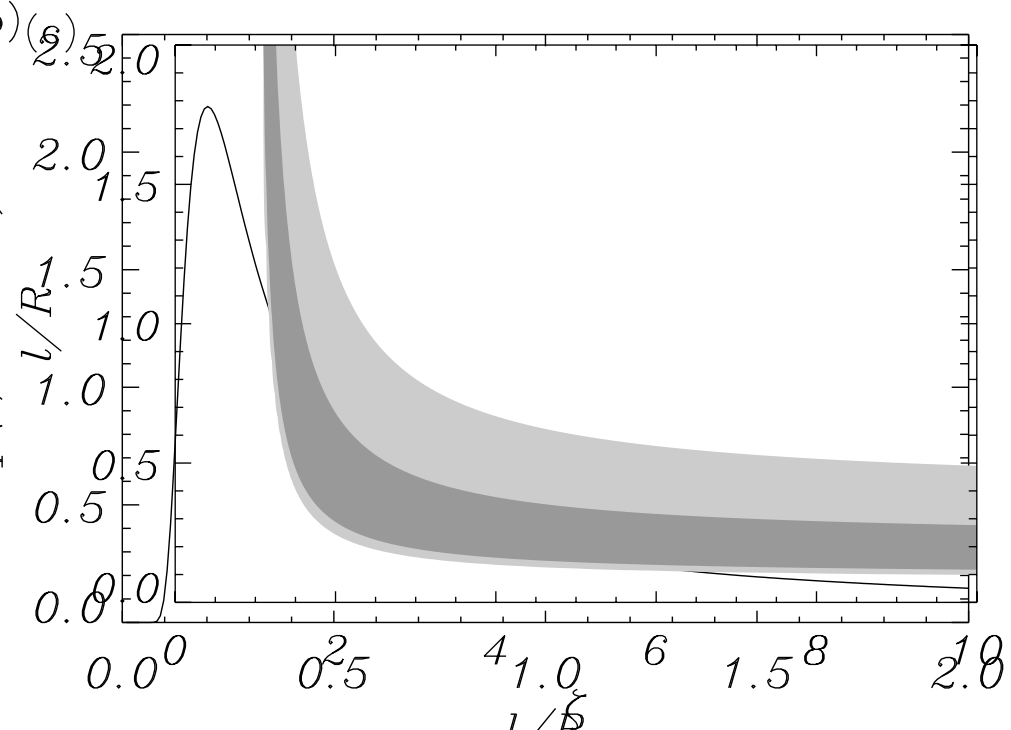
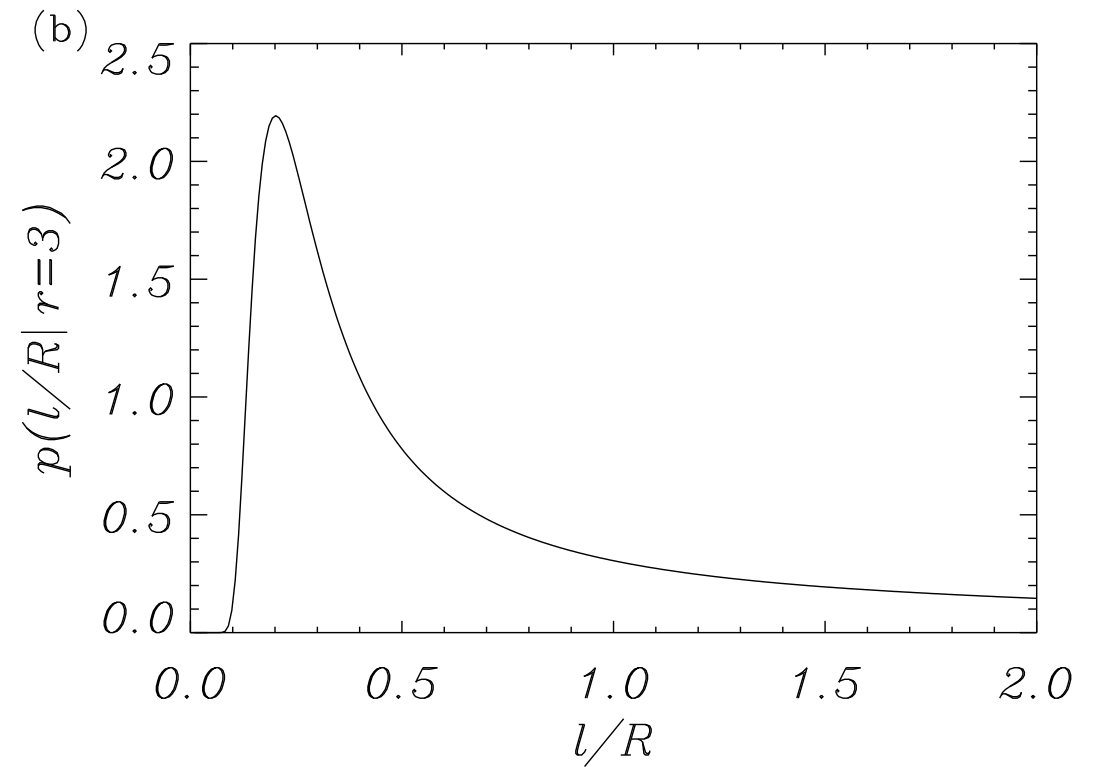
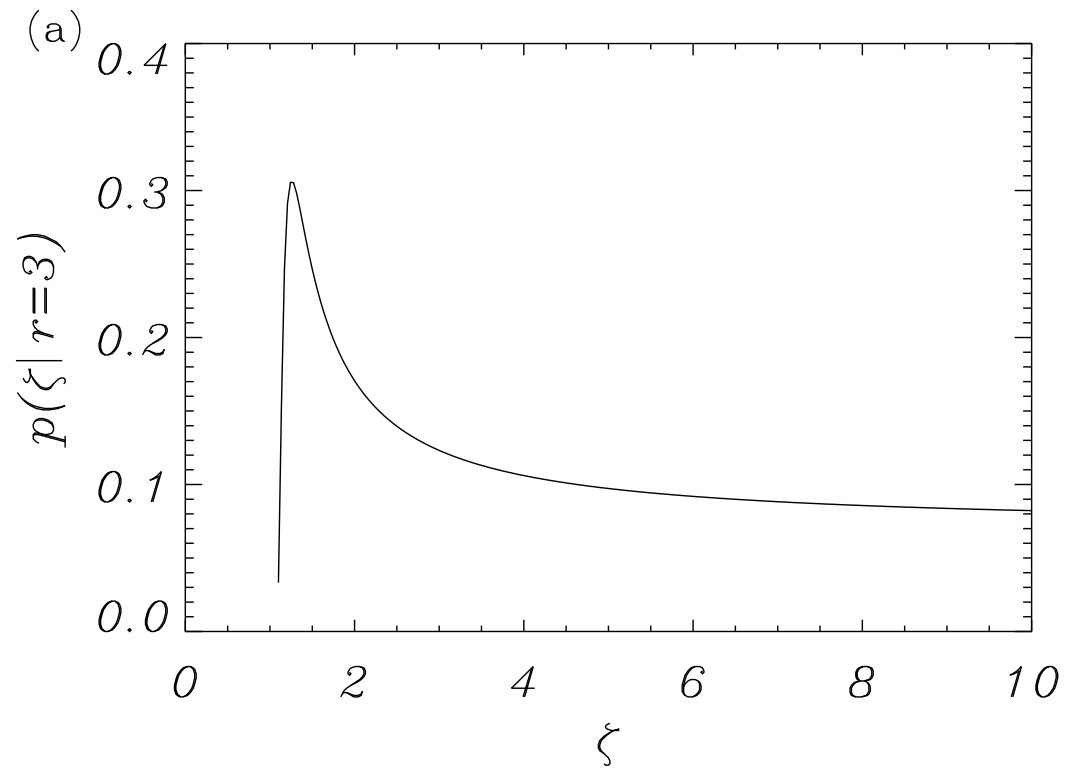
Bayes rule

Post \sim likelihood \times prior

$$p(\zeta|r) = \int p(\zeta, l/R|r) d(l/R)$$

$$p(l/R|r) = \int p(\zeta, l/R|r) d\zeta$$

Results: marginal posteriors



Well constrained marginal posteriors

Long tail for contrast - large uncertainty

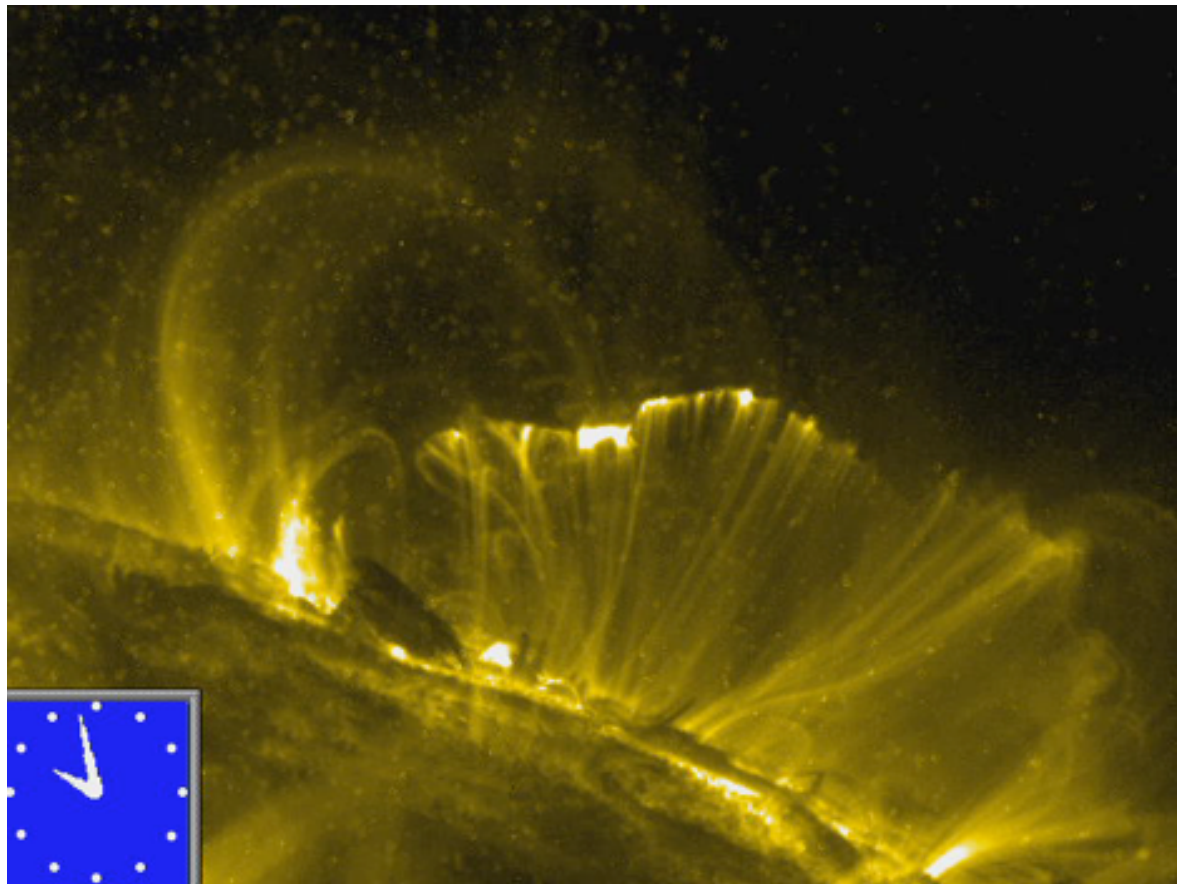
Example #4

Inference/model comparison of coronal density
scale height and magnetic field expansion
from multiple period transverse oscillations

Multiple mode harmonic oscillations

Verwichte et al. (2004); Andries et al. (2005); Andries, Arregui, & Goossens (2005)

Observations

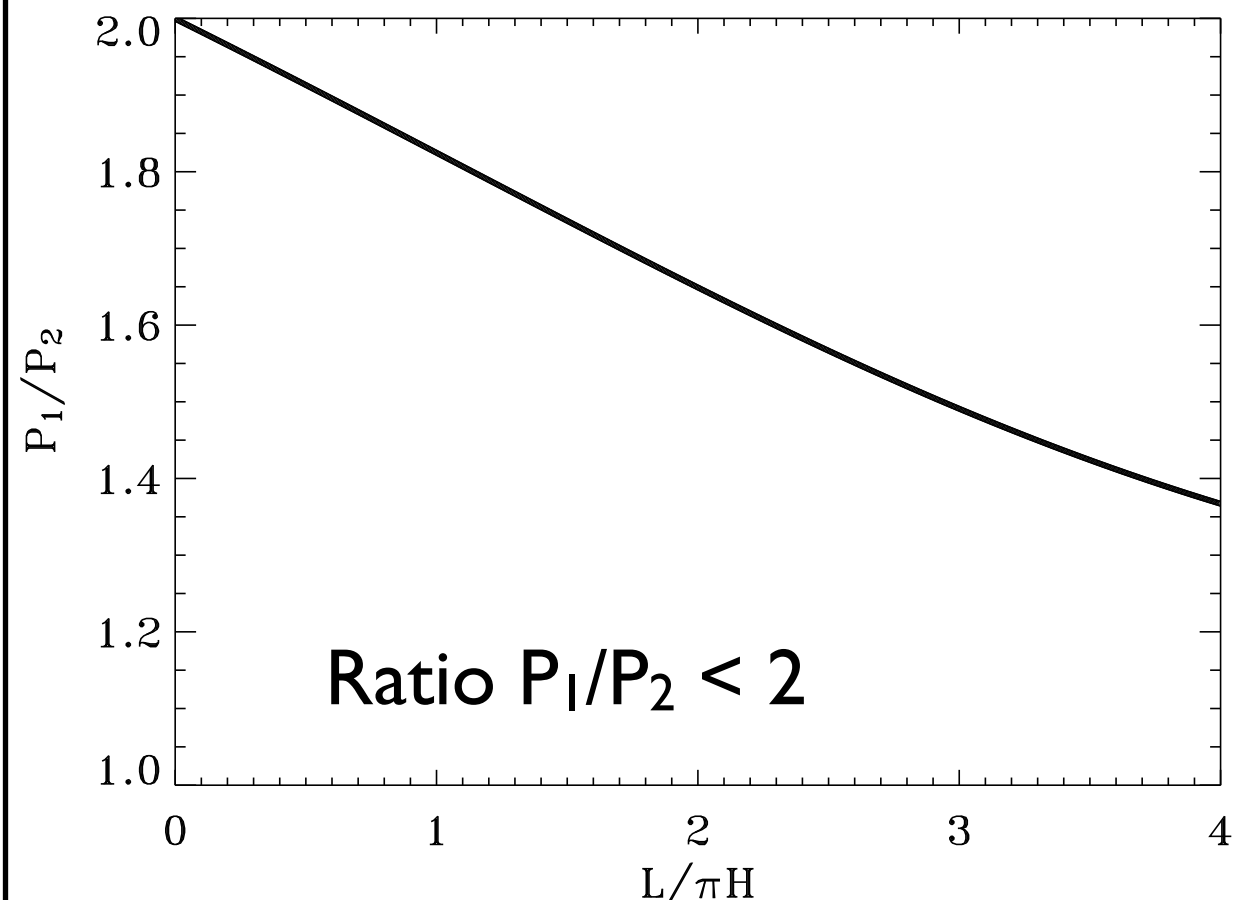


Detection of multiple harmonics in two coronal loops. **Simultaneous presence of fundamental and first harmonic**

Verwichte et al. (2004)

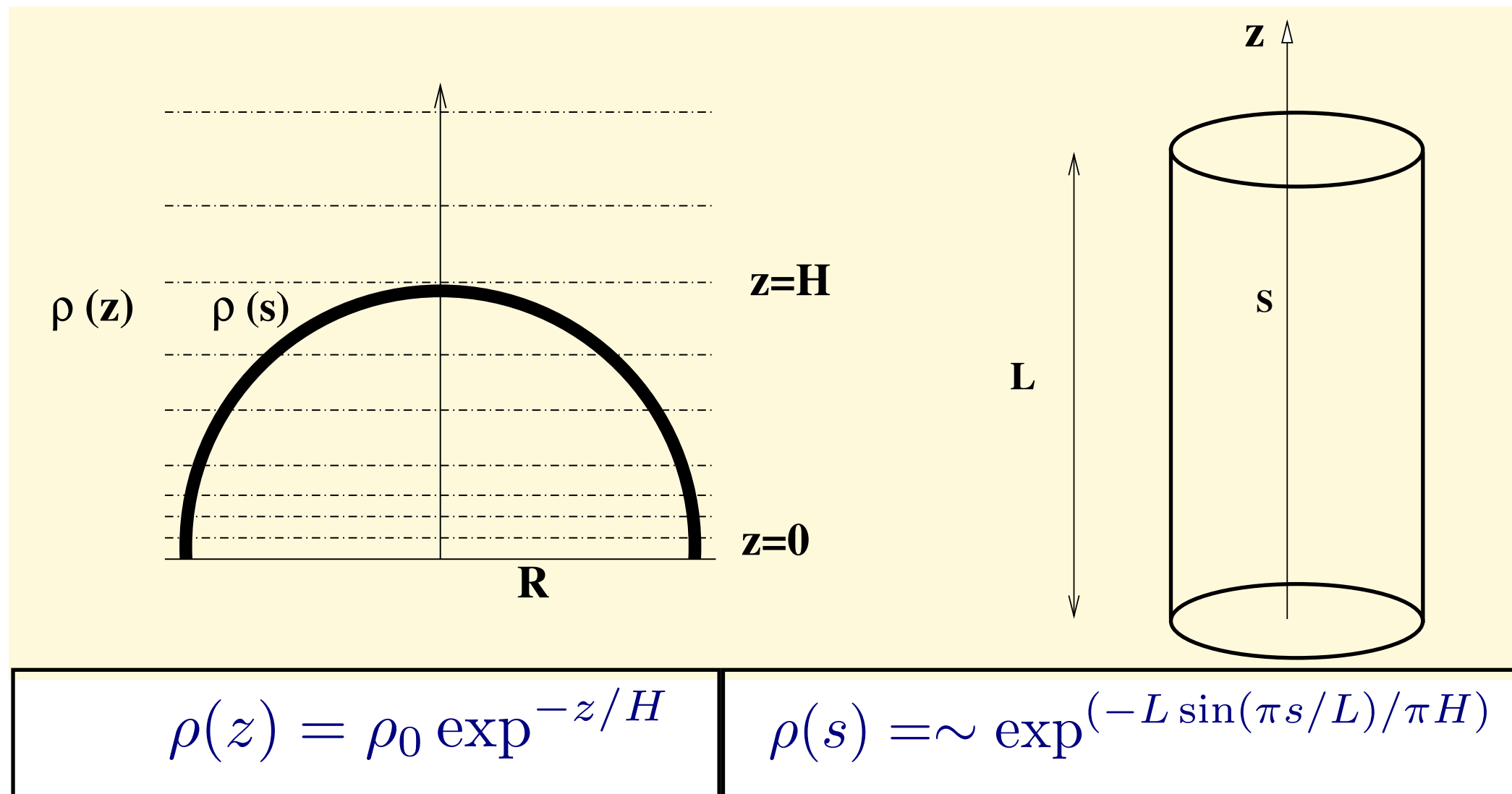
Theory

In a longitudinally inhomogeneous flux tube **the period ratio** of first overtone to fundamental mode is smaller than 2 and **depends on density stratification**



Estimate of density scale-height

Consider a vertically stratified atmosphere and a curved coronal loop

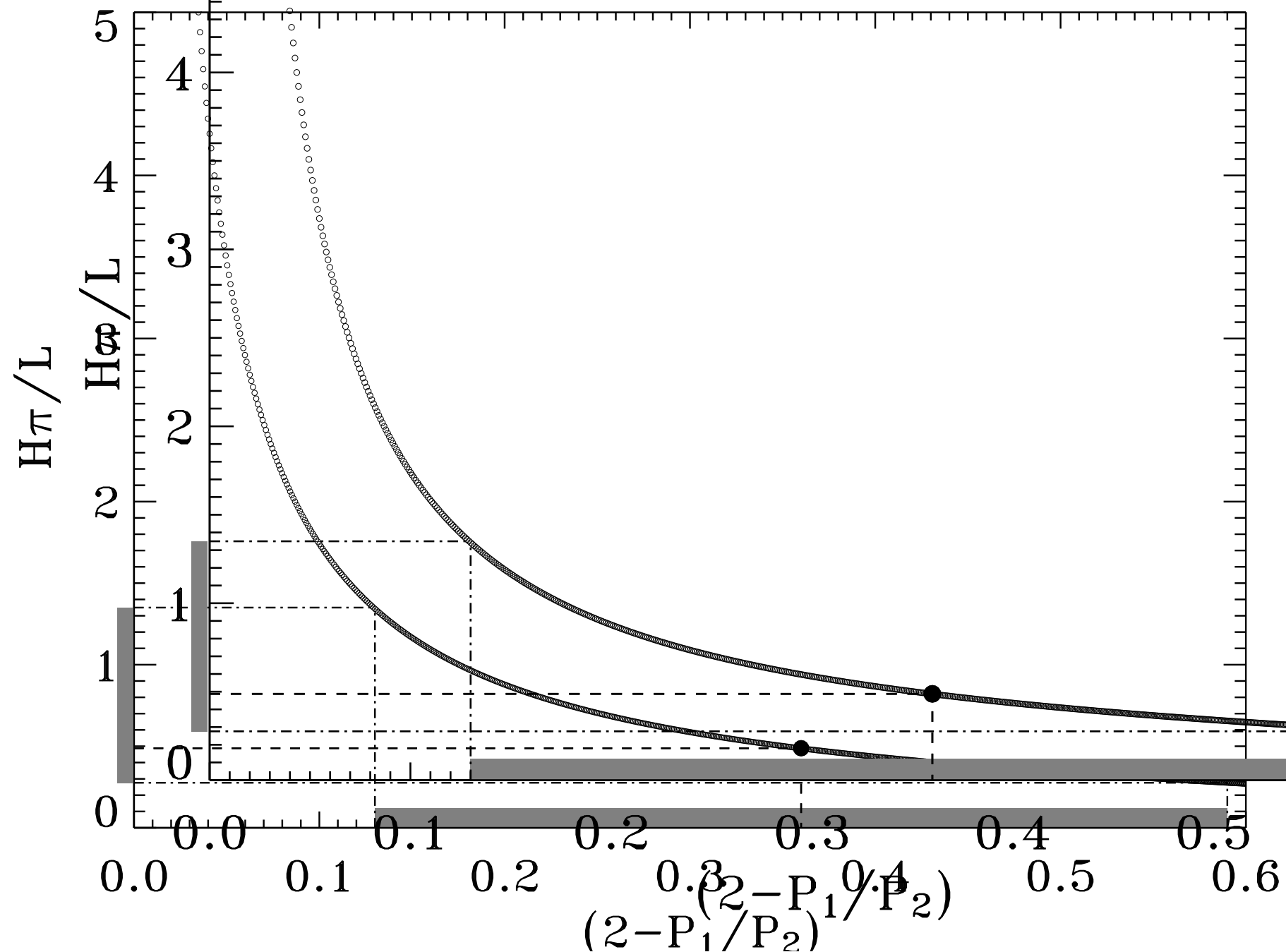


We can mimic an exponentially stratified atmosphere using a straight tube model by projecting the vertical density variation onto a semicircular loop of length L and height L/π

And use the observed period ratio together with theoretical calculations to estimate the density scale-height in the solar atmosphere

Result for case I: Path D in Verwichte et al. (2004)

(Andries, Arregui, & Goossens 2005)

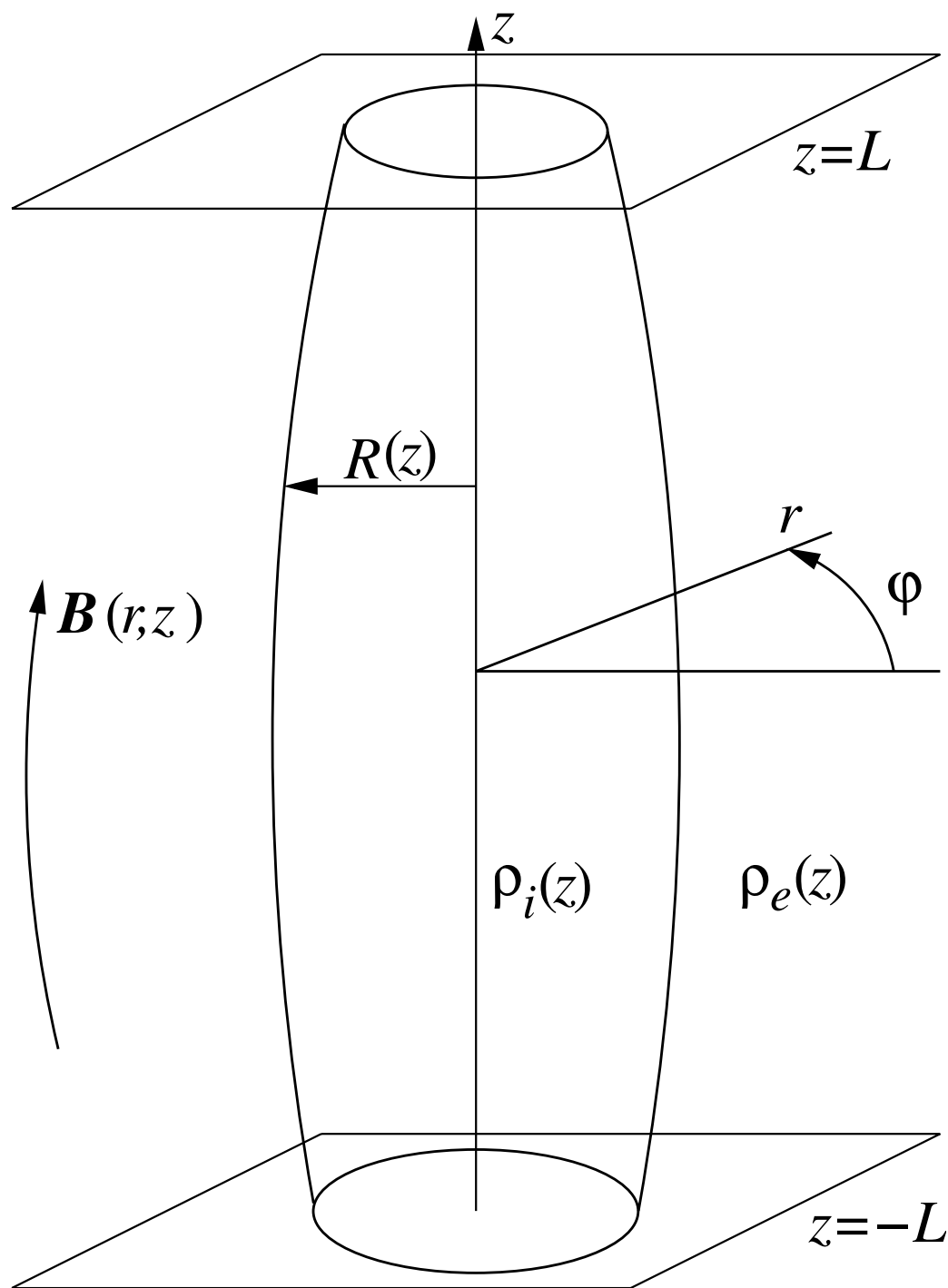


$2 - \frac{P_1}{P_2} = 0.36 \pm 0.23 \implies \frac{H\pi}{L}: [0.276, 1.35]$ with an estimated value $\frac{H\pi}{L} = 0.48$

$H: [20, 99]$ Mm with an estimated value of $H = 36$ Mm

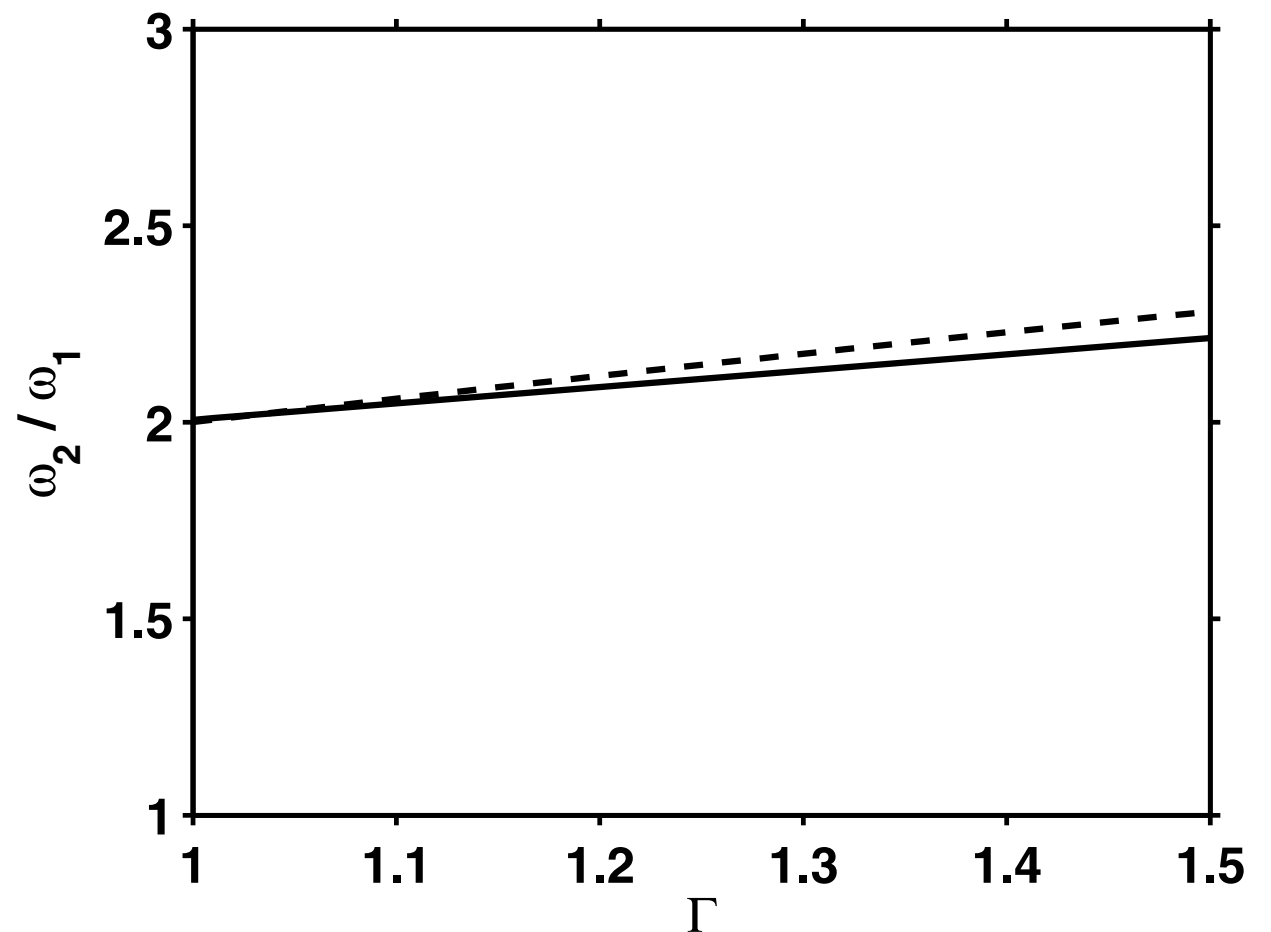
Magnetic flux tube expansion

Verth & Erdélyi (2008); Ruderman et al. (2008); Verth et al. (2008)



Expansion of magnetic loop affects period ratio

The period ratio between fundamental mode and first overtone is larger than 2 and depends on magnetic expansion



Bayesian inference

Arregui, Asensio Ramos, Díaz (2013, ApJL 765 L23)

Model 1: density stratification

$$r_1 = \frac{P_1}{2P_2} = 1 - \frac{4}{5} \left(\frac{\eta}{\eta + 3\pi^2} \right)$$

$$\eta = L/\pi H$$

Safari et al. (2007)

Model 2: magnetic expansion

$$r_2 = \frac{P_1}{2P_2} = 1 + \frac{3(\Gamma^2 - 1)}{2\pi^2}$$

$$\Gamma = r_a/r_f$$

Verth & Erdélyi (2008)

Parameter Inference: compute posteriors for given value of measured period ratios r

Gaussian likelihoods

$$p(r|\eta, M_1) = \frac{1}{\sqrt{2\pi}\sigma} \exp\left[-\frac{(r - r_1)^2}{2\sigma^2}\right]$$

$$p(r|\Gamma, M_2) = \frac{1}{\sqrt{2\pi}\sigma} \exp\left[-\frac{(r - r_2)^2}{2\sigma^2}\right]$$

Uniform priors

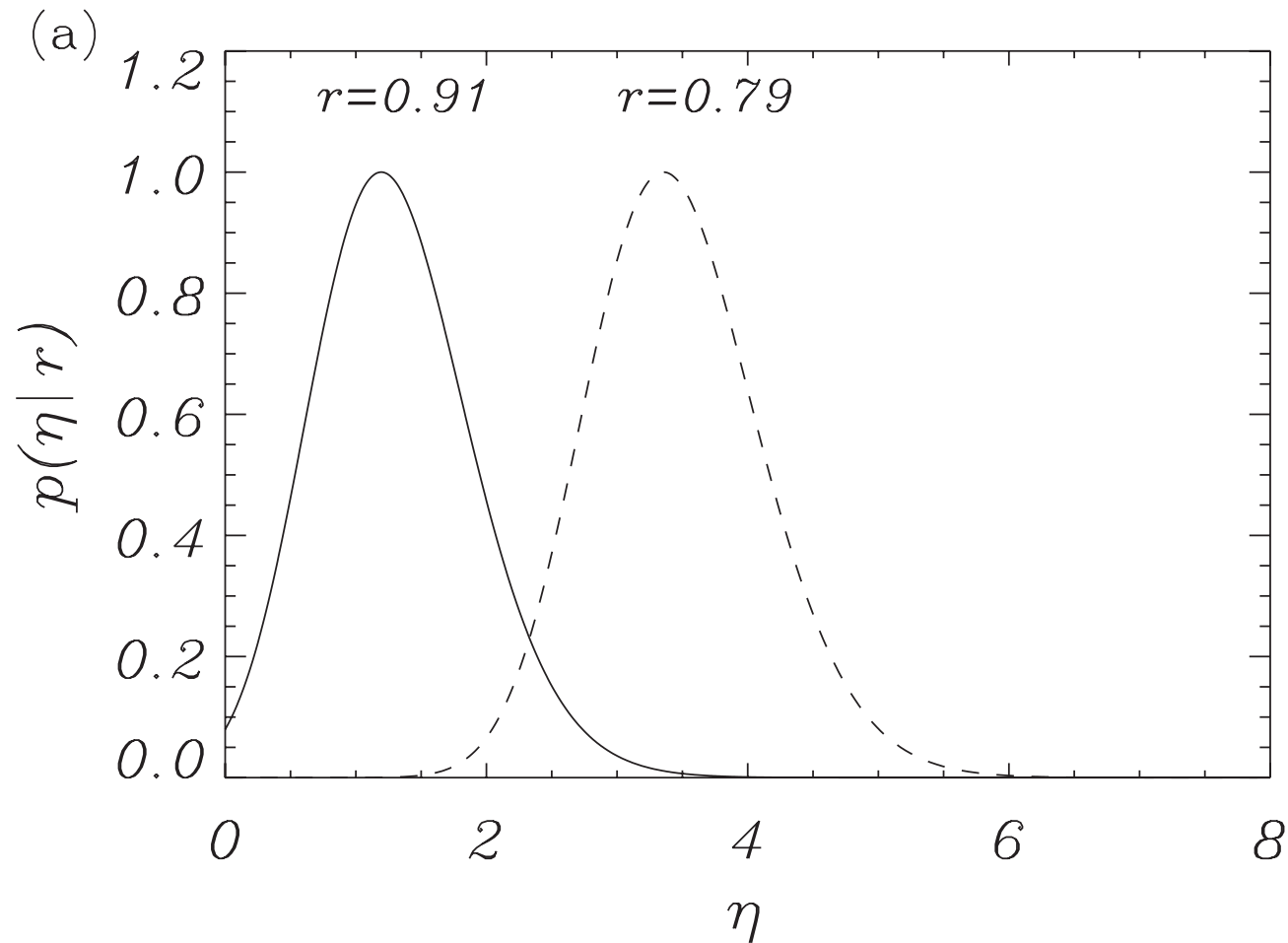
$$p(\eta|M_1) = \frac{1}{\eta^{\max} - \eta^{\min}} \text{ for } \eta^{\min} \leq \eta \leq \eta^{\max} \quad p(\Gamma|M_2) = \frac{1}{\Gamma^{\max} - \Gamma^{\min}} \text{ for } \Gamma^{\min} \leq \Gamma \leq \Gamma^{\max}$$

Marginalise

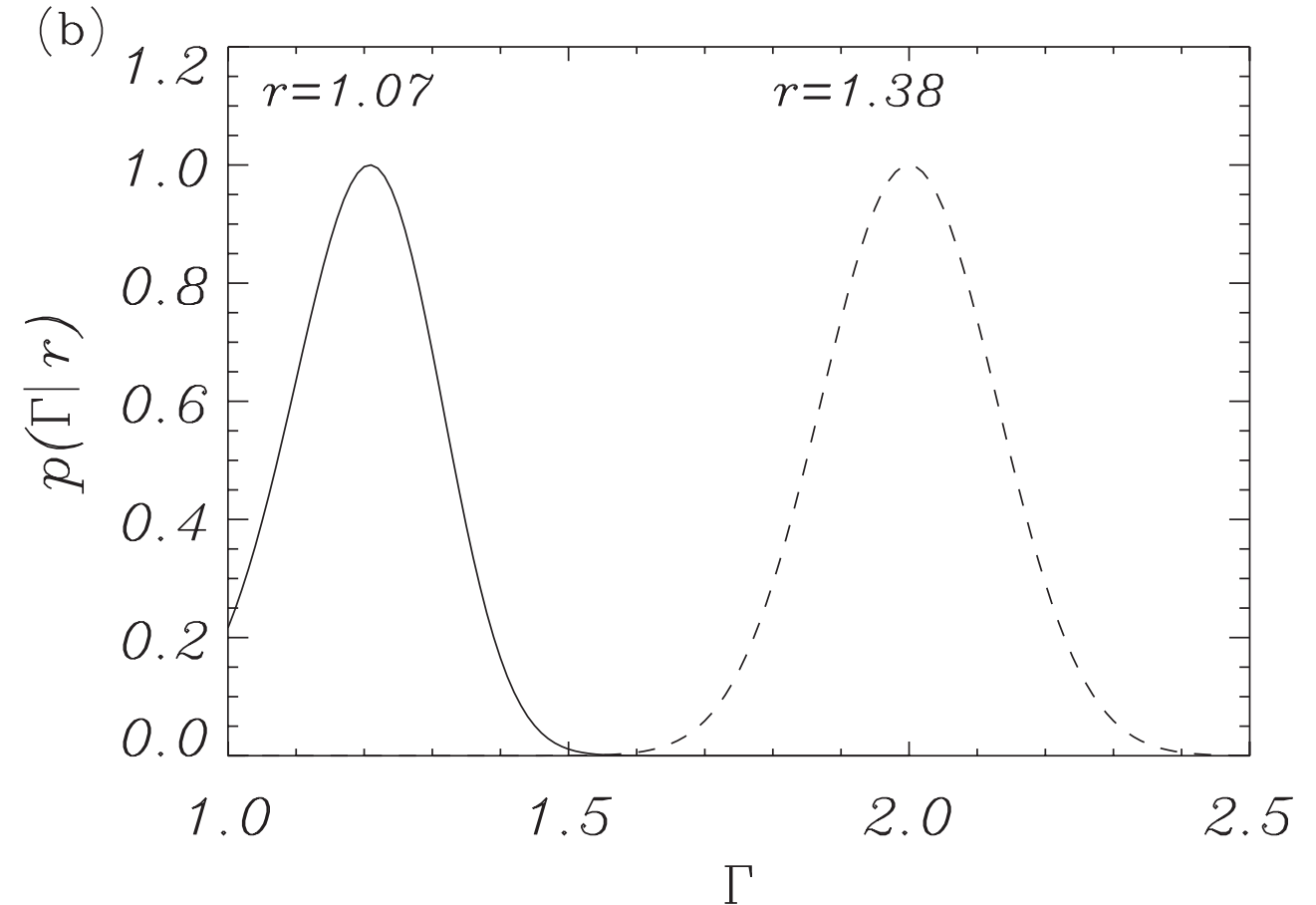
$$p(\theta_i|d) = \int p(\boldsymbol{\theta}|d) d\theta_1 \dots d\theta_{i-1} d\theta_{i+1} \dots d\theta_N$$

Bayesian inference results

Model 1: density stratification



Model 2: magnetic expansion



Well-defined posteriors. Inference with correctly propagated uncertainties from data to inferred parameters

Coronal density scale height: $H \sim 21$ Mm and $H \sim 56$ Mm (for $L/\pi = 70$ Mm)

Magnetic tube expansion factor: $\Gamma \sim 1.20$ and 1.87

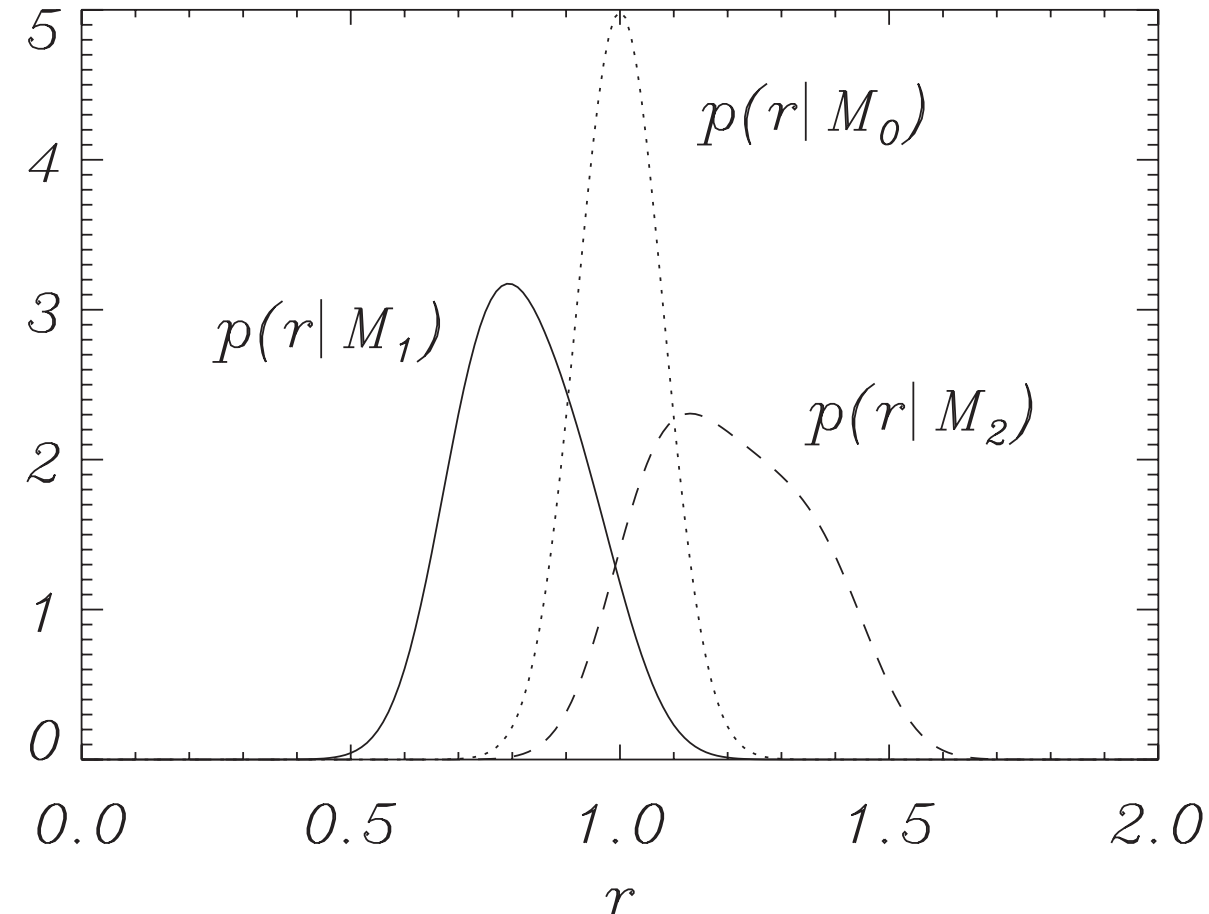
Bayesian model comparison

Assess the performance of 3 models in explaining data:

- M0 uniform loop - Uniform likely for $r \sim 1$
- M1 stratified loop - Stratified likely for $r < 1$
- M2 expanding loop - Expanding likely for $r > 1$

Marginal Likelihoods

$$p(r|M_i) = \int_{\theta_{\min}}^{\theta_{\max}} p(r, \theta|M_i) d\theta = \int_{\theta_{\min}}^{\theta_{\max}} p(r|\theta, M_i) p(\theta|M_i) d\theta$$



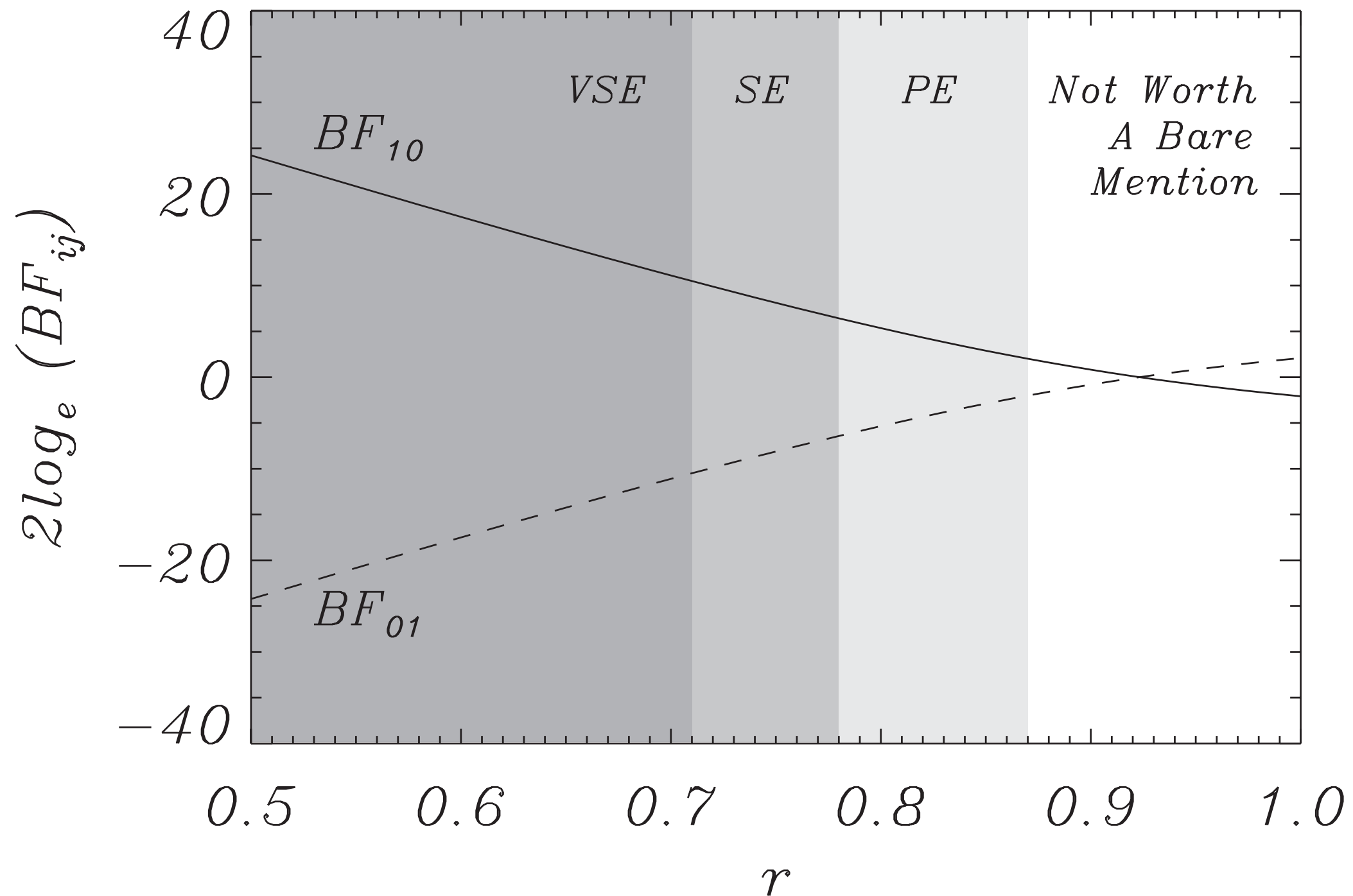
Quantitative model comparison: compute Bayes factors as a function of measured period ratios and use Jeffreys' scale (Jeffreys 1961; Kass & Raftery 1995)

$$\frac{p(M_i|r)}{p(M_j|r)} = \frac{p(r|M_i) p(M_i)}{p(r|M_j) p(M_j)}$$

$$BF_{ij} = \frac{p(r|M_i)}{p(r|M_j)}$$

$2 \log_e BF$	Evidence
0-2	Not worth more than a bare mention
2-6	Positive Evidence (PE)
6-10	Strong Evidence (SE)
> 10	Very Strong Evidence (VSE)

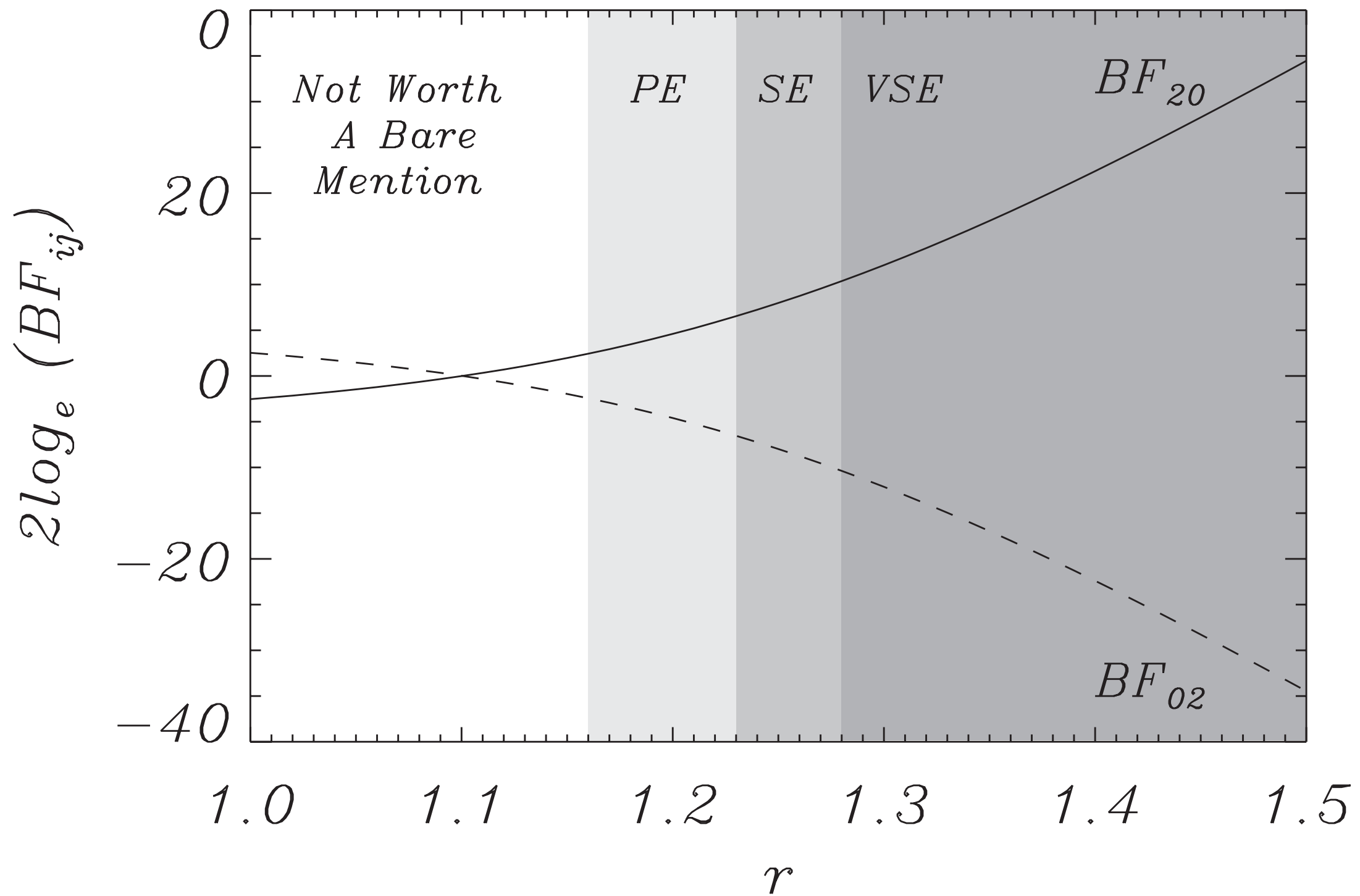
Model I against Model 0



A period ratio smaller than one is not sufficient evidence for density stratification

Level of evidence depends on data and their uncertainties

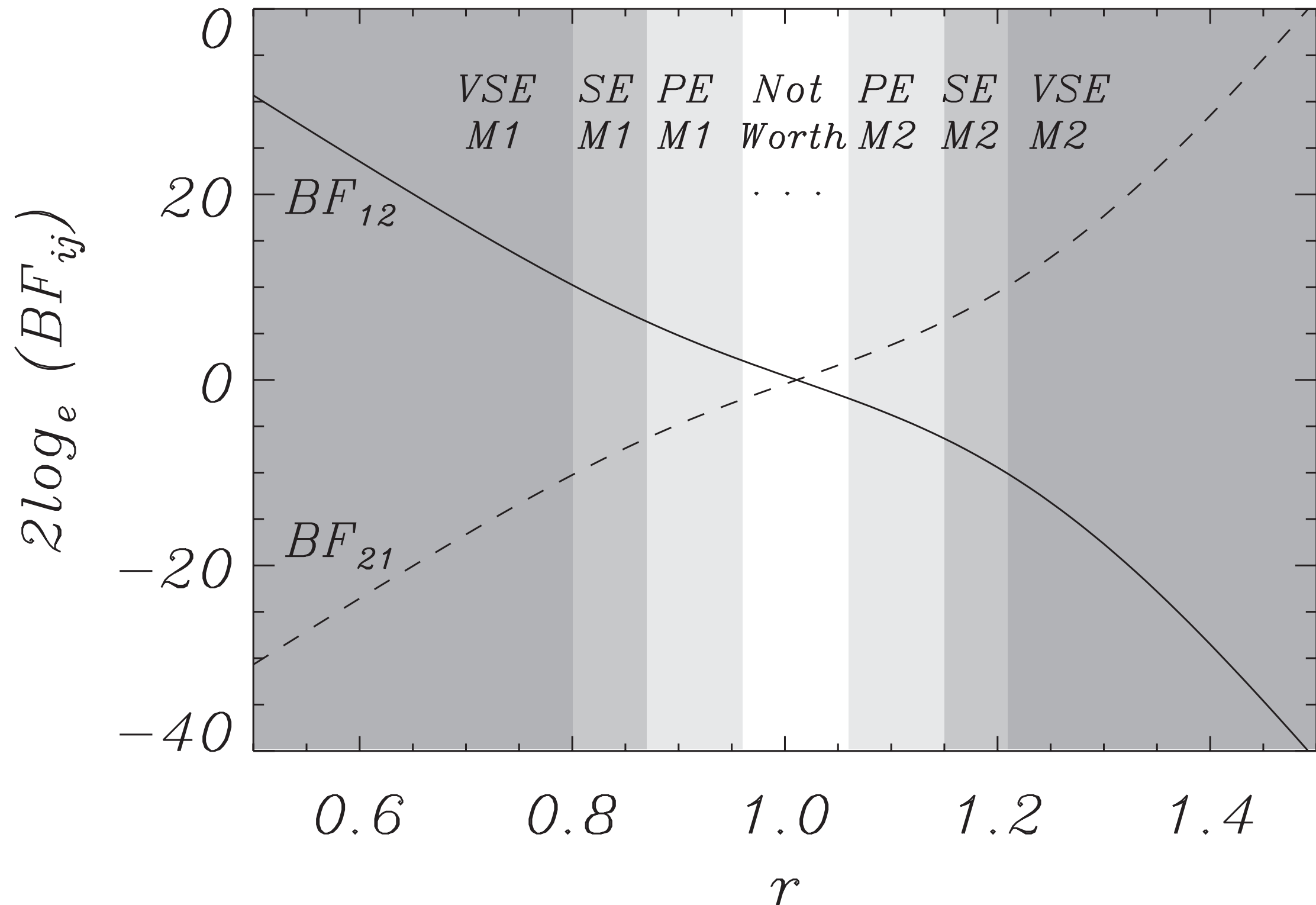
Model 2 against Model 0



A period ratio larger than one is not sufficient evidence for magnetic expansion

Level of evidence depends on data and their uncertainties

Model 1 against Model 2



Different levels of evidence for density stratification and magnetic tube expansion

Example #5

Application of the three levels of Bayesian inference to the problem of the cross-field density structure

The damping formula

Sakurai (1991); Goossens et al. (1995); Tirry & Goossens (1996); Ruderman & Roberts (2002)

Analytical expression for the period and damping by resonant absorption can be obtained under the thin tube and thin boundary approximations ($R/L \ll 1$; $l/R \ll 1$)

$$P = \tau_{Ai} \sqrt{2} \left(\frac{\zeta + 1}{\zeta} \right)^{1/2}$$

F numerical factor
depends on the radial density profile

$$\frac{\tau_d}{P} = F \frac{R}{l} \frac{\zeta + 1}{\zeta - 1}$$

Relevant parameters

Alfvén travel time

$$\tau_{Ai}$$

Density contrast

$$\zeta = \frac{\rho_i}{\rho_e}$$

Transverse inhomogeneity length-scale

$$\frac{l}{R}$$

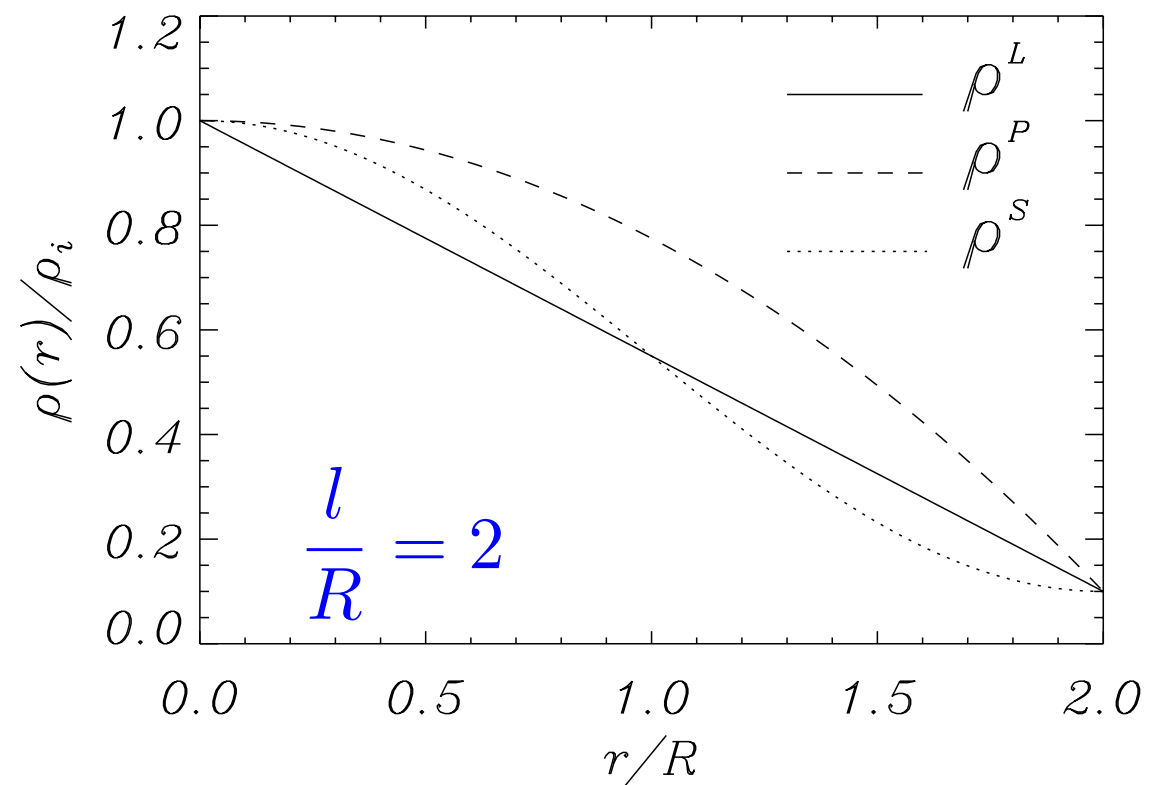
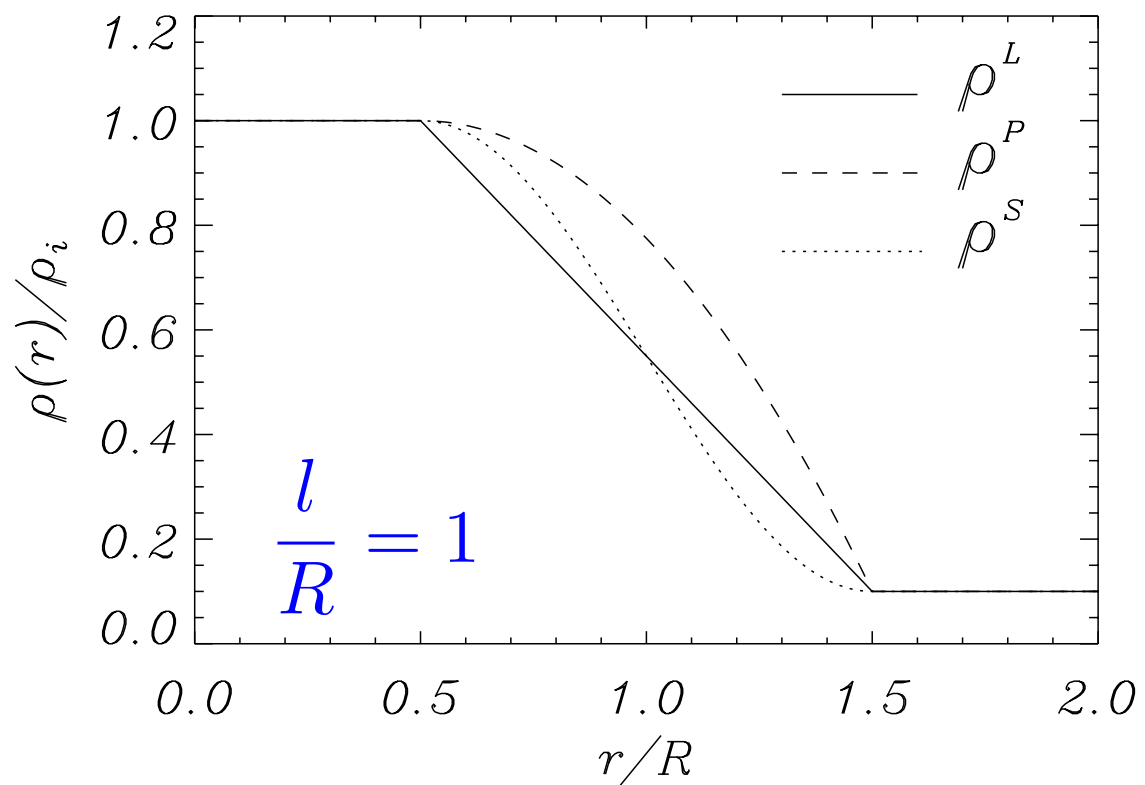
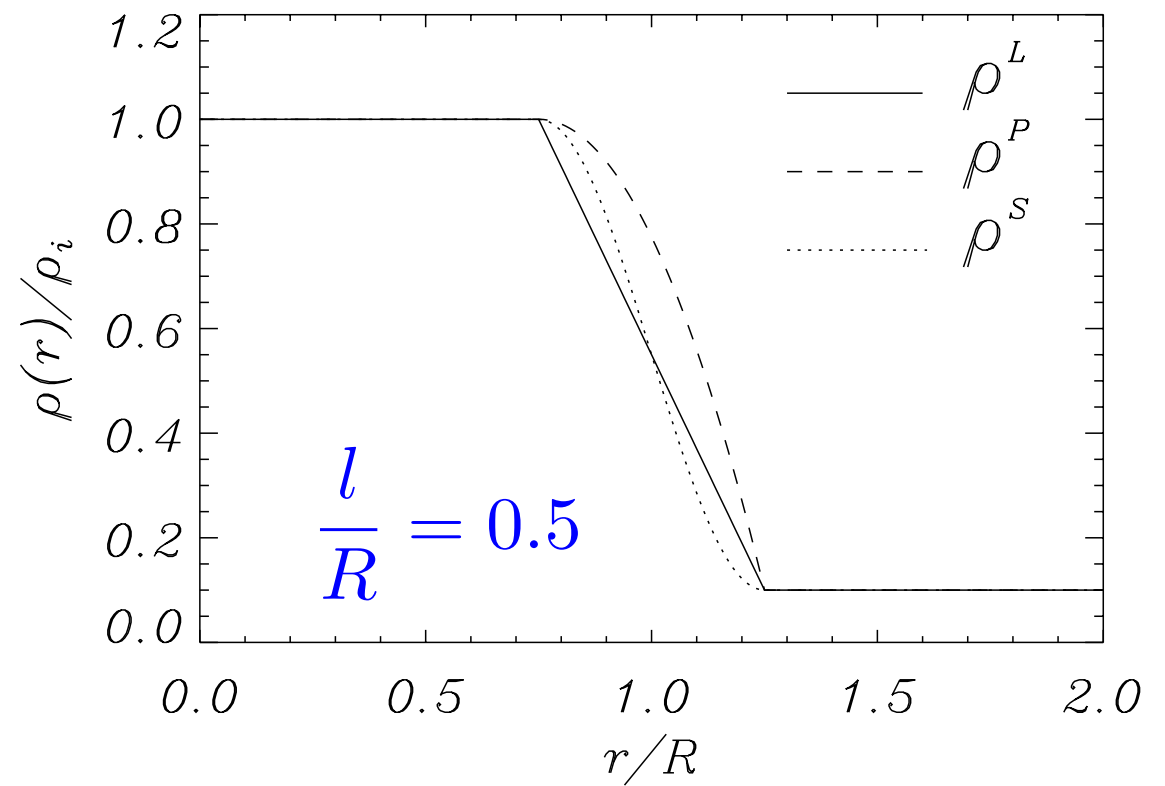
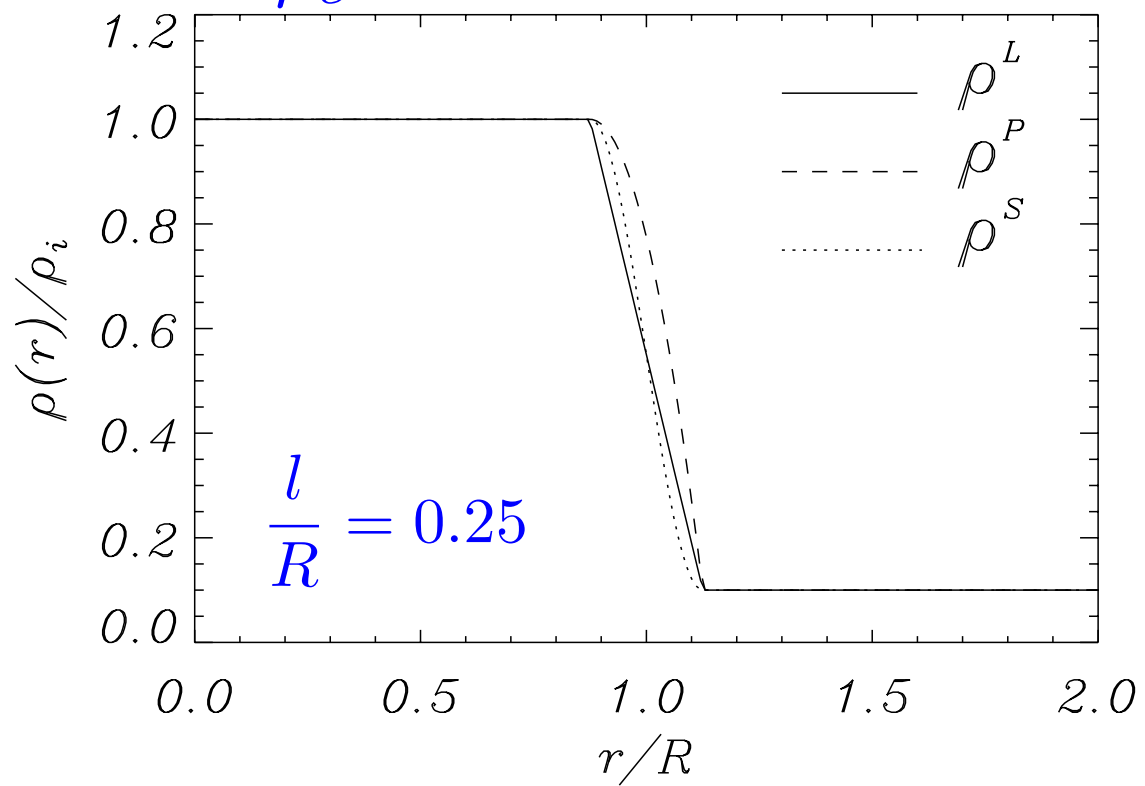
Alternative density models

$$\zeta = \frac{\rho_i}{\rho_e} = 10$$

S: sinusoidal

L: linear

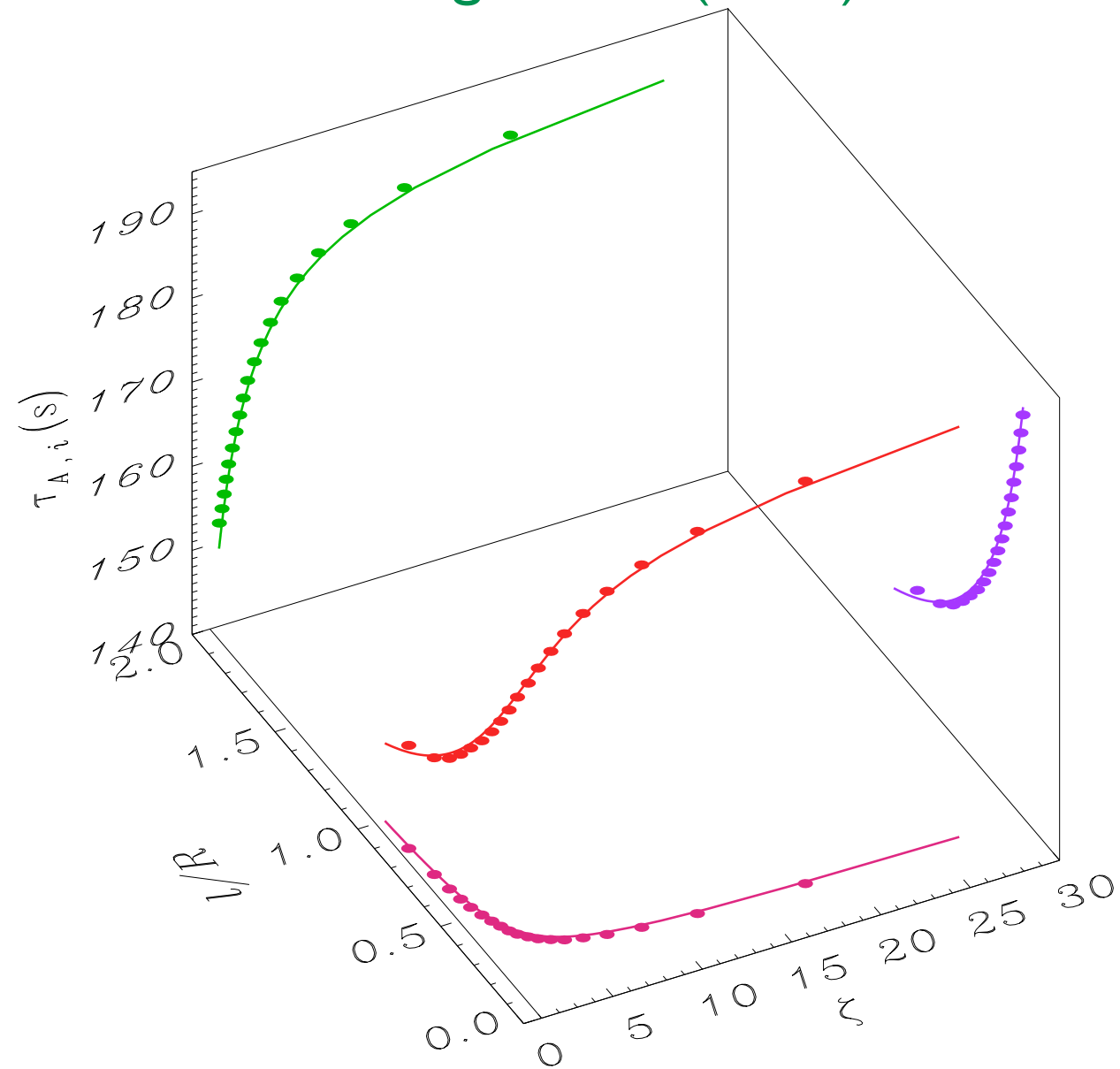
P: parabolic



Classic Inversion Result

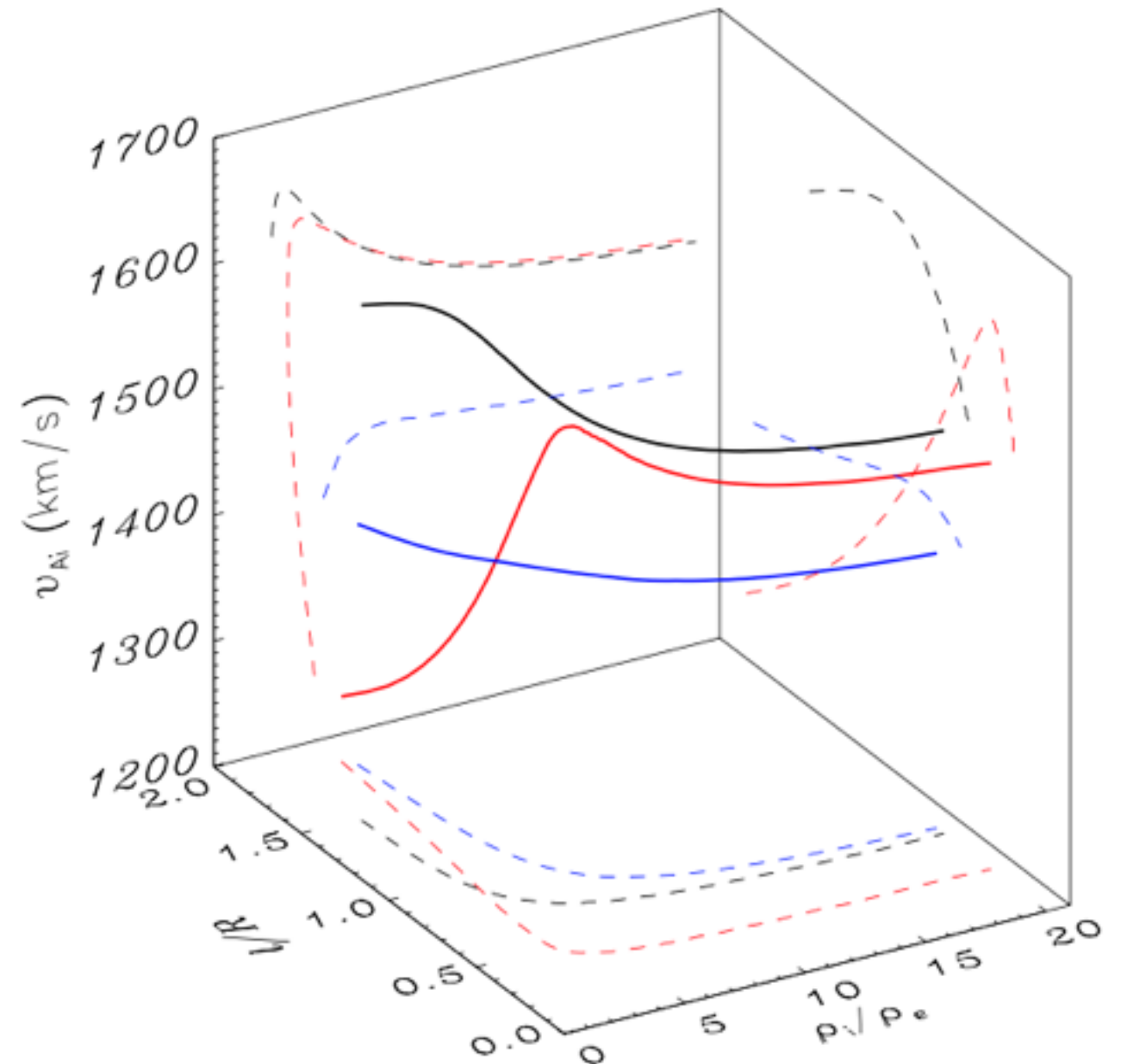
Inversion of: density contrast, transverse inhomogeneity, and Alfvén travel time, using observed period and damping

Arregui et al. (2007)



ID solution space for loop models that reproduce observations

Soler et al. (2014)



Inversion for 3 alternative density models seems to lead to significant differences

Infer the unknown physical parameters from observed oscillation properties:

Bayes Theorem

$$p(\{\tau_{Ai}, \zeta, l/R\} | \{P, \tau_d\}, M) \propto p(\{p, \tau_d\} | \{\tau_{Ai}, \zeta, l/R\}, M) p(\{\tau_{Ai}, \zeta, l/R\}, M)$$

Posterior	Likelihood	Prior
------------------	-------------------	--------------

Marginalise

$$p(\tau_{Ai} | \{P, \tau_d\}, M) = \int p(\{\tau_{Ai}, \zeta, l/R\} | \{P, \tau_d\}, M) d\zeta d(l/R)$$

$$p(\zeta | \{P, \tau_d\}, M) = \int p(\{\tau_{Ai}, \zeta, l/R\} | \{P, \tau_d\}, M) d\tau_{Ai} d(l/R)$$

$$p(l/R | \{P, \tau_d\}, M) = \int p(\{\tau_{Ai}, \zeta, l/R\} | \{P, \tau_d\}, M) d\tau_{Ai} d\zeta$$

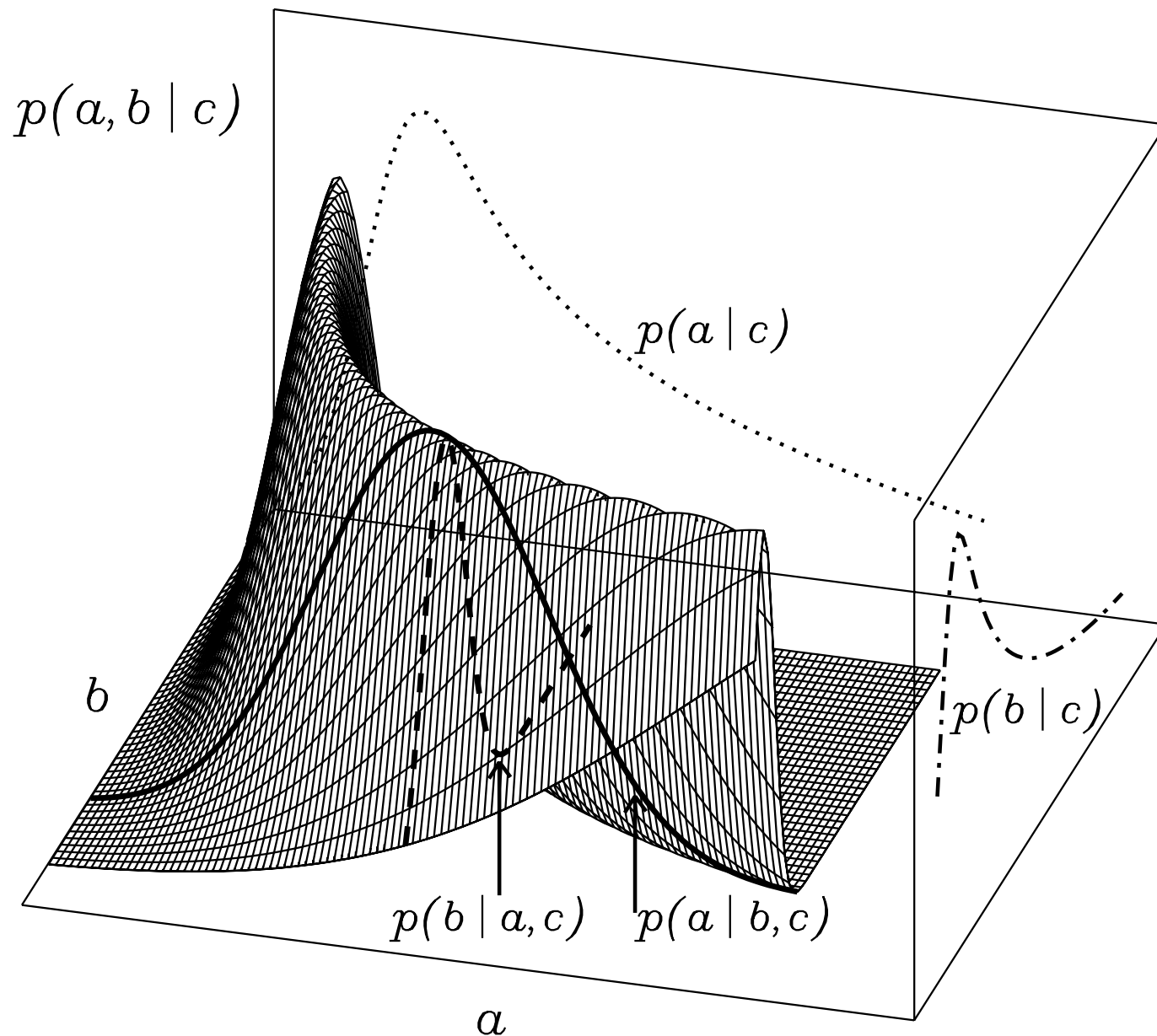
What we really do

Conditional probability and marginal posteriors

Arregui & Asensio Ramos (2014)

$$c = a \cdot b$$

Joint probability of a and b , given c $p(a,b|c)$



$p(b|a,c)$: probability of b , given a and c

$p(a|b,c)$: probability of a , given b and c

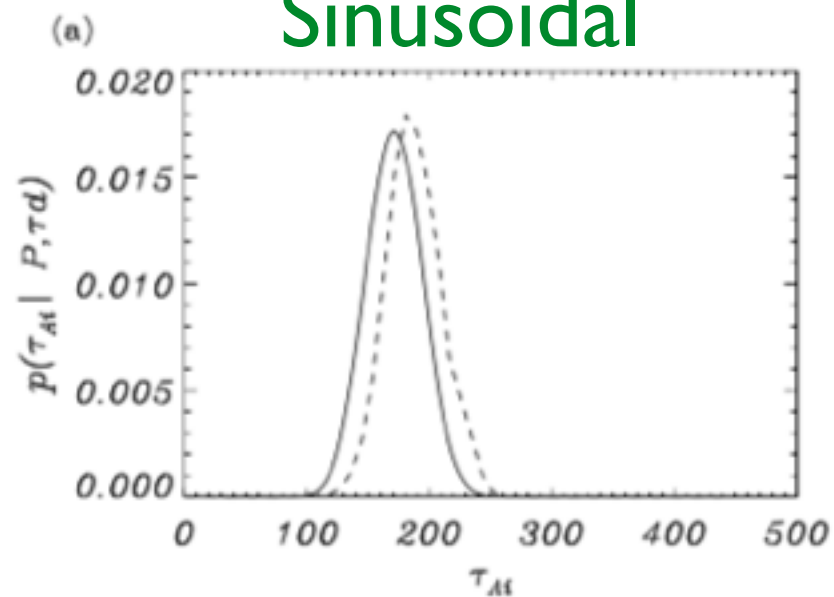
$p(b|c)$: probability of b , given c

$p(a|c)$: probability of a , given c

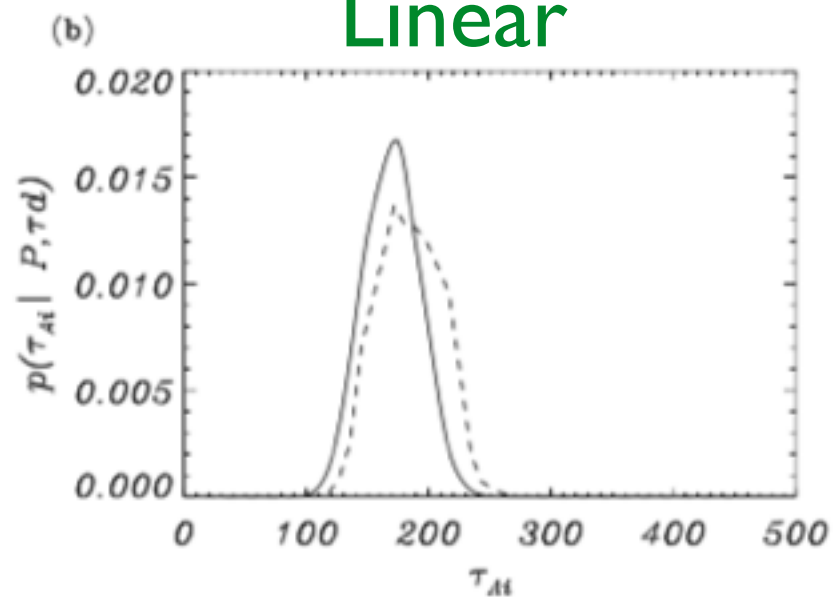
*All animals are equal,
but some animals are more equal than others*
George Orwell, Animal Farm (1945)

Solid: TTTB approximations - Dashed: numerical

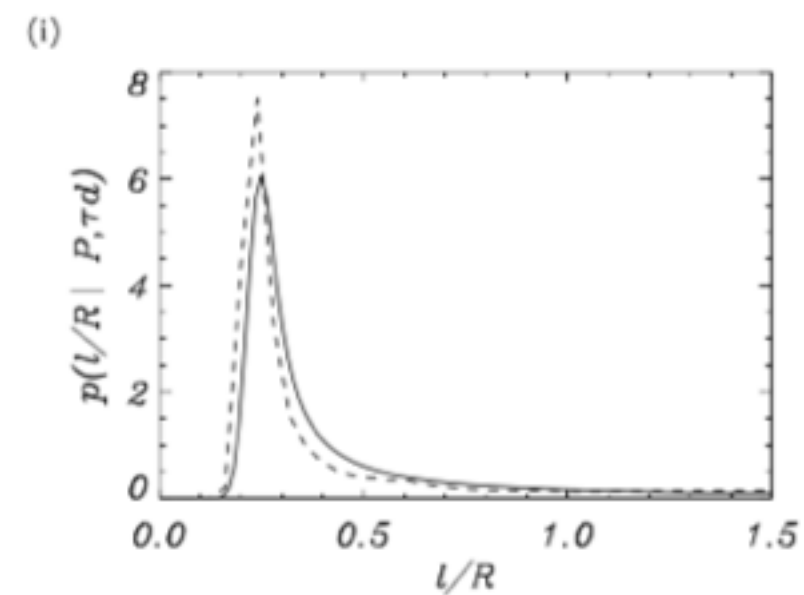
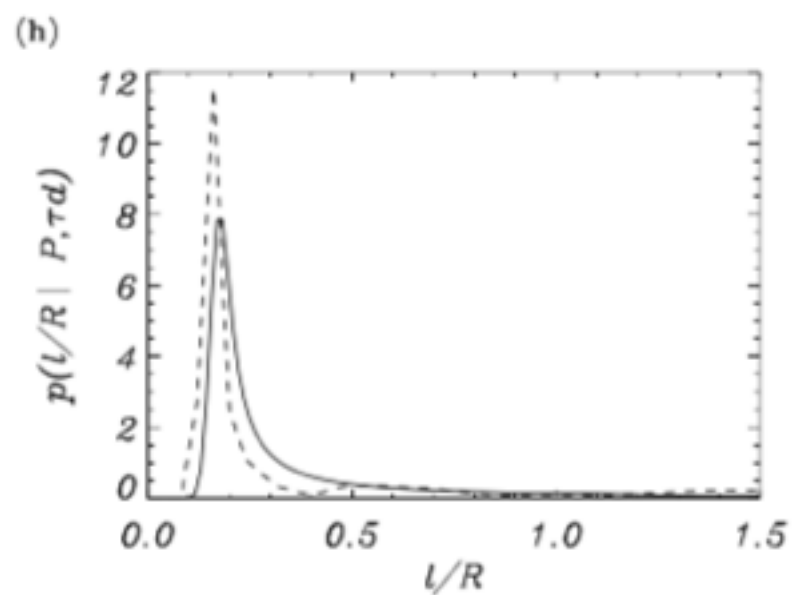
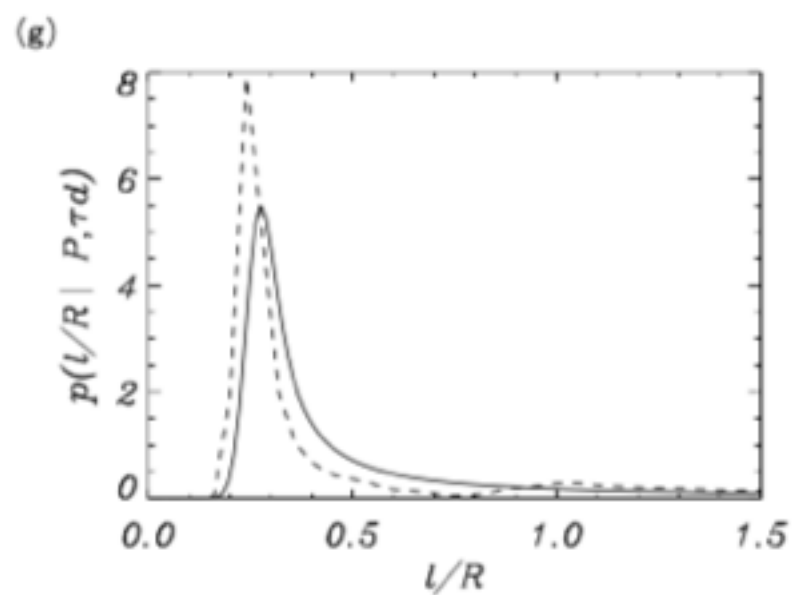
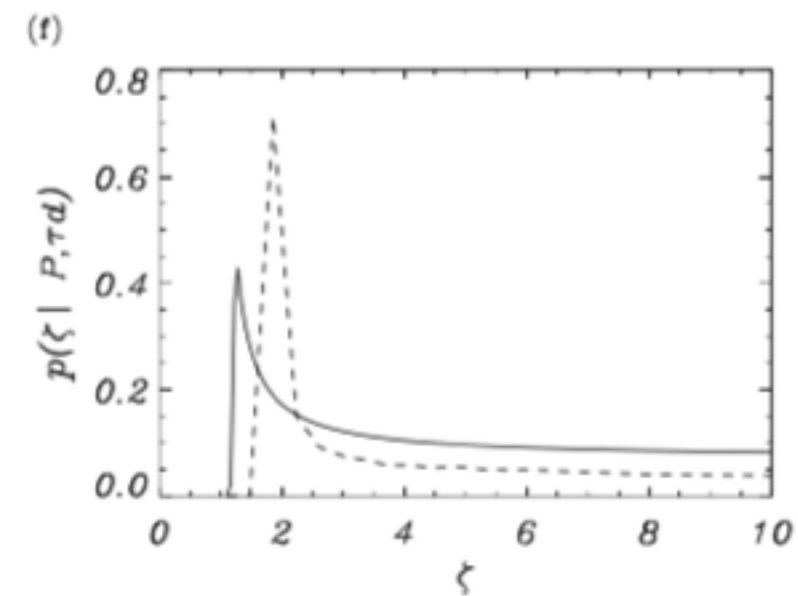
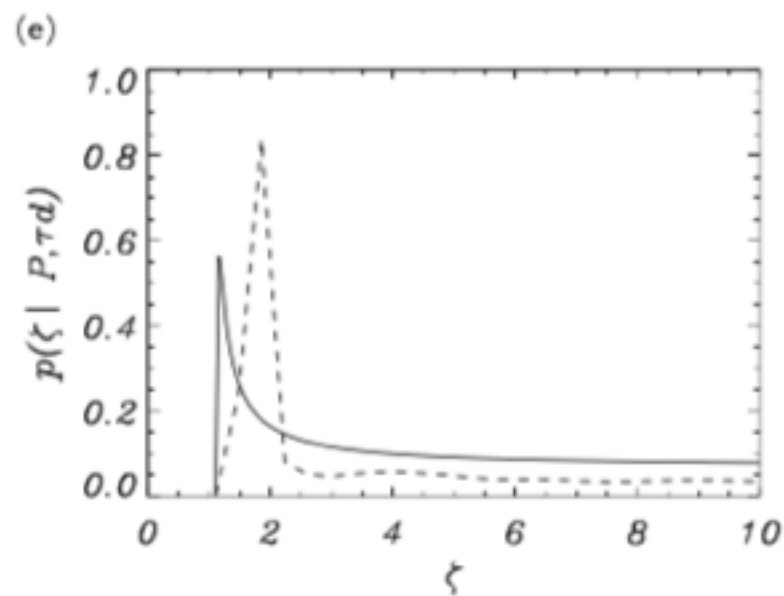
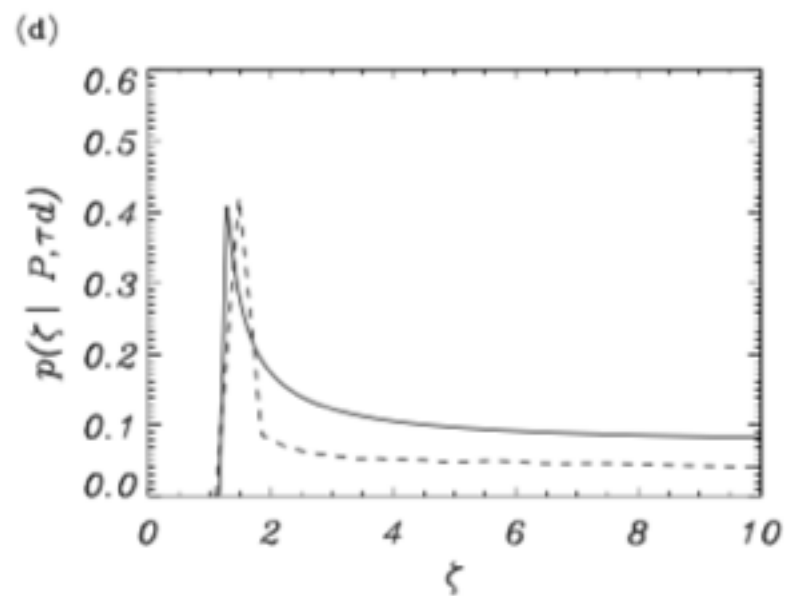
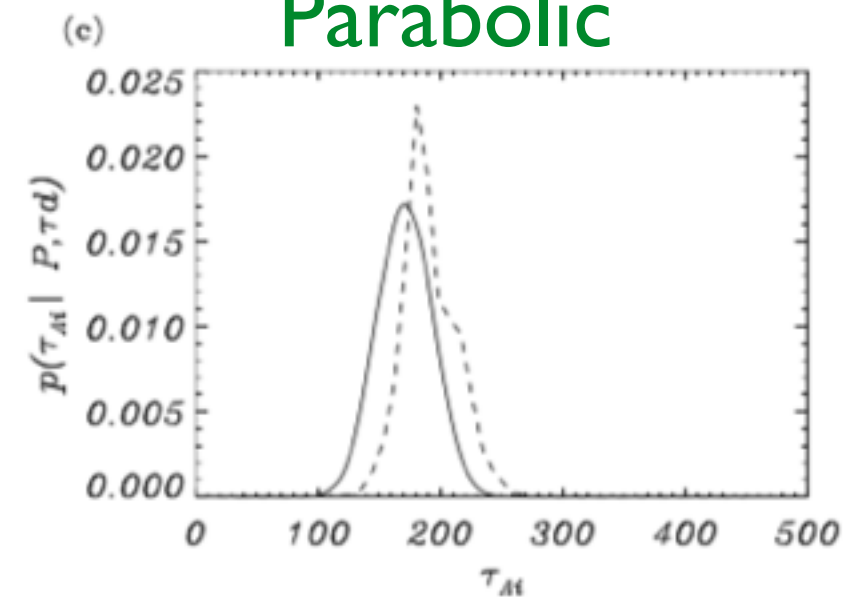
Sinusoidal



Linear



Parabolic



Solid: sinusoidal - Dotted: linear - Dashed parabolic

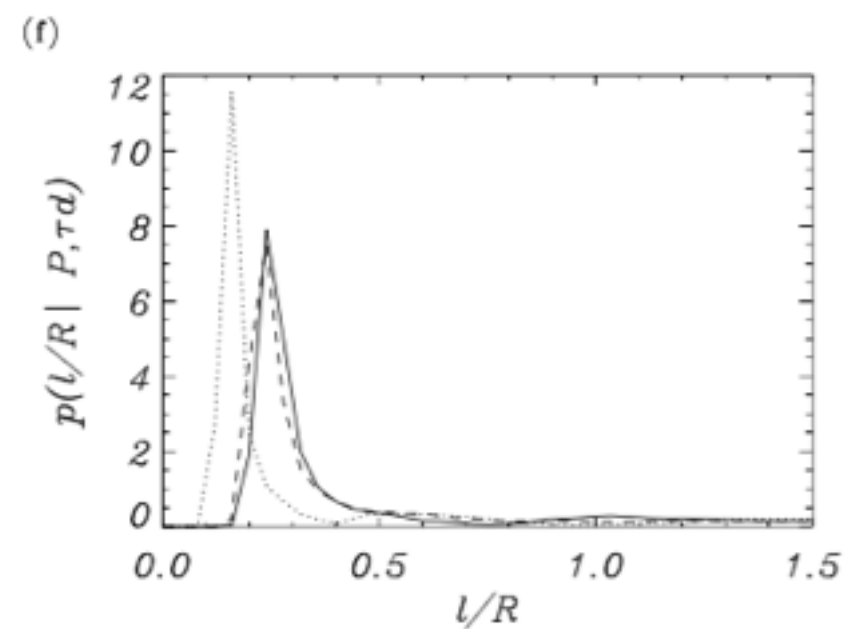
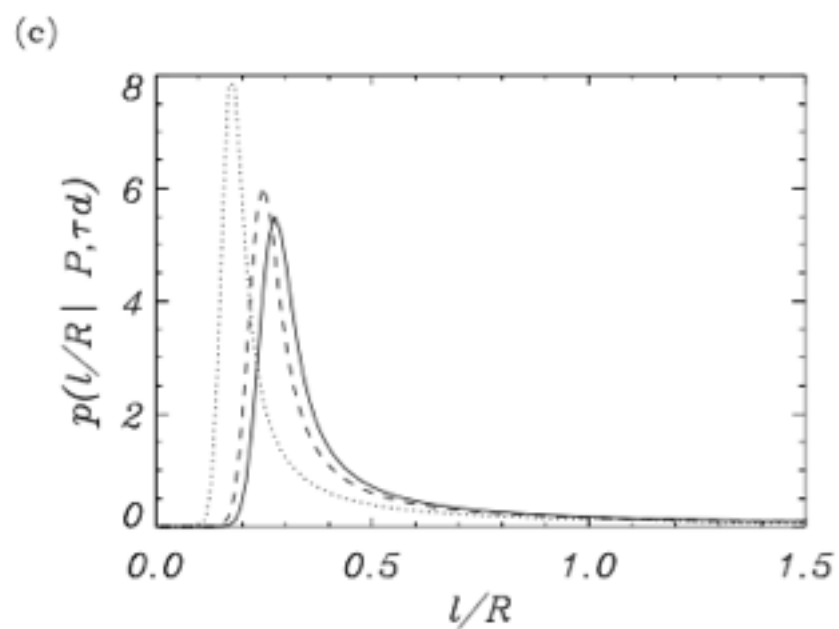
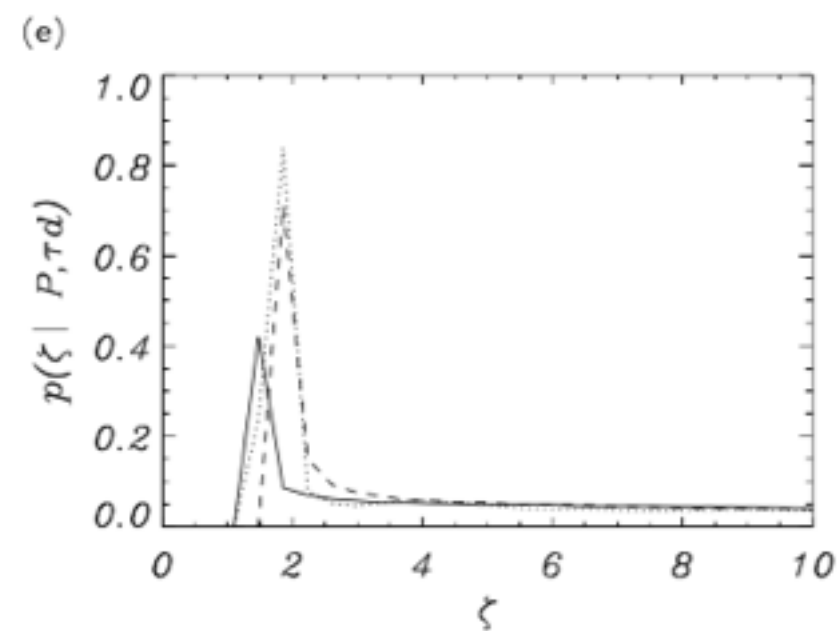
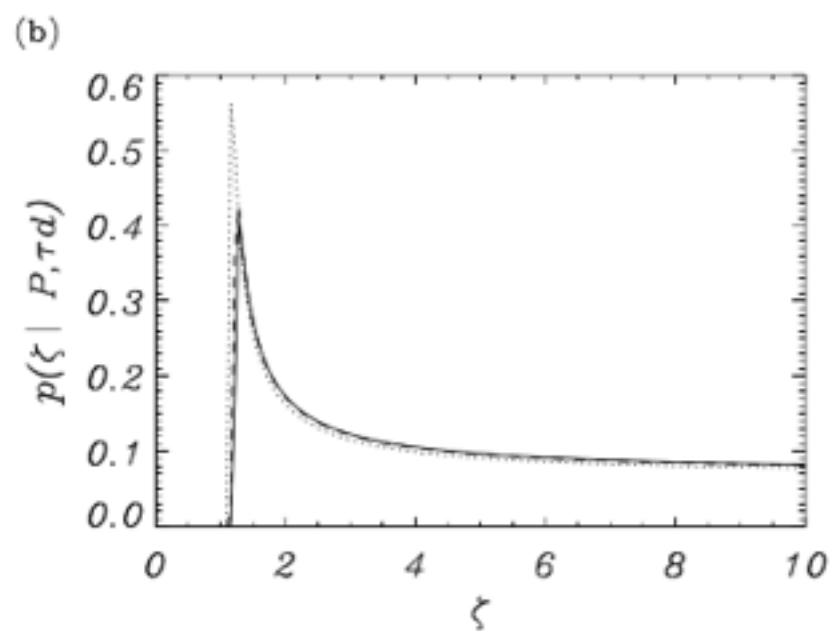
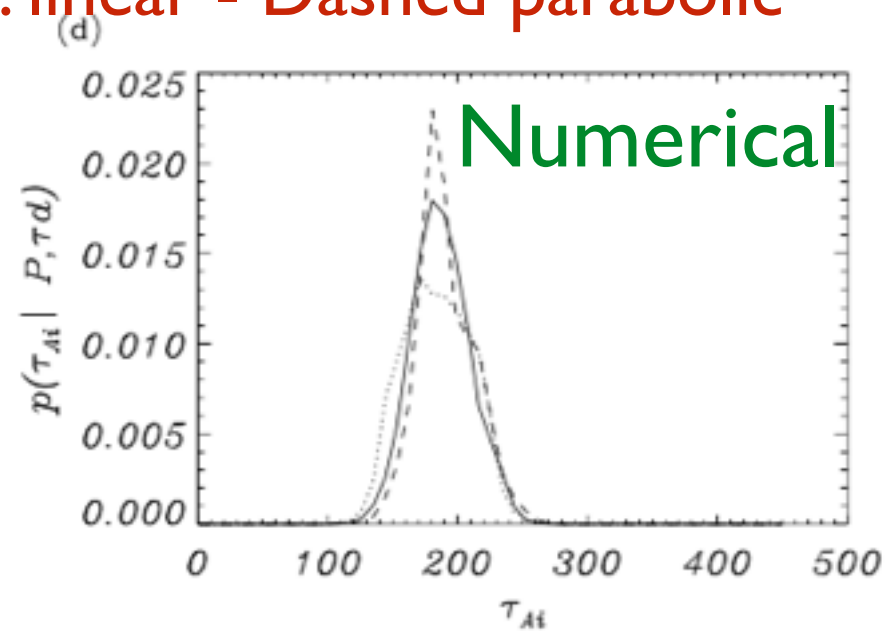
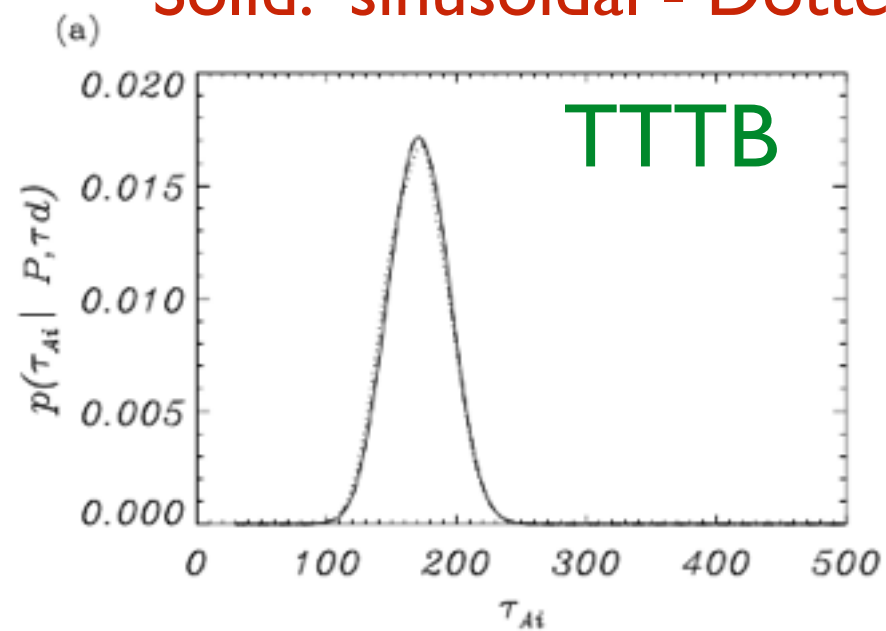


Table 1

Summary of inference results for the case with weak damping for the three alternative models by employing the TTTB and numerical forward solutions. $P = 272$ (s); $\tau_d = 849$ (s); $\sigma_P = \sigma_{\tau_d} = 30$ (s).

θ_i	TTTB approximation			Numerical		
	M ^S	M ^L	M ^P	M ^S	M ^L	M ^P
τ_{Ai}	171^{+22}_{-24}	169^{+24}_{-24}	171^{+21}_{-24}	177^{+24}_{-20}	169^{+29}_{-21}	181^{+21}_{-18}
ζ	$4.4^{+3.7}_{-2.6}$	$4.1^{+3.9}_{-2.2}$	$4.3^{+3.8}_{-2.6}$	$7.9^{+8.2}_{-6.1}$	$4.6^{+10.8}_{-2.9}$	$6.7^{+9.0}_{-4.8}$
l/R	$0.3^{+0.4}_{-0.1}$	$0.2^{+0.4}_{-0.1}$	$0.3^{+0.4}_{-0.1}$	$0.3^{+0.5}_{-0.1}$	$0.2^{+0.8}_{-0.1}$	$0.3^{+0.4}_{-0.1}$

The adopted density model does not seem to influence that much the inference result

Numerical results lead to basically the same conclusion

Model comparison

Compare the plausibility of alternative models to explain observed data

Posterior ratio for two competing models

$$\frac{p(M_i|d)}{p(M_j|d)} = \frac{p(d|M_i) p(M_i)}{p(d|M_j) p(M_j)}$$

A priori equally probable models > Bayes factors

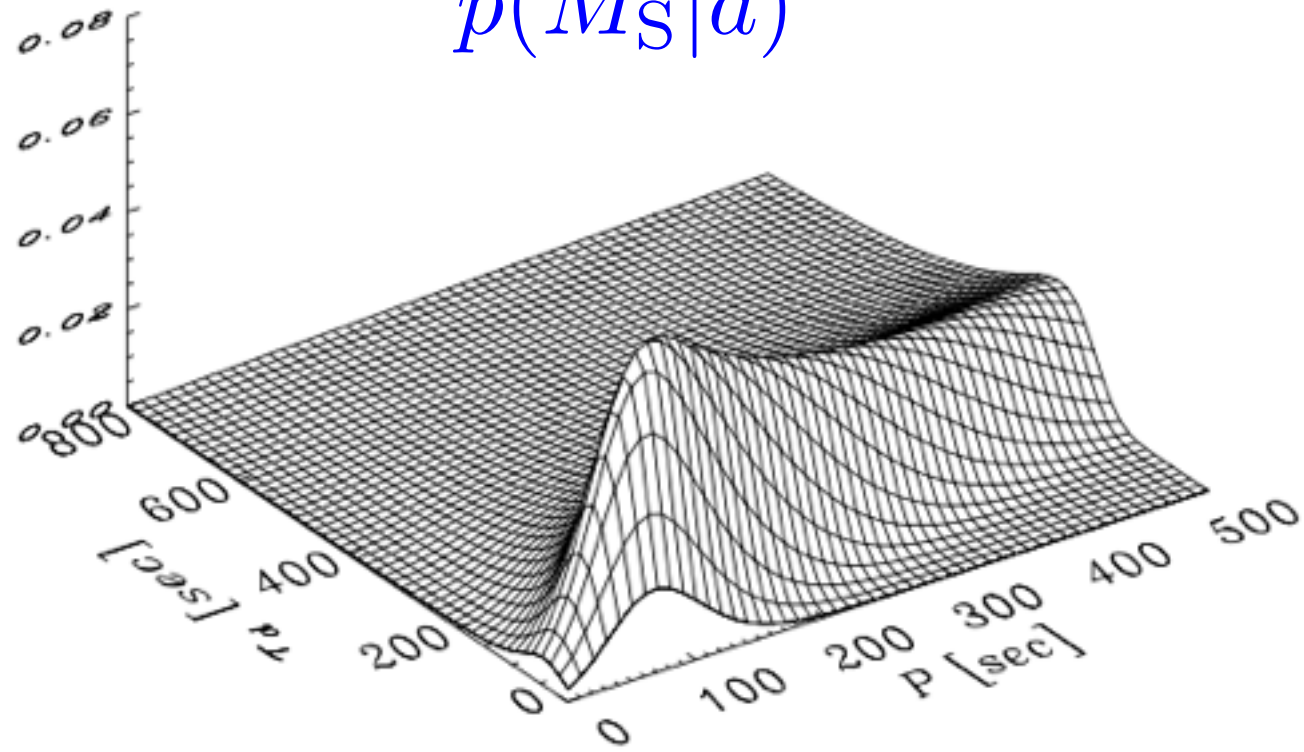
$$BF_{ij} = \frac{p(d|M_i)}{p(d|M_j)}$$

Quantitative model comparison: compute Bayes factors as a function of measured period and damping time and use Jeffreys' scale [Jeffreys\(61\)](#); [Kass & Raftery\(95\)](#)

$2 \log_e BF$	Evidence
0-2	Minimal Evidence (ME)
2-6	Positive Evidence (PE)
6-10	Strong Evidence (SE)
> 10	Very Strong Evidence (VSE)

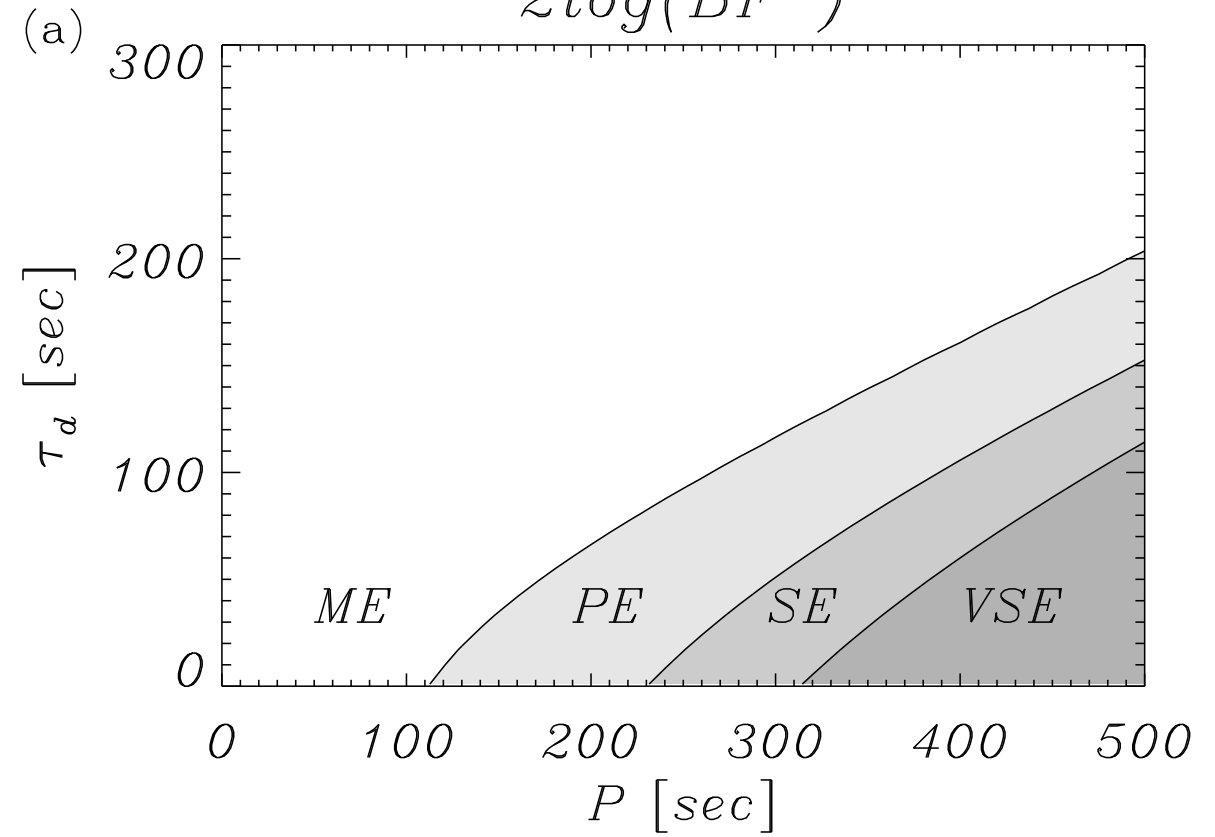
Example model evidence

$$p(M_S|d)$$



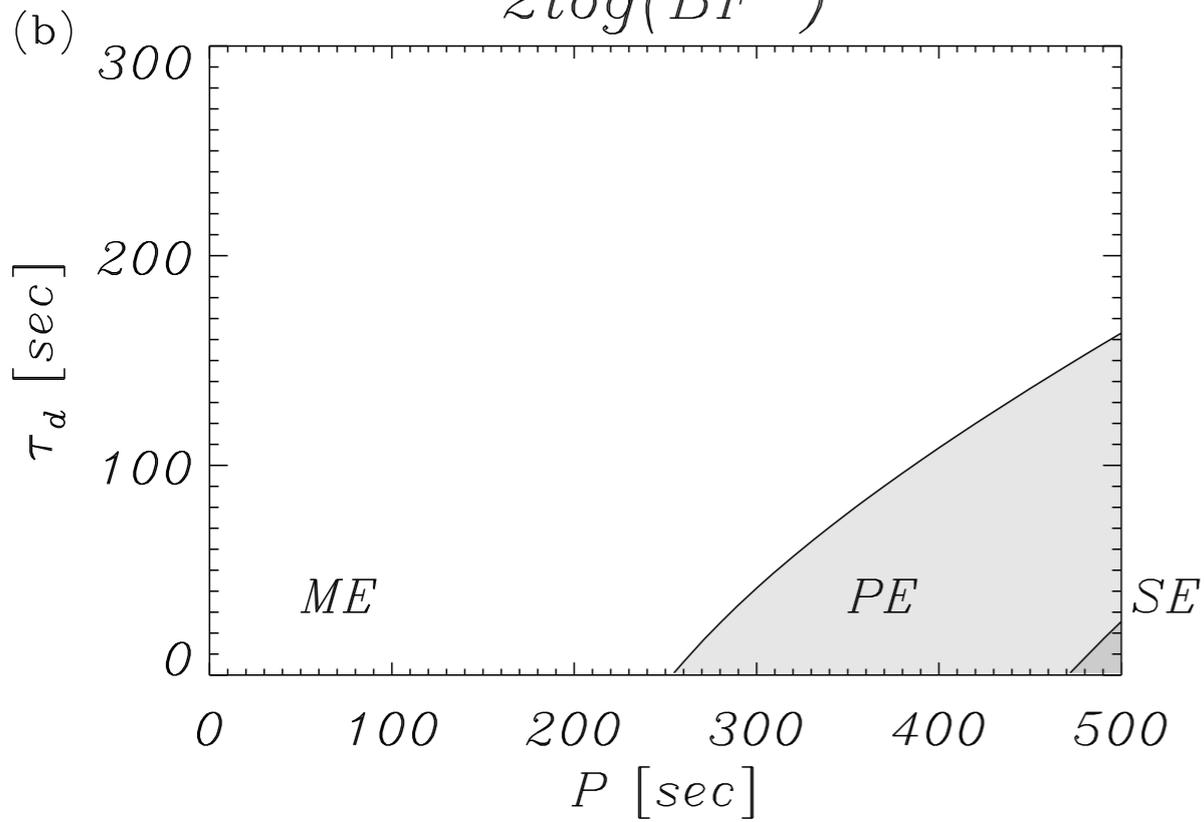
linear vs. sinusoidal

$$2\log(BF^{LS})$$



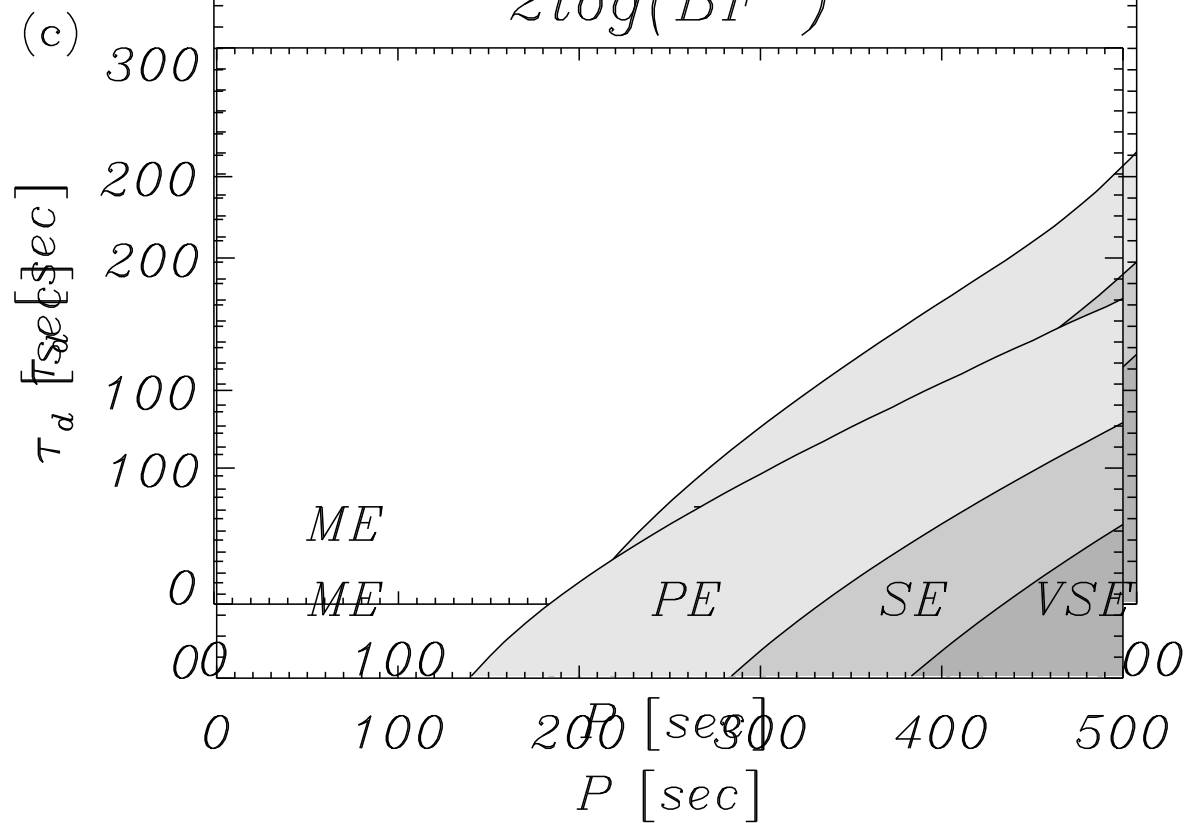
parabolic vs. sinusoidal

$$2\log(BF^{PS})$$



linear vs. parabolic

$$2\log(BF^{LP})$$



Model averaging

Weight posteriors from alternative models with the relative evidence for each one

Model-averaged posterior for parameter θ is

$$p(\theta|d) = \sum_{i=1}^N p(\theta|d, M_i)p(M_i|d) = p(M_1|d) \sum_{i=1}^N B_{i1}p(\theta|d, M_i)$$

Take e.g., model M_1 as reference model and compute **Bayes factors** with respect to it

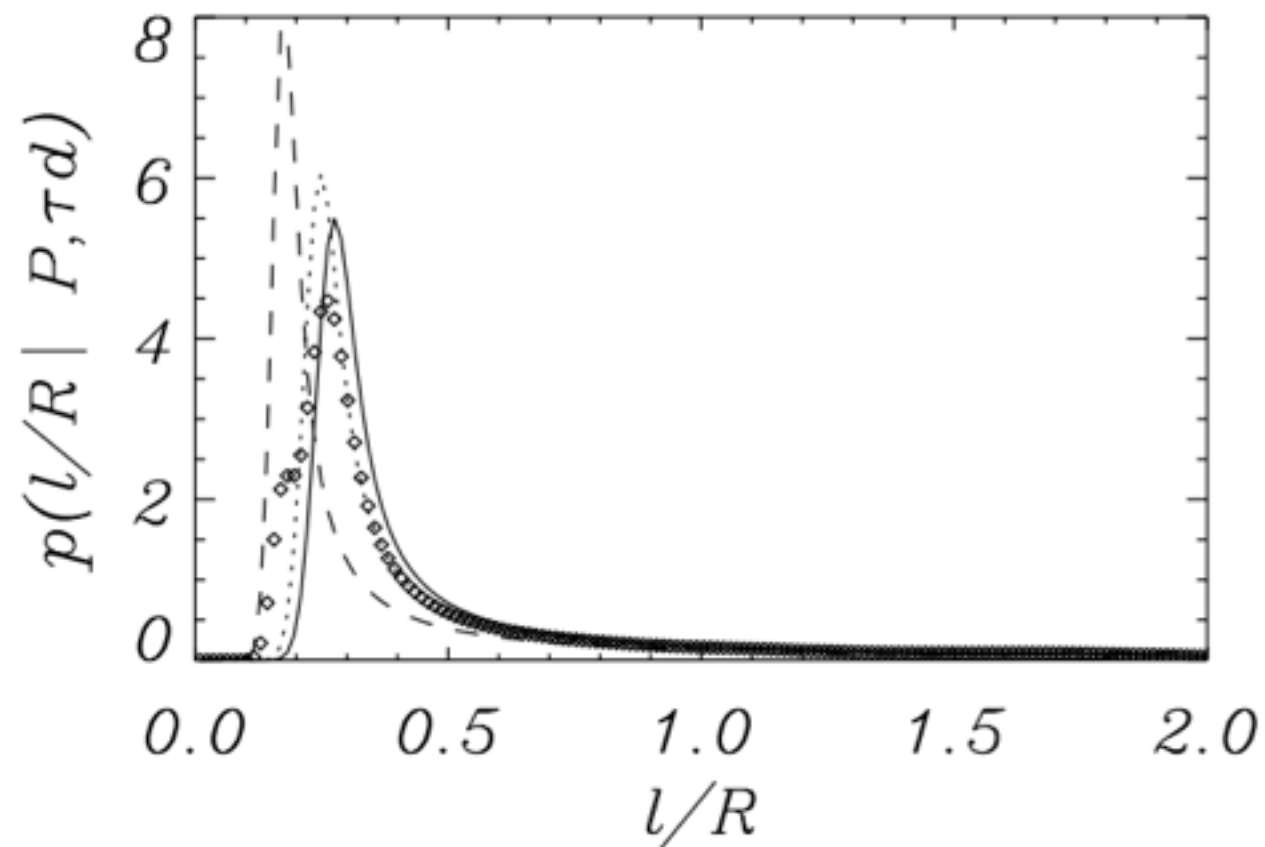
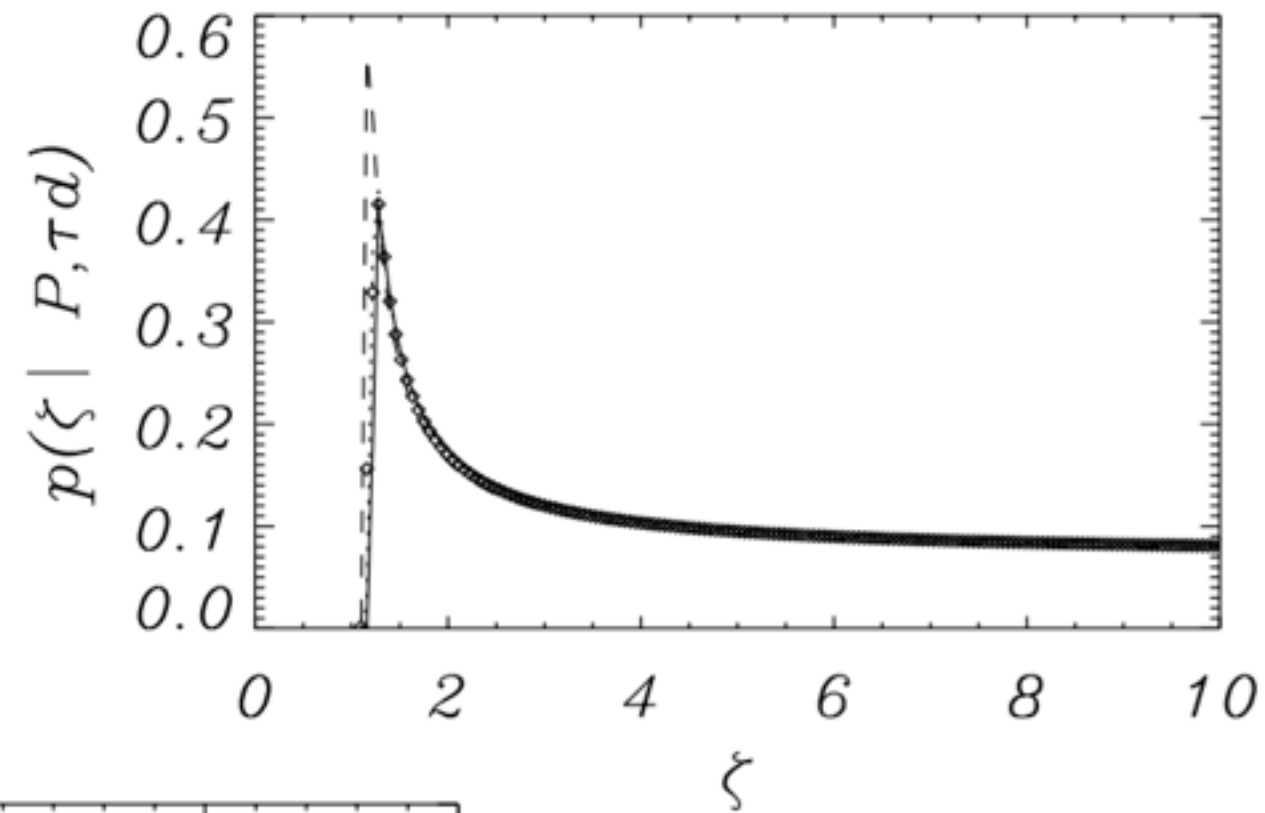
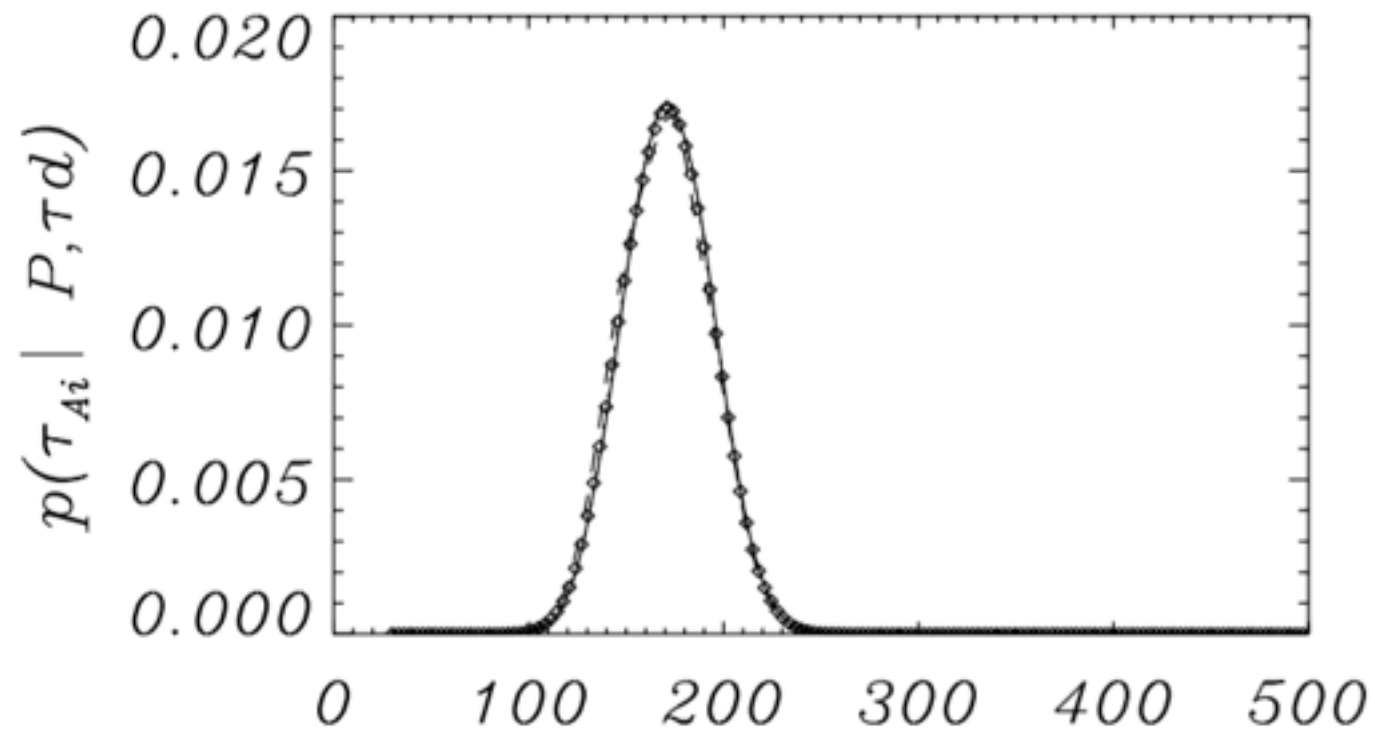
Further assume that prior probabilities for the N models are all equal $p(M_i)=1/N$

With these assumptions, the posterior for the reference model M_1 is given by

$$p(M_1|d) = \frac{1}{1 + \sum_{i=2}^N B_{i1}}$$

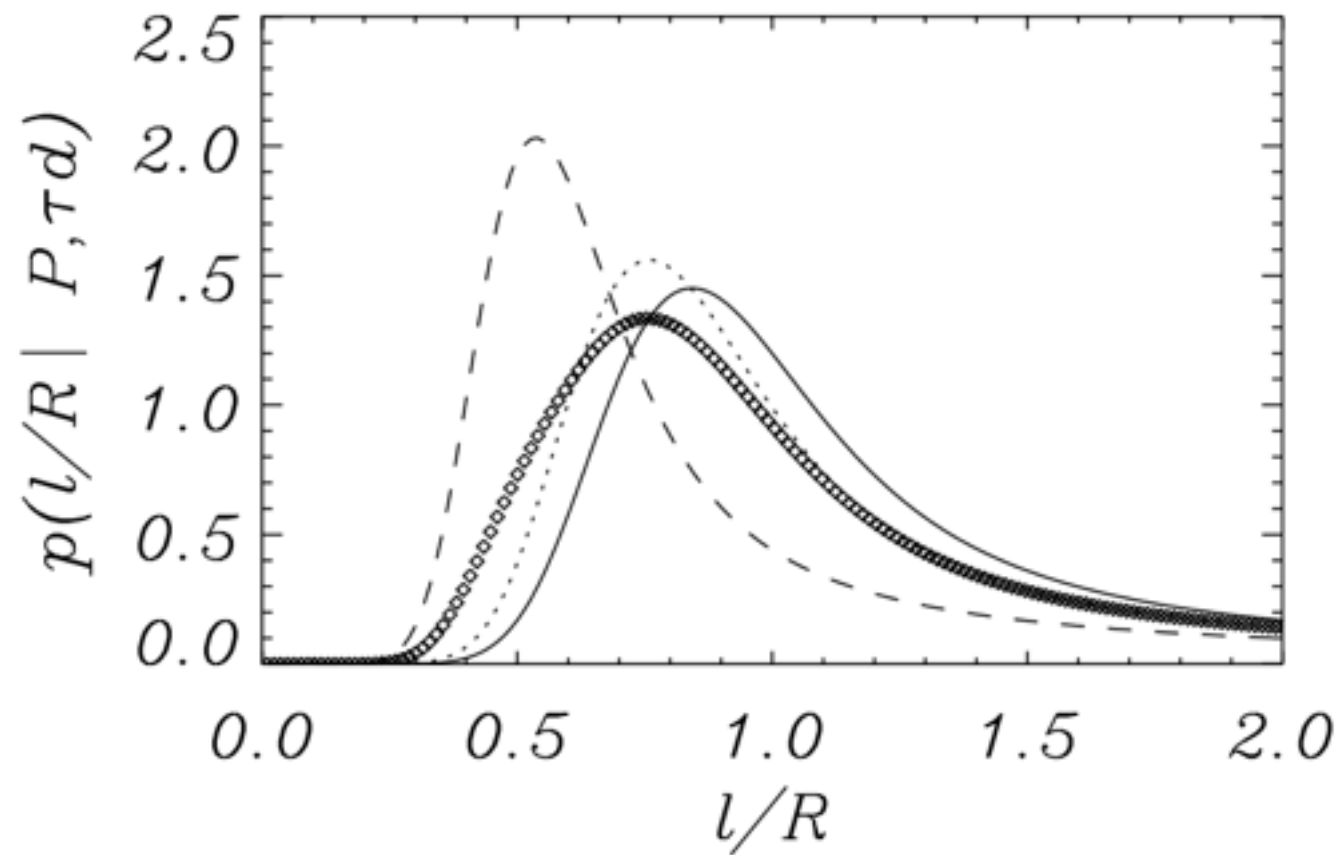
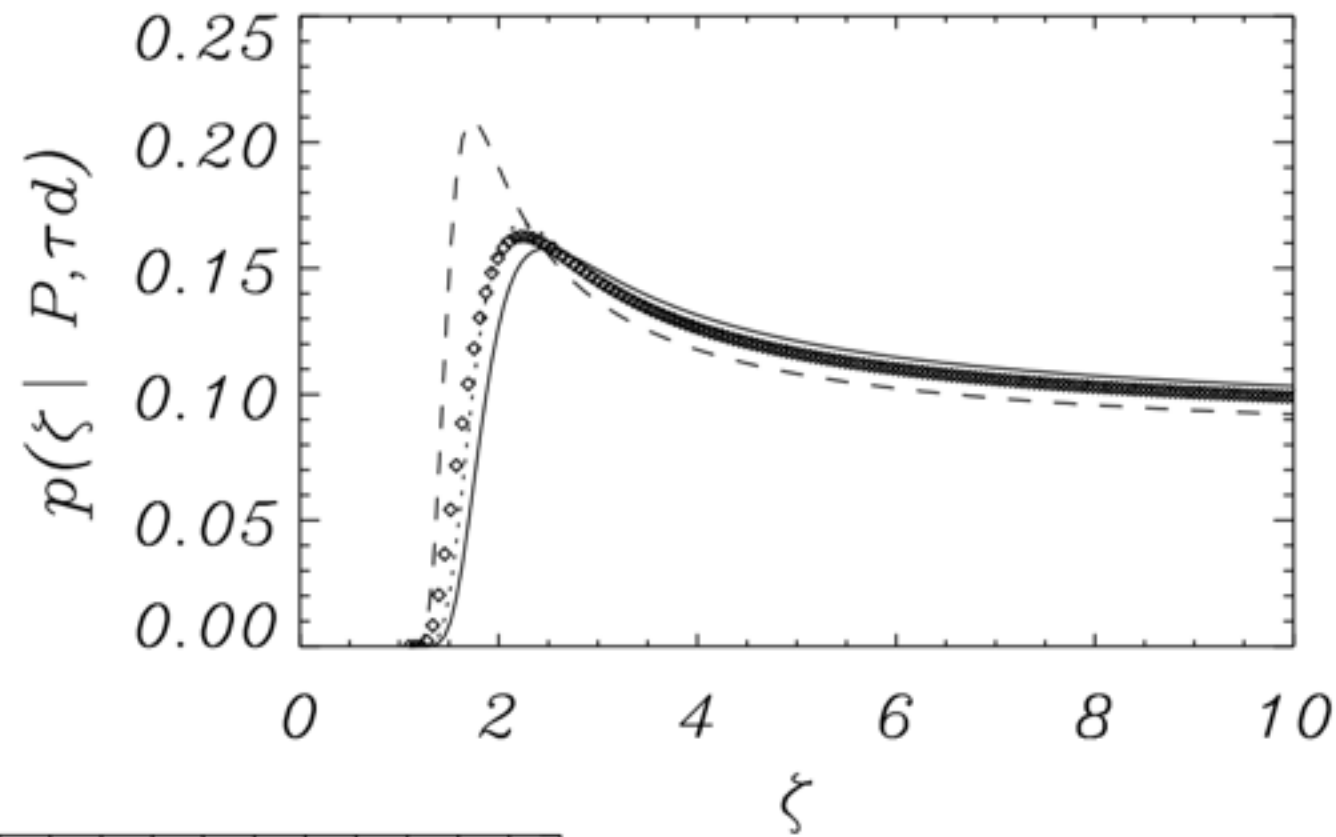
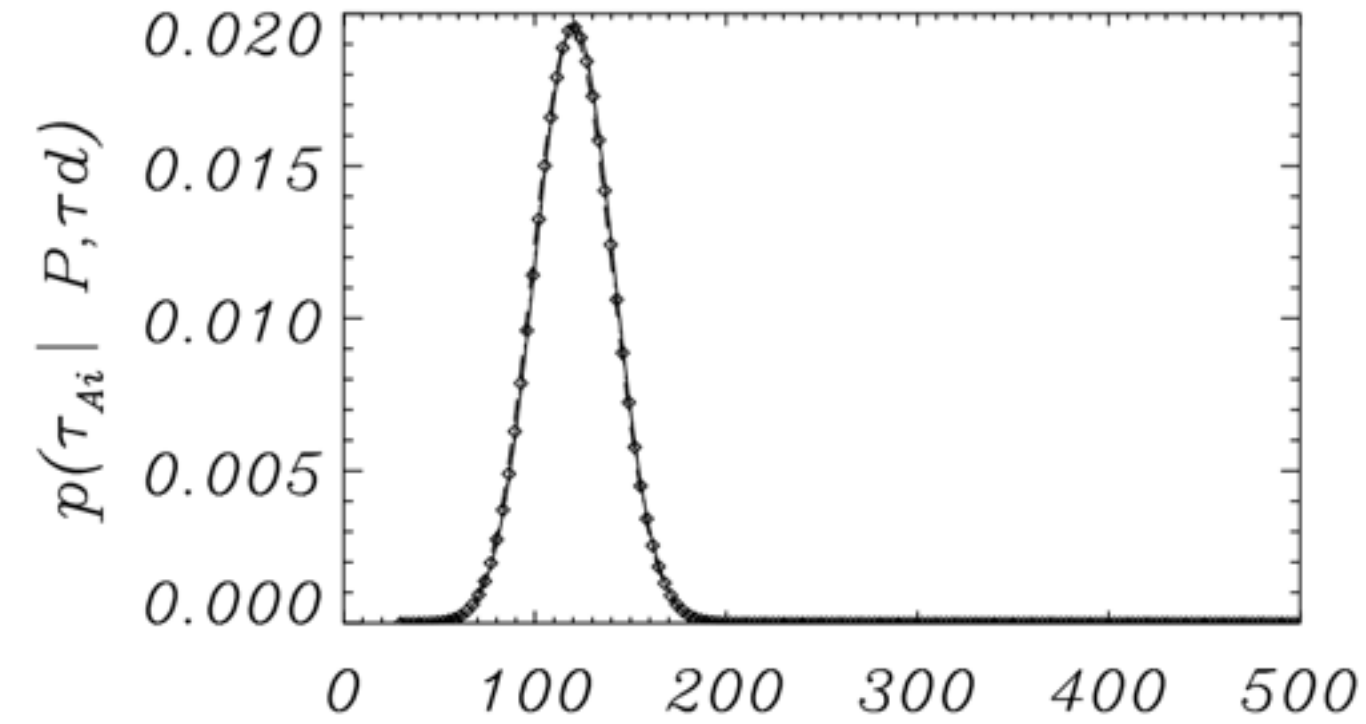
Model averaging result - case I

Solid: sinusoidal - Dashed: linear - Dotted: parabolic - symbols: averaged posterior



Model averaging result - case 2

Solid: sinusoidal - Dashed: linear - Dotted: parabolic - symbols: averaged posterior



Conclusions

Bayesian analysis tools enable us to apply the three levels of Bayesian inference to the problem of obtaining information on the physical parameters in oscillating coronal waveguides, to assess the plausibility of alternative models, and to obtain model averaged posteriors when the evidence does not strongly support any model.

Parameter inference successful in determining Alfvén travel times, density contrasts, and transverse inhomogeneity length-scales. Model comparison successful in assessing alternative density models.

Method incorporates consistently calculated credible intervals and uncertainty. Enables to quantify plausibility of alternative models in view of data

MCMC sampling of the full posterior can be substituted by integration for the marginal posteriors in low-dimensional problems.

The methods here developed can help to solve more involved problems such as the ones considered by our Team.

References

- I. Arregui, A. Asensio Ramos, “Bayesian Magnetohydrodynamic Seismology of Coronal Loops”, *The Astrophysical Journal*, 740, 44 (10pp) (2011)
- I. Arregui, A. Asensio Ramos, & A. J. Diaz, “Bayesian Analysis of Multiple Harmonic Oscillations in the Solar Corona”, *The Astrophysical Journal Letters*, 765, L23 (5pp) (2013)
- I. Arregui, A. Asensio Ramos, & D. J. Pascoe, “Determination of Transverse Density Structuring from Propagating Magnetohydrodynamic Waves in the Solar Atmosphere”, *The Astrophysical Journal Letters*, 769, L34 (6pp) (2013)
- A. Asensio Ramos & I. Arregui, “Coronal Loop Physical Parameters from the Analysis of Multiple Observed Transverse Oscillations”, *Astronomy and Astrophysics*, 554, A7 (2013)
- I. Arregui & A. Asensio Ramos, “Determination of the Cross-Field Density Structuring in Coronal Waveguides Using the Damping of Transverse Waves” (Research Note), *Astronomy and Astrophysics*, 565, A78 (2014)
- I. Arregui & R. Soler, “Model Comparison for the Density Structure Along Solar Prominence Threads”, *Astronomy and Astrophysics*, accepted (2015).
- I. Arregui, R. Soler, & A. Asensio Ramos, “Model Comparison for the Density Structure Across Solar Coronal Waveguides”, *The Astrophysical Journal*, submitted (2015).
- I. Arregui & A. Asensio Ramos, “Inference of the Magnetic Field Strength in Coronal Waveguides”, *Astronomy and Astrophysics*, in preparation (2015).